

SUPPORTING INFORMATION

Gene-guided discovery and engineering of branched cyclic peptides in plants

Roland D. Kersten^{a,1}, Jing-Ke Weng^{a,b,1}

^a Whitehead Institute for Biomedical Research, 455 Main Street, Cambridge, MA, United States

^b Department of Biology, Massachusetts Institute of Technology, Cambridge, MA, United States

¹ Corresponding authors: Roland D. Kersten, E-mail: rkersten@wi.mit.edu, Jing-Ke Weng, E-mail: wengj@wi.mit.edu

Table of contents

Figure/Table	Description	Page
Table S1	NMR data of lyciumin A	10
Table S2	NMR data of lyciumin B	11
Table S3	NMR data of lyciumin D	12
Table S4	Genome mining of candidate lyciumin precursor genes in plants	13
Table S5	Core peptide sequences from predicted lyciumin precursor genes	14
Table S6	NMR data of lyciumin C	15
Table S7	NMR data of lyciumin I	16
Table S8	Bioinformatic analysis of lyciumin precursor genes and co-clustered glutamine cyclotransferase genes in genomes of <i>Beta vulgaris</i> and <i>Chenopodium quinoa</i>	17
Table S9	LC-MS dataset accessions (MassIVE, GNPS)	17
Figure S1	MS analysis of lyciumin A	18
Figure S2	¹ H NMR spectrum of lyciumin A	19
Figure S3	¹³ C NMR spectrum of lyciumin A	19
Figure S4	MS analysis of lyciumin B	20
Figure S5	¹ H NMR spectrum of lyciumin B	21
Figure S6	MS analysis of lyciumin D	22
Figure S7	¹ H NMR of spectrum lyciumin D	23
Figure S8	Candidate transcripts of lyciumin precursor peptide gene from <i>Lycium barbarum</i> root transcriptome	24
Figure S9	Signal peptide prediction of LbaLycA with SignalP-4.1	24
Figure S10	Precursor gene-guided genome mining workflow for lyciumin discovery	25
Figure S11	Genome mining of lyciumins from <i>Amaranthus hypochondriacus</i>	26/27
Figure S12	¹ H NMR spectrum of lyciumin C	28
Figure S13	Genome mining of lyciumins from <i>Beta vulgaris</i>	29/30
Figure S14	Genome mining of lyciumins from <i>Chenopodium quinoa</i>	31/32
Figure S15	Genome mining of lyciumins from <i>Glycine max</i>	33-35
Figure S16	¹ H NMR of spectrum of lyciumin I	36
Figure S17	¹ H- ¹ H COSY spectrum of lyciumin I	37
Figure S18	¹ H- ¹ H TOCSY spectrum of lyciumin I	38
Figure S19	¹ H- ¹³ C HSQC spectrum of lyciumin I	39
Figure S20	¹ H- ¹³ C HMBC spectrum of lyciumin I	40
Figure S21	¹ H- ¹ H ROESY spectrum of lyciumin I	41
Figure S22	Genome mining of lyciumins from <i>Solanum melongena</i>	42/43
Figure S23	Genome mining of lyciumins from <i>Medicago truncatula</i>	44
Figure S24	Lyciumin precursor gene expression in <i>Amaranthus hypochondriacus</i> , <i>Chenopodium quinoa</i> , <i>Glycine max</i> , <i>Medicago truncatula</i> and <i>Solanum tuberosum</i>	45
Figure S25	Lyciumin chemotyping in source plant tissues	46
Figure S26	Genome and transcriptome mining of lyciumins from <i>Solanum tuberosum</i>	47-55
Figure S27	Detection of candidate dehydrothreonine-lyciumin derivatives in Amaranthaceae	56-60
Figure S28	Phylogenetic analysis of predicted and characterized lyciumin precursors from analyzed plant genomes	61
Figure S29	Detection of [Gln]-lyciumins after heterologous expression of <i>LbaLycA</i> in <i>Nicotiana benthamiana</i>	62-64
Figure S30	Characterization of <i>Lycium barbarum</i> glutamine cyclotransferase (LbaQC)	65
Figure S31	Detection of C-terminally extended lyciumins after <i>LbaLycA</i> heterologous expression in <i>Nicotiana benthamiana</i>	66-70
Figure S32	Heterologous expression of <i>Sali3-2</i> -[QAYGVYTW] in <i>Nicotiana benthamiana</i>	71
Figure S33	Heterologous expression of <i>Sali3-2</i> -[QPAGVYTW] in <i>Nicotiana benthamiana</i>	72
Figure S34	Heterologous expression of <i>Sali3-2</i> -[QPYAVYTW] in <i>Nicotiana benthamiana</i>	73
Figure S35	Heterologous expression of <i>Sali3-2</i> -[QPYGAYTW] in <i>Nicotiana benthamiana</i>	74
Figure S36	Heterologous expression of <i>Sali3-2</i> -[QPYGVATW] in <i>Nicotiana benthamiana</i>	75
Figure S37	Heterologous expression of <i>Sali3-2</i> -[QPYGVYAW] in <i>Nicotiana benthamiana</i>	76
Figure S38	Heterologous expression of <i>Sali3-2</i> -[QPYTVYTW] in <i>Nicotiana benthamiana</i>	77/78
Figure S39	Heterologous expression of <i>Sali3-2</i> -[QPWGVGTW] in <i>Nicotiana benthamiana</i>	79
Figure S40	Heterologous expression of <i>Sali3-2</i> -[QPWGVGAW] in <i>Nicotiana benthamiana</i>	80
Figure S41	Heterologous expression of <i>Sali3-2</i> -[QPWGVYTW] in <i>Nicotiana benthamiana</i>	81
Figure S42	Heterologous expression of <i>Sali3-2</i> -[QPFVYTW] in <i>Nicotiana benthamiana</i>	82
Figure S43	Heterologous expression of <i>Sali3-2</i> -[QPFVFFSW] in <i>Nicotiana benthamiana</i>	83
Figure S44	Heterologous expression of <i>Sali3-2</i> -[QPYGVYFW] in <i>Nicotiana benthamiana</i>	84
Figure S45	Heterologous expression of <i>Sali3-2</i> -[QPWGVYSW] in <i>Nicotiana benthamiana</i>	85

SUPPORTING TEXT

Chemotyping of lyciumin peptides from plant material

For comparative chemotyping of lyciumin concentrations in different plant tissues, peptides were extracted from plant tissues as described above from three different plants of the same age. Analyzed tissues of *Amaranthus hypochondriacus* and *Chenopodium quinoa* (three month old) were flower, leaf, root, seed and stem. Analyzed tissues of *Beta vulgaris* (three month old) were leaf, root, seed and stem. Analyzed tissues of *Glycine max* (three month old) were bean, leaf, pod, root and stem. Analyzed tissues for *Solanum tuberosum* (three week old) were sprout and tuber. Peptide extracts were subjected to low resolution MS analysis by selected-ion monitoring (SIM) of lyciumin masses specific to each plant with the following LC-MS parameters: LC – Phenomenex Kinetex® 2.6 µm C18 reverse phase 100 Å 150 x 3 mm LC column, LC gradient: solvent A – 0.1% formic acid, solvent B – acetonitrile (0.1% formic acid), 0-1 min: 5% B, 1-8 min: 5-95% B, 8-10 min: 95% B, 10-15 min: 5% B, MS – positive ion mode, SIM (*Amaranthus hypochondriacus*: 872.8-873.8 m/z and 963.8-964.8 m/z, *Chenopodium quinoa*: 869.8-870.8 m/z and 972.8-973.8 m/z, *Beta vulgaris*: 894.8-895.8 m/z, *Glycine max*: 910.8-911.8 m/z and 993.8-994.8 m/z, *Solanum tuberosum*: 880.8-881.8 m/z, 896.8-897.8 m/z, 913.8-914.8 m/z, 922.8-923.8 m/z, 947.8-948.8 m/z, 972.8-973.8 m/z and 1048.8-1049.8 m/z). Lyciumin ion abundance values were determined by peak area integration from each lyciumin SIM chromatogram in QualBrowser in the Thermo Xcalibur software package (version 3.0.63, ThermoScientific).

Phylogenetic analysis of lyciumin precursor peptides

Protein sequences of characterized and predicted lyciumin precursors from genomes (Dataset S1, except 3'-partial sequences) and four founding members of the BURP domain family (NP_001303011.1 - BURP domain-containing protein BNM2A precursor [*Brassica napus*], NP_001234835.1 - Polygalacturonase-1 non-catalytic subunit beta precursor [*Solanum lycopersicum*], CAA31603.1/CAA31602.1 - Embryonic abundant protein USP87 / Embryonic abundant protein USP92 [*Vicia faba*], NP_197943.1 - BURP domain protein RD22 [*Arabidopsis thaliana*]) (1-4) were reduced to their BURP domain (Pfam PF03181) and aligned using Muscle algorithm (5) in MEGA (ver. 7.0.9) (6). A neighbor-joining phylogenetic tree was generated with 2000 bootstrap generations using the p-distance method (7) in MEGA.

Lyciumin engineering in *Nicotiana benthamiana*

IDT gblocks® of *Sali3-2* for lyciumin engineering (from Figure 4B, core peptide sequences are in [brackets]):

```
>Sali3-2
ATGGAATTCGATGCTCAGTCATCTCTTTTACCATTCTCTTCTCTCTTGGCTCTTGCAGGAGAGAGCCATGTCCATGCATCGTACCTGAGGAAGATTATTGGGAAGCTGTT
TGGCCAAACACTCCCATTCCCAGTGCAGTGCAGAGAGCTTCTAAAGCCTCTCCCTGCAGGTGTTGAAATCGATGAACTCCCTAAGCAAATTTGATGATACACAGTACCCAAAA
ACATTTCTTCTATAAAGAAGACCTTCATCCAGGCAAAAACAATGAAAGTACAATTCACCAAGCGTCCCTATGCACAACCTTATGGTGTATATACATGGTTAACGGATATTAAA
GACACCTCTAAGAAGGATATAGTTTTGAAGAGATATGCATCAAGAAGAAGCGTTTGAGGAGAGAAGAGAAATTTGTGCAAAATCCTTGGGAACAGTAATTTGGTTTTGCC
ATTTCAAAGCTGGGAAGAAGACATTCAAGTACTTTCAAGTTCCTTTGTCAATAAGCAAGAGCAATACACTGTGGAAGGAGTGCAGAAATCTGGAGACAAAGCAGTATGTGT
CATGGGCTAAATTCAGAAGTGCAGTATTTTACTGCCATAAAGTCCGTGAAACAACAGCTTTCATGGTTCCATTGGTGGCTGGTATGGAACCAAACTCAGGCACCTTGCT
GTTTGCCACTCAGATACTTCTGGAATGAATCATCATGCTTTCATGAACTCATGGGAGTTGATCCTGGAACTAACCCCTGTTTGCCATTTCTTGGGAAGCAAGGCCATTTTA
TGGGTACCCAATTTATCTATGGACACTGCCTATCAGACTAACGTTGTTGTTTAA
```

```
>Sali3-2-[QPWGVYTW]
ATGGAATTCGATGCTCAGTCATCTCTTTTACCATTCTCTTCTCTCTTGGCTCTTGCAGGAGAGAGCCATGTCCATGCATCGTACCTGAGGAAGATTATTGGGAAGCTGTT
TGGCCAAACACTCCCATTCCCAGTGCAGTGCAGAGAGCTTCTAAAGCCTCTCCCTGCAGGTGTTGAAATCGATGAACTCCCTAAGCAAATTTGATGATACACAGTACCCAAAA
ACATTTCTTCTATAAAGAAGACCTTCATCCAGGCAAAAACAATGAAAGTACAATTCACCAAGCGTCCCTATGCACAACCTTGGGGTGTATATACATGGTTAACGGATATTAAA
GACACCTCTAAGAAGGATATAGTTTTGAAGAGATATGCATCAAGAAGAAGCGTTTGAGGAGAGAAGAGAAATTTGTGCAAAATCCTTGGGAACAGTAATTTGGTTTTGCC
ATTTCAAAGCTGGGAAGAAGACATTCAAGTACTTTCAAGTTCCTTTGTCAATAAGCAAGAGCAATACACTGTGGAAGGAGTGCAGAAATCTGGAGACAAAGCAGTATGTGT
CATGGGCTAAATTCAGAAGTGCAGTATTTTACTGCCATAAAGTCCGTGAAACAACAGCTTTCATGGTTCCATTGGTGGCTGGTATGGAACCAAACTCAGGCACCTTGCT
GTTTGCCACTCAGATACTTCTGGAATGAATCATCATGCTTTCATGAACTCATGGGAGTTGATCCTGGAACTAACCCCTGTTTGCCATTTCTTGGGAAGCAAGGCCATTTTA
TGGGTACCCAATTTATCTATGGACACTGCCTATCAGACTAACGTTGTTGTTTAA
```

```
>Sali3-2-[QPYGVYFW]
ATGGAATTCGATGCTCAGTCATCTCTTTTACCATTCTCTTCTCTCTTGGCTCTTGCAGGAGAGAGCCATGTCCATGCATCGTACCTGAGGAAGATTATTGGGAAGCTGTT
TGGCCAAACACTCCCATTCCCAGTGCAGTGCAGAGAGCTTCTAAAGCCTCTCCCTGCAGGTGTTGAAATCGATGAACTCCCTAAGCAAATTTGATGATACACAGTACCCAAAA
ACATTTCTTCTATAAAGAAGACCTTCATCCAGGCAAAAACAATGAAAGTACAATTCACCAAGCGTCCCTATGCACAACCTTATGGTGTATATTTCTGGTTAACGGATATTAAA
GACACCTCTAAGAAGGATATAGTTTTGAAGAGATATGCATCAAGAAGAAGCGTTTGAGGAGAGAAGAGAAATTTGTGCAAAATCCTTGGGAACAGTAATTTGGTTTTGCC
ATTTCAAAGCTGGGAAGAAGACATTCAAGTACTTTCAAGTTCCTTTGTCAATAAGCAAGAGCAATACACTGTGGAAGGAGTGCAGAAATCTGGAGACAAAGCAGTATGTGT
```


CATGGGCTAAATTCAGAACTGCAGTATTTACTGCCATAAAGTCCGTGAAACAACAGCTTTCATGGTTCATTGGTGGCTGGTATGGAACCAAACTCAGGCCTTGCT
GTTTGCCACTCAGATACTTCTGGAATGAATCATCATGCTTTCATGAACTCATGGGAGTTGATCCTGGAACCTAACCCCTGTTTGGCCATTTCTTGGAGCAAGGCCATTTTA
TGGGTACCAATTTATCTATGGACTGCCTATCAGACTAACGTTGTTGTTTAA

>Sali3-2- [QYGVYTW]

ATGGAATTCGATGCTCAGTCACTCTCTTTTACCATTCTCTTCTCTCTTGGCTCTTGCAGGAGAGGCCATGTCCATGCATCGTACCTGAGGAAGATTATGGGAAGCTGTT
TGGCCAAACACTCCCATTCCCCTGCAGTGCAGAGCTTCTAAAGCCTCTCCCTGCAGGTGTTGAAATCGATGAACTCCCTAAGCAAATTTGATGATACACAGTACCCAAAA
ACATTTCTTATAAAGAAGACCTTCCATCCAGGCAAAACAATGAAAGTACAATTCACCAAGCGTCCCTATGCACAATATGGTGTATATACATGGTTAACGGATATTAAAGAC
ACCTCTAAAGAAGGATATAGTTTGAAGAGATATGCATCAAGAAAGAAGCGTTTGGAGGAGAAGAGAAGTTTGTGCAAAAATCCTTGGGAACAGTAATTTGGTTTGGCCATT
TCAAAGCTGGGAAAGAACATTCAGTACTTTCAAGTTCCTTTGTCAATAAGCAAGAGCAATACACTGTGGAAGGAGTGCAGAATCTTGGAGACAAAGCAGTGTATGTCAT
GGGCTAAATTCAGAACTGCAGTATTTACTGCCATAAAGTCCGTGAAACAACAGCTTTCATGGTTCATTGGTGGCTGGTATGGAACCAAACTCAGGCCTTGCTGTT
TGCCACTCAGATACTTCTGGAATGAATCATCATGCTTTCATGAACTCATGGGAGTTGATCCTGGAACCTAACCCCTGTTTGGCCATTTCTTGGAGCAAGGCCATTTTATGG
GTACCAATTTATCTATGGACTGCCTATCAGACTAACGTTGTTGTTTAA

>Sali3-2- [QGVYTW]

ATGGAATTCGATGCTCAGTCACTCTCTTTTACCATTCTCTTCTCTCTTGGCTCTTGCAGGAGAGGCCATGTCCATGCATCGTACCTGAGGAAGATTATGGGAAGCTGTT
TGGCCAAACACTCCCATTCCCCTGCAGTGCAGAGCTTCTAAAGCCTCTCCCTGCAGGTGTTGAAATCGATGAACTCCCTAAGCAAATTTGATGATACACAGTACCCAAAA
ACATTTCTTATAAAGAAGACCTTCCATCCAGGCAAAACAATGAAAGTACAATTCACCAAGCGTCCCTATGCACAAGGTGTATATACATGGTTAACGGATATTAAAGACACC
TCTAAAGAGGATATAGTTTGAAGAGATATGCATCAAGAAAGAAGCGTTTGGAGGAGAAGAGAAGTTTGTGCAAAAATCCTTGGGAACAGTAATTTGGTTTGGCCATTTCA
AAGCTGGGAAAGAACATTCAGTACTTTCAAGTTCCTTTGTCAATAAGCAAGAGCAATACACTGTGGAAGGAGTGCAGAATCTTGGAGACAAAGCAGTGTATGTCATGGG
CTAAATTCAGAACTGCAGTATTTACTGCCATAAAGTCCGTGAAACAACAGCTTTCATGGTTCATTGGTGGCTGGTATGGAACCAAACTCAGGCCTTGCTGTTTGC
CACTCAGATACTTCTGGAATGAATCATCATGCTTTCATGAACTCATGGGAGTTGATCCTGGAACCTAACCCCTGTTTGGCCATTTCTTGGAGCAAGGCCATTTTATGGGTA
CCCAATTTATCTATGGACTGCCTATCAGACTAACGTTGTTGTTTAA

>Sali3-2- [QAPYGVYTW]

ATGGAATTCGATGCTCAGTCACTCTCTTTTACCATTCTCTTCTCTCTTGGCTCTTGCAGGAGAGGCCATGTCCATGCATCGTACCTGAGGAAGATTATGGGAAGCTGTT
TGGCCAAACACTCCCATTCCCCTGCAGTGCAGAGCTTCTAAAGCCTCTCCCTGCAGGTGTTGAAATCGATGAACTCCCTAAGCAAATTTGATGATACACAGTACCCAAAA
ACATTTCTTATAAAGAAGACCTTCCATCCAGGCAAAACAATGAAAGTACAATTCACCAAGCGTCCCTATGCACAAGCACCTTATGGTGTATATACATGGTTAACGGATATT
AAAGACACCTCTAAAGAAGGATATAGTTTGAAGAGATATGCATCAAGAAAGAAGCGTTTGGAGGAGAAGAGAAGTTTGTGCAAAAATCCTTGGGAACAGTAATTTGGTTT
GCCATTTCAAAGCTGGGAAAGAACATTCAGTACTTTCAAGTTCCTTTGTCAATAAGCAAGAGCAATACACTGTGGAAGGAGTGCAGAATCTTGGAGACAAAGCAGTGTATG
TGTGATGGGCTAAATTCAGAACTGCAGTATTTTACTGCCATAAAGTCCGTGAAACAACAGCTTTCATGGTTCATTGGTGGCTGGTATGGAACCAAACTCAGGCCTT
GCTGTTTGGCACTCAGATACTTCTGGAATGAATCATCATGCTTTCATGAACTCATGGGAGTTGATCCTGGAACCTAACCCCTGTTTGGCCATTTCTTGGAGCAAGGCCATT
TTATGGGTACCAATTTATCTATGGACTGCCTATCAGACTAACGTTGTTGTTTAA

Purification and structure elucidation of lyciumins

For lyciumin A, B and D isolation, *Lycium barbarum* roots (100 g wet weight) were ground with a tissue homogenizer and extracted for 16 h with methanol shaking at 225 rpm and 37 °C. For lyciumin C isolation, amaranth grain (4.5 kg) was ground in a tissue homogenizer and extracted for 16 h with methanol shaking at 225 rpm and 37 °C. Methanol extracts were filtered and dried *in vacuo*. Dried methanol extracts were resuspended in water and partitioned twice with hexane and twice with ethyl acetate and then extracted twice with n-butanol. n-butanol extracts were dried *in vacuo*. Dried n-butanol extracts were resuspended in 10% methanol and separated by flash liquid chromatography with Sephadex LH20 as a stationary phase and a gradient of 10-100% methanol as a mobile phase. Fractions were collected with a fraction collector and analyzed for lyciumin content by LC-QQQ-MS with the following LC-MS settings: LC – Phenomenex Kinetex® 2.6 µm C18 reverse phase 100 Å 150 x 3 mm LC column, LC gradient: solvent A – 0.1% formic acid, solvent B – acetonitrile (0.1% formic acid), 0.5 mL/min, 0-1 min: 5% B, 1-8 min: 5-95% B, 8-10 min: 95% B, 10-15 min: 5% B, MS – positive ion mode, Full MS: Lyciumin A/B/D - 860-920 m/z, Lyciumin C/I - 950-1010 m/z. LH20 fractions with lyciumins were combined, dried *in vacuo*, resuspended in 10% acetonitrile (0.1% trifluoroacetic acid) and subjected to preparative HPLC with a Phenomenex Kinetex® 5 µm C18 reverse phase 100 Å 150 x 21.2 mm LC column as a stationary phase for two rounds of separation. LC settings were as follows: solvent A – 0.1% trifluoroacetic acid, solvent B – acetonitrile (0.1% trifluoroacetic acid), 10 mL/min, Lyciumin A (20 mg) – 1.LC: 0-3 min: 10% B, 3-43 min: 10-50% B, 43-45 min: 50-95% B, 45-48 min: 95% B, 48-49 min: 95-10% B, 49-69 min: 10% B, 2.LC: 0-5 min: 35% B, 5-35 min: 35-50% B, 35-38 min: 50-95% B, 38-40 min: 95% B, 40-40.1 min: 95-35% B, 40.1-60 min: 35% B, Lyciumin B (13 mg) – 1.LC: 0-3 min: 20% B, 3-48 min: 20-40% B, 48-50 min: 40-95% B, 50-54 min: 95% B, 54-55 min: 95-20% B, 55-70 min: 20% B, 2.LC: 0-3 min: 30% B, 3-35 min: 30-45% B, 35-38 min: 45-95% B, 38-40 min: 95% B, 40-40.1 min: 95-30% B, 40.1-60 min: 30% B, Lyciumin C – 1.LC: 0-3 min: 10% B, 3-43 min: 10-50% B, 43-45 min: 50-95% B, 45-48 min: 95% B, 48-49 min: 95-10% B, 49-69 min: 10% B, 2.LC: 0-3 min: 40% B, 3-48 min: 40-55% B, 48-50 min: 55-95% B, 50-54 min: 95% B, 54-55 min: 95-40%, 55-70 min: 40% B, Lyciumin D (5 mg) – 1.LC: 0-3 min: 20% B, 3-48 min: 20-40% B, 48-50 min: 40-95% B, 50-54 min: 95% B, 54-55 min: 95-20% B, 55-70 min: 20% B, 2.LC: 0-3 min: 30% B, 3-48 min: 30-50% B, 48-50 min: 50-95% B, 50-54 min: 95% B, 54-55 min: 95-30% B, 55-70 min: 30% B, Lyciumin I – 1.LC: 0-3 min: 20% B, 3-48min: 20-

50% B, 48-50 min: 50-95% B, 50-54 min: 95% B, 54-55 min: 95-20% B, 55-70min: 20% B, 2.LC: 0-3 min: 25% B, 3-48 min: 25-45% B, 48-50 min: 45-95% B, 50-54 min: 95% B, 54-55 min: 95-25% B, 55-70min: 25% B. Preparative HPLC fractions with lyciumin C and lyciumin I, respectively, were combined, dried *in vacuo*, resuspended in 30% acetonitrile (0.1% trifluoroacetic acid) and subjected to semipreparative HPLC with a Phenomenex Kinetex® 5 µm C18 reverse phase 100 Å 250 x 10 mm LC column as a stationary phase. LC settings were as follows: Solvent A – 0.1% trifluoroacetic acid, solvent B – acetonitrile (0.1% trifluoroacetic acid), 1.5 mL/min, Lyciumin C (25 mg) - 0-5 min: 40% B, 5-15 min: 40-42% B, 15-17 min: 42-95% B, 17-20 min, 95% B, 20-20.1 min: 95-40% B, and lyciumin I (2.5 mg) - 0-5 min: 30% B, 5-30 min: 30-35% B, 30-32 min: 35-95% B, 32-36 min: 95% B, 36-40 min: 95-30% B, 40-60min: 30% B. For NMR analysis, lyciumin A, B, C, D and I were each dissolved in DMSO-d₆. Lyciumin A was analyzed for ¹H and ¹³C NMR data, lyciumin B, D and C were analyzed for ¹H NMR data. Lyciumin I was analyzed for ¹H NMR, ¹H-¹H COSY, ¹H-¹H TOCSY, HSQC, HMBC and ROESY data. NMR data was analyzed with TopSpin software (v3.5) from Bruker. Stereochemistry of crosslinked glycine α-carbons at the fourth position of lyciumins was inferred as (*R*) based on lyciumin A analysis (8) and same ROESY correlations of lyciumin I glycine-Hα as reported for lyciumin A (8). Stereochemistry of other amino acids of lyciumin I was inferred as (*L*)-amino acids because of its ribosomal biosynthesis and (*L*)-amino acid stereochemistry in all reported lyciumins (8-10).

Gene expression analysis of characterized lyciumin precursors

Gene expression of characterized lyciumin precursors was estimated by mapping raw sequencing reads to *de novo* assembled transcriptomes using RSEM (11). For *Solanum tuberosum*, gene expression of lyciumin precursor *PGSC0003DMG400047074* was analyzed in 16 tissue samples (NCBI SRA datasets: ERR029909, ERR029910, ERR029911, ERR029912, ERR029913, ERR029914, ERR029915, ERR029916, ERR029917, ERR029918, ERR029919, ERR029920, ERR029921, ERR029922, ERR029923, ERR029924) (12) by RSEM against the combined *de novo* Trinity (13)-assembled transcriptome of all 16 samples (Figure S24). For *Amaranthus hypochondriacus*, gene expression of lyciumin precursor *AHYPO_007393-RA* was analyzed in eight tissues and conditions (NCBI SRA: SRR1598916, SRR1598915, SRR1598914, SRR1598913, SRR1598912, SRR1598911, SRR1598910, SRR1598909) by RSEM against the combined *de novo* Trinity-assembled transcriptome of all eight samples (Figure S24). For *Chenopodium quinoa*, gene expression of lyciumin precursor *AUR62017095* was analyzed in 15 tissue samples (NCBI SRA: SRR5974430, SRR5974427, SRR5974436, SRR5974438, SRR5974437, SRR5974435, SRR5974432, SRR5974433, SRR5974425, SRR5974426, SRR5974424, SRR5974431, SRR5974428, SRR5974429, SRR5974434) against the combined *de novo* Trinity-assembled transcriptome of all 15 samples (Figure S24). For *Medicago truncatula*, gene expression of lyciumin precursor *Medtr2g081610* was assessed by the eFP bar.utoronto.ca webbrowser (14) of gene expression data from *Medicago truncatula* RNA-seq dataset (15) and displayed (Figure S24). For *Glycine max*, gene expression of lyciumin precursors *Sali3-2* and *Glyma.12G217300* was assessed by the eFP bar.utoronto.ca webbrowser (14) of gene expression data from *Glycine max* RNA-seq datasets (16,17) and displayed (Figure S24).

Glutamine cyclotransferase co-expression assays with *LbaLycA* in *Nicotiana benthamiana*

Glutamine cyclotransferase *LbaQC* was characterized as the closest homolog of *Chenopodium quinoa* glutamine cyclotransferase (AUR62017096, Phytozome v12.1) by blastp search of *L. barbarum* root transcriptome on an internal Blast server (18). *LbaQC* was synthesized as a gBlock® (ATGGTTTCTTCTACTTCATATCTACCTACCAATCACACAAAATGCCTCTGCTAAATCCAAGGTTTCTA GTCATAAGCTTGATTGTTCTACTGAGCATCACCGTATTCAGAGAAGCTGAAGCATCATATAGAGTTTAC AAAGTCAAAGTAGTCAATGAATTCCCTCACGACCCCAAGCCTACACTCAGGGGCTTCTCTATGCAGA AAATAATACACTCTTTGAATCAACTGGACTTTACGGACGTTTCATCTGTTTCGAAAAGTTGCATTGCTGGA CGGTAAGGTTGAGAGACTTCATGAAATGGAGTCTTCTTACTTTGGAGAGGGTCTAACTCTTCTTGGTGA GAGGTTGTTCCAACATAACATGGTTGCTGGATACAGGTTTTCATATATGATCGATACAACTTCAGCAAATT CAAAAAGTTTACTCATCACATGCAAGATGGTTGGGGATTGGCAACCGATGGGAAAGTACTTTTTGGAA GTGATGGAACATCAACATTATATAAGATTGACCCTAAAACAATGAAAGTCATCAGAAAACAAGTTGTC AAGTCTCAAGGCATGAAGTGCCTACCTGAATGAGCTGGAGTATGTGAAAGCTGAAGTCTGGGCAA

ATGTTTATGTGACTGATTGCATTGCTAGAAATTCACCAAAAGATGGCACTGTGATCGGGTGGATTCTCC TTCAATCTCTAAGAGAAGAGTTAATATCAAGAGGATATAAGGACTTCGAGGTCCTGAATGGAATCGCA TGGGACAGAGATGGTGACCGTATTTTTGTGACAGGGAACTATGGCCAAAGCTCTTTGAGATCAAGTT GCTCCCCCTCACACCGAATGATCCATTGGCTGGAGAAATCAATAACTTGTGCATCCCGAAAACCAGTT TTCTCTTGGAATTTAG) with a 5'-adapter (tgcccaaatcgcgaccggt) and a 3'-adapter (ctcaggcctttaactctgg) for Gibson assembly (19). pEAQ-HT (20) was digested by AgeI and XhoI restriction enzymes and the *LbaQC* gBlock® was cloned into linearized pEAQ-HT with Gibson Assembly Master Mix (New England Biolabs). pEAQ-HT-*LbaQC* was verified by Sanger sequencing. For glutamine cyclotransferase co-expression assays, pEAQ-HT-*LbaQC* and pEAQ-HT-*LbaLycA* were transformed into *Agrobacterium tumefaciens* LBA4404 for heterologous expression as described above. For co-expression assay, leaves of three plants of *Nicotiana benthamiana* (six week old) were infiltrated with a 1:1 mixture of resuspended *A. tumefaciens* LBA4404 pEAQ-HT-*LbaQC* (OD 0.8) and *A. tumefaciens* LBA4404 pEAQ-HT-*LbaLycA* (OD 0.8). For *LbaLycA* control expression without *LbaQC*, leaves of three plants of *Nicotiana benthamiana* (six week old) were infiltrated with resuspended *A. tumefaciens* LBA4404 pEAQ-HT-*LbaLycA* (OD 0.4). Infiltrated plants were cultivated as described before for six days for heterologous expression. After six days, leaves of three plants of the *LbaQC*-*LbaLycA* co-expression and leaves of three plants of *LbaLycA* expression control were collected and freeze-dried. For comparative chemotyping of [Gln1]-lyciumin B, [Gln1]-lyciumin D, lyciumin B and lyciumin D, peptides were extracted from 0.1 g of freeze-dried tobacco leaves as described above for peptide chemotyping from the *LbaQC*-*LbaLycA* co-expression plants and from the *LbaLycA* expression plants. Peptide extracts were subjected to low resolution MS analysis by selected-ion monitoring (SIM) of masses of [Gln1]-lyciumins and lyciumins with the following LC-MS parameters: LC – Phenomenex Kinetex® 2.6 µm C18 reverse phase 100 Å 150 x 3 mm LC column, LC gradient: solvent A – 0.1% formic acid, solvent B – acetonitrile (0.1% formic acid), 0.5 mL/min, 0-1 min: 5% B, 1-8 min: 5-95% B, 8-10 min: 95% B, 10-15 min: 5% B, MS – positive ion mode, SIM: 896.8-897.8 m/z (lyciumin B), 899.8-900.8 m/z (lyciumin D), 913.8-914.8 m/z ([Gln1]-lyciumin B), 916.8-917.8 m/z ([Gln1]-lyciumin D). Lyciumin and [Gln1]-lyciumin ion abundance values were determined by peak area integration from each peptide SIM chromatogram in QualBrowser in the Thermo Xcalibur software package (version 3.0.63, ThermoScientific).

LbaLycA-based lyciumin production in *Nicotiana benthamiana* in comparison to source plant extraction

LbaLycA precursors with one, five or ten core peptide repeats of lyciumin B (QPWGVGSW) were designed manually by combination of different spacer (non-core peptide) sequences from Solanaceae lyciumin precursors with multiple core peptides with lyciumin B core peptide sequences and synthesized as gBlocks® with a 5'-adapter (tgcccaaatcgcgaccggt) and a 3'-adapter (ctcaggcctttaactctgg) for Gibson assembly (19). pEAQ-HT was digested by AgeI and XhoI restriction enzymes and the *LbaLycA* gBlocks® were cloned into linearized pEAQ-HT with Gibson Assembly Master Mix (New England Biolabs). pEAQ-HT-*LycA*-1x/5x/10x-QPWGVGSW were verified by Sanger sequencing. For expression assays, pEAQ-HT-*LycA*-1x-QPWGVGSW, pEAQ-HT-*LycA*-5x-QPWGVGSW or pEAQ-HT-*LycA*-10x-QPWGVGSW were transformed into *Agrobacterium tumefaciens* LBA4404 for heterologous expression as described above. Multiple leaves of three plants of *Nicotiana benthamiana* (six week old) were infiltrated with resuspended *A. tumefaciens* LBA4404 pEAQ-HT-*LycA*-1x-QPWGVGSW, pEAQ-HT-*LycA*-5x-QPWGVGSW or pEAQ-HT-*LycA*-10x-QPWGVGSW (OD 0.8). Infiltrated plants were cultivated as described before for six days for heterologous expression. After six days, infiltrated leaves of the three plants were collected and freeze-dried. For source plant extraction, roots of three *Lycium barbarum* plants (one year old) were collected and freeze-dried. For comparative lyciumin B chemotyping, 0.1 g of freeze-dried leaves of each *N. benthamiana* plant and 0.1 g of freeze-dried roots were extracted as described above. Peptide extracts were subjected to low resolution MS analysis by selected-ion monitoring (SIM) of lyciumin B with the following LC-MS parameters: LC – Phenomenex Kinetex® 2.6 µm C18 reverse phase 100 Å 150 x 3 mm LC column, LC gradient: solvent A – 0.1% formic acid, solvent B – acetonitrile (0.1% formic acid), 0.5 mL/min, 0-1 min: 5% B, 1-8 min: 5-95% B, 8-10 min: 95% B, 10-15 min: 5% B, MS – positive ion mode, SIM: 896.8-897.8 m/z (lyciumin B). Lyciumin B ion abundance values were determined by peak area integration from each peptide SIM chromatogram in QualBrowser in the Thermo Xcalibur software package (version 3.0.63, ThermoScientific).

>LycA-1x-QPWGVGSW
ATGGAGTTGCATCACCATTACTTCTTCATACTTCTTTCTCTTGTCTTTATAGCAAGTCATGCAGCTAATTTATCTCCTGAGGTGTATTGGAAAGTCAAGCTGCCAACACT
CCTATGCCAGACCCATTAAAGGATGCTCTACACTATTCTGAAGCCTCCGAGGGTGACGTTTCAACAAGTTGCGCCAACCATGGGGAGTGGGTTCTGGTATAACTGCTTACA
AAGAAAGATGTTAATGAAACCTCCAGTCCACCCCTACTTTTGTAAACAGATTTACATCAAGGAAAAAGATGAATCTTCCATCTCAAAAAATTATAATCCAGCTCCC
ATTTTGCCTCGCAAAGTTGCAGATTCCATCCCTTCTCATCAGACAAGATTGAAGAAATTTCAAAGCACTTTTCCATTGATAAGGACTCAGAGGGGGTAAAAATGATCAAG
AAAACATATAAAGATGTGTGAGGAGCAAGCGGTAATGGCCGAGAAGAAATATTGTGCCACTTCTTGAATCAATGGTTGATTTACCTCATCTTATCTGGGAACAAATAAT
ATTATAGCACTTCCACTTTAGTAGAGAAGGAACTCCAGAGTGCAAAATATATACCATCGAAGAAGTGAAGAGAAAGCAAAATGGCAAAGCGGTGATATGCCAAAGTG
GCTTACCCGATGCGATACATTATTGCCATAGTGTAGGAAGCACAAGGACCTTTATGGTCTCAATGGTGGGTTCTGATGGAACAAAAGTTAATGCAGTATCAGAGTGTCTAT
GAGGATACGACCCATGAACCTAAGGCATTGCCTTTTCAATTGCTCAACGTTAAGCCAGGAGATAAACCTATTGTGCCATTTTCAATTTGGATGATCAGATTGCCTTAGTT
CCTTCTCAAGACGCAACTCAAGTGTCTGAAAACTAA

>LycA-5x-QPWGVGSW
ATGGAGTTGCATCACCATTACTTCTTCATACTTCTTTCTCTTGTCTTTATAGCAAGTCATGCAGCTAATTTATCTCCTGAGGTGTATTGGAAAGTCAAGCTGCCAACACT
CCTATGCCAGACCCATTAAAGGATGCTCTACACTATTCTGAAGCCTCCGAGGGTGACGTTTCAACAAGTTGCGCCAACCATGGGGAGTGGGTTCTGGTATAAGCAGCAAAAC
GAGGTTGATGTTAAAAAATTAGCCAGCCTTGGGGTGTGGGCTCTTGGTATAAGGCTGCCCCAGAGGACGAGCTTCAAAAAATAGCCAGCCCTGGGGCGTGGGATCCTGG
TATCAAGCTGCCAAAGAGAAATGACCTACCAGAATGCCAGCCTGGGGGTAGGGAGTTGGTATCAGGCTGCCCCGAGAACGAGCTTCAAAAGTACGGCAGCCATGG
GGCGTGGAAAGTGTACCAACCCGAGCAGAAAGGGGATTTACACAAGCTCCGATATAAATCTGCTACAAAGAAAGATGTTAATGAAACCTCCAGTCCACCCCTACTTT
TTTGAACAGATTTACATCAAGGAAAAAGATGAATCTTCCATCTCTCAAAAATATAATCCAGCTCCCATTTTGCCTCGCAAAGTTGCAGATTCCATCCCTTCTCATCA
GACAAGATTGAAGAAATTTCAAGCACTTTTCCATTGATAAGGACTCAGAGGGGGTAAAAATGATCAAGAAACTATAAATGTTGTAGGAGCAAGCGGTAATGGCGAG
AAGAAATATTGTGCCACTTCTTAGAATCAATGGTTGATTTACCTCATCTTATCTGGGAACAAAATAATATTATAGCACTTCCACTTTAGTAGAGAAGGAACTCCAGAG
GTGCAAAATATATACCATCGAAGAAGTGAAGAGAAAGCAAAATGGCAAAGCGGTGATATGCCCAAAGTGGTTACCCGATGCGATACATTATTGCCATAGTGTAGGAAGC
ACAAGGACCTTTATGGTCTCAATGGTGGGTTCTGATGGAACAAAAGTTAATGCAGTATCAGAGTGTCTGATGAGGATACTGCACCCATGAACCTAAGGCATTGCCCTTTCAA
TTGCTCAACGTTAAGCCAGGAGATAAACCTATTGTGCCATTTTCAATTTGGATGATCAGATTGCCTTAGTTCTTCTCAAGACGCAACTCAAGTGTCTGAAAACTAA

>LycA-10x-QPWGVGSW
ATGGAGTTGCATCACCATTACTTCTTCATACTTCTTTCTCTTGTCTTTATAGCAAGTCATGCAGCTAATTTATCTCCTGAGGTGTATTGGAAAGTCAAGCTGCCAACACT
CCTATGCCAGACCCATTAAAGGATGCTCTACACTATTCTGAAGCCTCCGAGGGTGACGTTTCAACAAGTTGCGCCAACCATGGGGAGTGGGTTCTGGTATAAGCAGCAAAAC
GAGGTTGATGTTAAAAAATTAGCCAGCCTTGGGGTGTGGGCTCTTGGTATAAGGCTGCCCCAGAGGACGAGCTTCAAAAAATAGCCCAACCCCTGGGGCGTGGGATCCTGG
TATCAAGCTGCCAAAGAGAAATGACCTACCAGAATGCCAGCCTGGGGGTAGGGAGTTGGTATCAGGCTGCCCCGAGAACGAGCTTCAAAAGTACGGCAACCATGG
GGCGTGGAAAGTGTACCAACCCGAGCAGAAAGGGGATTTACACAAGCTCCGACAGCCTTGGGGCGTGGGGAGTTGGTACAAACGACGACCCAGAGAATGAATCCATAAG
TTCCGTTCAACCTGGGGAGTTGGATCGTGGTACAGGGCAGCTACTGAAGGGGACGTTCAAAAAGCTGCGTCAAGCCGTTGGGGCTCGGCTCATGGTACCAAGCAGCAAAACGAG
GGAGACATTAAGAAGCTACGGCAGCCATGGGGAGTCCGCTCTTGGTACAGAGCCGCTACTGAGGGTGACGTTTCAAGAAGTAAAGACGACCCCTGGGGGTGGTGTGGTAT
AATACTGCTACAAAGAAAGATGTTAATGAAACCTCCAGTCCACCCCTACTTTTGTAAACAGATTTACATCAAGGAAAAAGATGAATCTTCCATCTCTCAAAAATTTAT
AATCCAGCTCCCATTTTGCCTCGCAAAGTTGCAGATTCCATCCCTTCTCATCAGACAAGATTGAAGAAATTTCAAAGCACTTTTCCATTGATAAGGACTCAGAGGGGCT
AAAATGATCAAGAAACTATCAAAATGTGTGAGGAGCAAGCGGTAATGGCGAGAAGAAATATTGTGCCACTTCTTAGAATCAATGGTTGATTTACCTCATCTTATCTG
GGAAACAAAATAATATTATAGCACTTCCACTTTAGTAGAGAAGGAACTCCAGAGTGCAAAATATATACCATCGAAGAAGTGAAGAGAAAGCAAAATGGCAAAGCGGTGATA
TGCCACAAAGTGGCTTACCCGATGCGATACATTATTGCCATAGTGTAGGAAGCACAAGGACCTTTATGGTCTCAATGGTGGGTTCTGATGGAACAAAAGTTAATGCAGTA
TCAGAGTGTATGAGGATACTGCACCCATGAACCTAAGGCATTGCCTTTTCAATTTGCTCAACGTTAAGCCAGGAGATAAACCTATTGTGCCATTTTCAATTTGGATGATCAG
ATTGCTTAGTTCTTCTCAAGACGCAACTCAAGTGTCTGAAAACTAA

LbaLycA-based lyciumin precursors with 1, 5 or 10 core peptides of lyciumin B (BURP domain underlined, core peptides in red):

>LycA-1x-QPWGVGSW
MELHHHYFFILLSLAFIASHAANLSPEVYKVKLPNTMPRPRIKDALHYSEASEGDVHKLRL**QPWGVGSW**YNTATKKDVNENLVPVTPYFFETD
LHQGKMNLP**SLK**NYNPAPILPRKVADSI**PFSSDKIEEILKHFS**IDKDSEGA**KMIKKT**IKMCEE**QAGN**GEKKYCAT**SL**ESMVDFTSSYLG**TN**
NIIALSTLVEKETPEVQIY**Y**TIIEVKEKANGKGV**ICH**KVAYPYAIHYCHSVG**STR**TFMVSMVGS**DG**TKVNAVSECH**ED**TAPMNP**KALP**
FQ**LLN**VKPGDK**PI**CH**FILDDQ**IALVPSQ**DATQ**VSEN

>LycA-5x-QPWGVGSW
MELHHHYFFILLSLAFIASHAANLSPEVYKVKLPNTMPRPRIKDALHYSEASEGDVHKLRL**QPWGVGSW**YQAANEGDVK**KLRLQPWGVGSW**YK
AAPEDELHKIR**QPWGVGSW**YQAANENLPRMS**QPWGVGSW**YQAAPENELHKV**RPQPWGVGSW**YQAAEGDLHLK**RLYNTATKKDVNENLVPVTPY**
FFETDLHQG**KMNLP****SLK**NYNPAPILPRKVADSI**PFSSDKIEEILKHFS**IDKDSEGA**KMIKKT**IKMCEE**QAGN**GEKKYCAT**SL**ESMVDFTSS
YLG**TN**NI**I**ALSTLVEKETPEVQIY**Y**TIIEVKEKANGKGV**ICH**KVAYPYAIHYCHSVG**STR**TFMVSMVGS**DG**TKVNAVSECH**ED**TAPMNP**KALP**
FQ**LLN**VKPGDK**PI**CH**FILDDQ**IALVPSQ**DATQ**VSEN

>LycA-10x-QPWGVGSW
MELHHHYFFILLSLAFIASHAANLSPEVYKVKLPNTMPRPRIKDALHYSEASEGDVHKLRL**QPWGVGSW**YQAANEGDVK**KLRLQPWGVGSW**YK
AAPEDELHKIR**QPWGVGSW**YQAANENLPRMS**QPWGVGSW**YQAAPENELHKV**RPQPWGVGSW**YQAAEGDLHLK**RLQPWGVGSW**YNDAPENELH
KFR**QPWGVGSW**YRAATEGDVQ**KLRLQPWGVGSW**YQAANEGDI**KKLRLQPWGVGSW**YRAATEGDVQ**KLRLQPWGVGSW**YNTATKKDVNENLVPVTPY
FFETDLHQG**KMNLP****SLK**NYNPAPILPRKVADSI**PFSSDKIEEILKHFS**IDKDSEGA**KMIKKT**IKMCEE**QAGN**GEKKYCAT**SL**ESMVDFTSS
YLG**TN**NI**I**ALSTLVEKETPEVQIY**Y**TIIEVKEKANGKGV**ICH**KVAYPYAIHYCHSVG**STR**TFMVSMVGS**DG**TKVNAVSECH**ED**TAPMNP**KALP**
FQ**LLN**VKPGDK**PI**CH**FILDDQ**IALVPSQ**DATQ**VSEN

Table S1 | NMR analysis of lyciumin A from *Lycium barbarum* (600 MHz, DMSO-d6).

Residue	C	$\delta(^{13}\text{C})$ [ppm] ^[a]	$\delta(^{13}\text{C})$ [ppm] ^[b]	H	$\delta(^1\text{H})$ (int, m, <i>J</i>) [ppm] ^[c]	$\delta(^1\text{H})$ (int, m, <i>J</i>) [ppm] ^[d]
PyroGlu ¹	α	54.8	54.6	α	4.35 (1H, m)	4.35 (m)
	β	23.9	23.9	β_1	2.28 (1H, m)/1.89 (m)	2.29 (m)/1.9 (m)
	γ	26.5	27.3	γ	2.10 (m)	2.10 (2H, m)
	δ	177.4	177.3	NH	7.9 (m)	n/a
Pro ²	α	59.5	59.4	α	4.35 (1H, m)	4.35 (m)
	β	29.1	29.0	β	2.11 (m)/1.75 (m)	2.16 (m)/1.75 (m)
	γ	24.4	24.2	γ	1.81 (m)/1.69 (m)	1.82 (m)/ 1.68 (m)
	δ	46.2	46.1	δ	3.63 (m)/3.36 (m)	3.60 (m)/3.35 (m)
Tyr ³	α	53.9	53.8	α	4.33 (1H, m)	4.33 (t, 7)
	β	36.3	36.3	β	2.63 (2H, m)	2.63 (2H, d, 7)
	C1	126.6	126.5	H2	6.68 (1H, d, 8.4)	6.63 (1H, d, 8)
	C2	129.9	129.8	H3	6.35 (1H, d, 8.3)	6.38 (1H, d, 8)
	C3	114.8	114.9	OH	7.73 (1H, s)	7.71 (s, OH)
	C4	155.8	155.6	H5	6.35 (1H, d, 8.3)	6.38 (1H, d, 8)
	C5	114.8	114.9	H6	6.68 (1H, d, 8.4)	6.63 (1H, d, 8)
	C6	129.9	129.8	NH	7.94 (m)	7.97 (br d, 7)
Gly ⁴	α	61.0	61.4	α	6.66 (1H, d, 8.4)	6.67 (d, 8)
				NH	9.28 (1H, d, 8.4)	9.37 (d, 8)
Val ⁵	α	51.7	56.3	α	4.00 (1H, t, 8.1)	3.99 (t, 7)
	β	28.9	29.0	β	2.05 (m)	2.03 (m)
	γ_1	19.6	19.2	γ_1	0.91 (3H, d, 6.7)	0.87 (3H, d, 7)
	γ_2	18.9	18.5	γ_2	0.86 (3H, d, 6.8)	0.82 (3H, d, 7)
Gly ⁶	α	43.1	43.5	α	4.02 (1H, m)/ 3.22 (1H, m)	4.08 (dd, 6, 15)/ 3.23 (dd, 6, 15)
				NH	8.53 (1H, t, 6)	8.68 (t, 6)
Ser ⁷	α	55.2	55.4	α	4.22 (1H, dd, 6, 13)	4.11 (dd, 7, 11)
	β	61.7	62.0	β	3.59 (m)/3.4 (m)	3.59 (m)/3.49 (m)
Trp ⁸				NH	7.90 (m)	7.72 (br d, 7)
	α	53.9	53.8	α	4.54 (1H, t)	4.40 (t, 7)
	β	28.6	28.3	β	3.30 (m)/3.16 (m)	3.30 (m)/ 3.01 (m)
	C2	123.8	124.7	H2	7.15 (s)	6.91 (s)
	C3	113.2	111.2	H4	7.53 (1H, d, 8.1)	7.54 (d, 8)
	C4	119.1	119.5	H5	7.08 (1H, t, 7.5)	7.04 (t, 8)
	C5	121.3	121.9	H6	7.18 (1H, t, 7.7)	7.14 (t, 8)
	C6	119.1	118.7	H7	7.37 (1H, d, 8.4)	7.38 (d, 8)
C7	109.4	109.8	NH	7.9 (m)	7.83 (d, 7)	
C=O		166.4	166.5			
		169.4	169.2			
		169.9	169.2			
		170.6	170.6			
		171.5	171.3			
		171.5	171.3			
		171.6	171.5			
	173.0	175.7				

[a] ¹³C NMR data of isolated lyciumin A in DMSO-d6. Values were derived from ¹³C NMR analysis (Figure S3) [b] ¹³C NMR data of lyciumin A in DMSO-d6 from reference 9. [c] ¹H NMR data of isolated lyciumin A in DMSO-d6. Multiplicity m (s=singlet, d=doublet, t=triplet, dd=double doublet, m=multiplet), intensity int, coupling constants *J* in Hertz (Figure S2). [d] ¹H NMR data of lyciumin A in DMSO-d6 from reference 9.

Table S2 | NMR analysis of lyciumin B from *Lycium barbarum* (600 MHz, DMSO-d6).

Residue	H	$\delta(^1\text{H})$ (int, m, J) [ppm] ^[a]	$\delta(^1\text{H})$ (int, m, J) [ppm] ^[b]
PyroGlu ¹	α	4.45 (1H, dd, 7, 13)	4.36 (m)
	β	2.23 (1H, m)/1.83 (1H, m)	2.21 (m)/1.83 (m)
	γ	2.08 (2H, m)	2.08 (2H, m)
	NH	7.89 (1H)	n/a
Pro ²	α	4.34 (1H, m)	4.36 (m)
	β	2.10 (m)/1.97 (m)	2.10 (m)/1.95 (m)
	γ	1.72 (2H, m)	1.72 (2H, m)
	δ	3.63 (m)/3.33 (m)	3.64 (dd, 5, 11)/3.11 (dd, 9, 11)
Trp ³	α	4.34 (1H, m)	4.32 (m)
	β	3.31 (m)/2.9 (1H, m)	3.26 (m)/2.93 (m)
	H2	6.86 (s)	6.87 (s)
	H4	7.53 (1H, d, 7.7)	7.56 (d, 8)
	H5	7.06 (1H, t, 7.5)	7.01 (t, 8)
	H6	7.14 (1H, t, 7.8)	7.08 (t, 8)
	H7	7.28 (1H, t, 8)	7.28 (t, 8)
	N(indole)H	10.68 (1H, s)	10.66 (s)
	NH	7.93 (1H, d, 7.6)	7.86 (d, 6)
Gly ⁴	α	6.61 (d, 8.2)	6.67 (d, 8)
	NH	9.30 (d, 8.1)	9.35 (d, 8)
Val ⁵	α	4.01 (m)	4.01 (t, 7)
	β	2.08 (m)	2.08 (m)
	γ 1	0.90 (3H, d, 6.7)	0.87 (3H, d, 7)
	γ 2	0.86 (3H, d, 6.8)	0.82 (3H, d, 7)
	NH	7.97 (1H, d, 6.3)	7.89 (br d, 7)
Gly ⁶	α	4.04 (m)/3.26 (1H, m)	4.08 (dd, 6, 15)/3.25 (m)
	NH	8.56 (1H, t, 6)	8.55 (br s)
Ser ⁷	α	4.22 (1H, dd, 6.1, 12.7)	4.18 (dd, 6, 12)
	β	3.55 (m)/3.36 (m)	3.55 (m)/3.30 (m)
	NH	7.93 (1H, d, 8)	7.69 (br d, 7)
Trp ⁸	α	4.53 (1H, dt, 3.3, 8.1)	4.52 (m)
	β	3.16 (1H, br s)/2.9 (1H, m)	3.26 (m)/2.93 (br s)
	H2	7.17 (s)	7.55 (s)
	H4	7.37 (d, 7.7)	7.37 (d, 8)
	H5	6.86 (1H, t)	6.86 (t, 8)
	H6	7.00 (1H, t, 7.6)	7.00 (t, 8)
	H7	7.26 (1H, d, 8)	7.26 (d, 8)
	NH	7.71 (s)	7.69 (br d, 7)

[a] ¹H NMR data of isolated lyciumin B in DMSO-d6. Multiplicity m (s=singlet, d=doublet, t=triplet, dd=double doublet, m=multiplet), intensity int, coupling constants J in Hertz (Figure S5). [b] ¹H NMR data of lyciumin B in DMSO-d6 from reference 9.

Table S3 | NMR analysis of lyciumin D from *Lycium barbarum* (600 MHz, DMSO-d6).

Residue	H	$\delta(^1\text{H})$ (int, m, J) [ppm] ^[a]	$\delta(^1\text{H})$ (int, m, J) [ppm] ^[b]
PyroGlu ¹	α	4.50 (1H, m)	4.36 (m)
	β	2.27 (m)/1.88 (m)	2.31 (m)/1.85 (m)
	γ	2.10 (2H, m)	2.10 (2H, m)
	NH	8.32 (1H, d, 7.5)	n/a
Pro ²	α	4.34 (1H, m)	4.36 (m)
	β	2.00 (1H, m)/1.80 (m)	1.97 (m)/1.80 (m)
	γ	1.83 (2H, m)	1.83 (2H, m)
	δ	3.57 (m)	3.58 (m)/3.41 (m)
Tyr ³	α	4.34 (1H, m)	4.33 (m)
	β	2.62 (2H, m)	2.64 (m)
	H2	6.66 (1H, d, 8.4)	6.52 (1H, d, 8)
	H3	6.33 (1H, d, 8.4)	6.35 (1H, d, 8)
	OH	9.05 (s)	7.53 (s)
	H5	6.33 (1H, d, 8.4)	6.35 (1H, d, 8)
	H6	6.66 (1H, d, 8.4)	6.52 (1H, d, 8)
	NH	7.90 (1H, d, 7.9)	7.85 (d, 5)
Gly ⁴	α	6.65 (d, 8.5)	6.67 (d, 9)
	NH	9.38 (1H, d, 8.5)	9.15 (d, 9)
Val ⁵	α	4.01 (m)	4.04 (m)
	β	2.01 (m)	2.10 (m)
	γ_1	0.87 (3H, d, 7)	0.86 (3H, d, 6)
	γ_2	0.85 (3H, d, 7)	0.84 (3H, d, 6)
	NH	7.73 (1H, m)	7.70 (d, 8)
Gly ⁶	α	4.00 (m)/3.30 (m)	4.01 (m)/3.29 (m)
	NH	8.39 (1H, t, 6)	8.30 (t, 5)
Ile ⁷	α	4.12 (1H, dd)	4.07 (m)
	β	1.76 (m)	1.77 (m)
	γ_1	1.48 (1H, m)	1.49 (m)
	γ_2	1.09 (1H, m)	1.14 (m)
	γ (Me)	0.86 (3H, d, 6.6)	0.83 (3H, d, 8)
	δ	0.81 (3H, t, 7.5)	0.82 (3H, t, 8)
	NH	7.39 (1H, d, 8.4)	7.47 (d, 7)
Trp ⁸	α	4.28 (1H, dd, 6.6, 12.8)	4.38 (m)
	β	3.20 (m)/3.12 (m)	3.20 (m)/3.00 (m)
	H2	6.56 (s)	6.84 (s)
	H4	7.54 (1H, d, 7.7)	7.54 (d, 8)
	H5	7.05 (1H)	7.01 (t, 8)
	H6	7.09 (1H, t, 7.5)	7.11 (t, 8)
	H7	7.18 (1H, t, 8.4)	7.39 (t, 8)
	NH	7.72 (1H, s)	7.56 (d, 6)

[a] ¹H NMR data of isolated lyciumin D in DMSO-d6. Multiplicity m (s=singlet, d=doublet, t=triplet, dd=double doublet, m=multiplet), intensity int, coupling constants J in Hertz (Figure S7). [b] ¹H NMR data of lyciumin D in DMSO-d6 from reference 9.

Table S5 | Core peptide sequences from predicted lyciumin precursor genes.

Core peptide	Chemotype	Organism(s)
QPYTVGSW*	Lyciumin A	<i>Amaranthus hypochondriacus</i>
QPYTVFSW*	Lyciumin C	<i>Amaranthus hypochondriacus</i>
QPYGVYTW*	Lyciumin I	<i>Arachis duranensis, Arachis ipaensis, Glycine max, Medicago truncatula, Solanum melongena, Trifolium pratense</i>
QPWTVYVGW		<i>Beta vulgaris</i>
QPWTVAGW		<i>Beta vulgaris</i>
QPFTISAW		<i>Beta vulgaris</i>
QPWTVAAW*	Lyciumin E	<i>Beta vulgaris</i>
QPYGGLTW		<i>Capsicum annuum</i>
QPWGVCLW		<i>Capsicum annuum</i>
QPWGVGSW*	Lyciumin B	<i>Capsicum annuum, Capsicum chinense, Solanum lycopersicum, Solanum melongena, Solanum pennellii, Solanum pimpinellifolium, Solanum tuberosum</i>
QPWGVGFW		<i>Capsicum annuum, Capsicum chinense</i>
QPWGVCFW		<i>Capsicum chinense</i>
QPFTVVGW*	Lyciumin G	<i>Chenopodium quinoa</i>
QPYTVMAW		<i>Chenopodium quinoa</i>
QPYTVWGW*	Lyciumin F	<i>Chenopodium quinoa</i>
QPYTVMGW		<i>Chenopodium quinoa</i>
QPYTVYGW		<i>Chenopodium quinoa</i>
QPFTVFGW		<i>Chenopodium quinoa</i>
QPYTVDGW		<i>Chenopodium quinoa</i>
QPFTVFAW		<i>Glycine max</i>
QPWGVGTW*	Lyciumin H	<i>Glycine max</i>
QPLLFIYW		<i>Medicago truncatula</i>
QPYGVYFW		<i>Medicago truncatula</i>
QPLTTRMW		<i>Medicago truncatula</i>
QPLTSMW		<i>Medicago truncatula</i>
QPITTHMW		<i>Medicago truncatula</i>
QPFGINIW		<i>Medicago truncatula, Trifolium pratense</i>
QPFVLTW		<i>Medicago truncatula</i>
QPFGFESW		<i>Medicago truncatula</i>
QPLPAHKW		<i>Medicago truncatula</i>
QPFRTIGW		<i>Medicago truncatula</i>
QPLGAVKW		<i>Medicago truncatula</i>
QPFGLTW		<i>Medicago truncatula</i>
QPFGVAW		<i>Medicago truncatula</i>
QPFGFRAW		<i>Medicago truncatula</i>
QPFEAHTW		<i>Medicago truncatula</i>
QPWGVYSW		<i>Nicotiana attenuata</i>
QPYGVFAW*	Lyciumin J	<i>Petunia axillaris, Solanum tuberosum</i>
QPFGVFAW		<i>Petunia axillaris</i>
QPYGPFGW		<i>Petunia inflata</i>
QPFGDYVW		<i>Petunia inflata</i>
QPYGVFGW		<i>Petunia inflata, Solanum tuberosum</i>
QPFGVFGW		<i>Petunia inflata, Solanum tuberosum</i>
QPFGVFEW		<i>Petunia inflata</i>
QPAPQLYW		<i>Prunus avium, Prunus persica</i>
QPARQLYW		<i>Prunus persica</i>
QPWGVGAW*	Lyciumin K	<i>Solanum lycopersicum, Solanum pennellii, Solanum pimpinellifolium, Solanum tuberosum</i>
QPWGVYRW		<i>Solanum lycopersicum</i>
QPYGVYRW*	Lyciumin M	<i>Solanum lycopersicum, Solanum pimpinellifolium, Solanum tuberosum</i>
QPYGVYSW		<i>Solanum lycopersicum, Solanum pimpinellifolium</i>
QPWGVNSW		<i>Solanum melongena</i>
QPWGVLRW		<i>Solanum melongena</i>
QPWGVLGW		<i>Solanum melongena</i>
QPFVYRW		<i>Solanum pennellii</i>
QPWGVFERW		<i>Solanum pennellii</i>
QPYGVYSW		<i>Solanum pimpinellifolium</i>
QPWGVDSW		<i>Solanum tuberosum</i>
QPYGVGVW		<i>Solanum tuberosum</i>
QPFVGRW		<i>Solanum tuberosum</i>
QPWGVGRW*	Lyciumin O	<i>Solanum tuberosum</i>
QPFVVAW		<i>Solanum tuberosum</i>
QPYGVLAW		<i>Solanum tuberosum</i>
QPYGVSRW*	Lyciumin N	<i>Solanum tuberosum</i>
QPWGVVAW*	Lyciumin L	<i>Solanum tuberosum</i>
QPYGVFERW		<i>Solanum tuberosum</i>
QPYGVFAW		<i>Solanum tuberosum</i>
QPYGVGDW		<i>Solanum tuberosum</i>
QPLGTWIW		<i>Trifolium pratense</i>
QPFGLAAW		<i>Trifolium pratense</i>
QPSGVYIW		<i>Trifolium pratense</i>
QPATLLAW		<i>Vigna unguiculata</i>

Multi-species peptides	11 (16%)
Single-species peptides	60 (84%)
Total core peptides	71
* Detected peptides	13 (18%)

Table S6 | NMR analysis of lyciumin C from *Amaranthus hypochondriacus* (600 MHz, DMSO-d6).

Residue	H	$\delta(^1\text{H})$ (int, m, J) [ppm] ^[a]	$\delta(^1\text{H})$ (int, m, J) [ppm] ^[b]
PyroGlu ¹	α	4.36 (1H, m)	4.36 (m)
	β	1.79 (m)/2.26 (1H, m)	1.79 (m)/2.24 (m)
	γ	2.10 (2H, m)	2.09 (2H, m)
	NH	8.10 (1H, s)	n/a
Pro ²	α	4.36 (1H, m)	4.36 (m)
	β	1.79 (1H, m)/2.01 (m)	1.79 (m)/1.96 (m)
	γ	1.79 (2H, m)	1.79 (2H, m)
	δ	3.38 (1H, m)/3.64 (1H, t, 7.6)	3.41 (m)/3.73 (t, 7)
Tyr ³	α	4.36 (1H, m)	4.36 (m)
	β	2.68 (2H, m)	2.74 (m)
	H2	6.69 (1H, d, 8.3)	6.68 (1H, d, 8)
	H3	6.35 (1H, d, 8.4)	6.39 (1H, d, 8)
	H5	6.35 (1H, d, 8.4)	6.39 (1H, d, 8)
	H6	6.69 (1H, d, 8.3)	6.68 (1H, d, 8)
	OH	7.27 (1H, m)	7.54 (s, OH)
	NH	8.08 (1H, m)	7.99 (d, 6)
Gly ⁴	α	6.65 (1H, d, 7.9)	6.63 (d, 8)
	NH	9.29 (1H, d, 8.1)	9.15 (d, 8)
Val ⁵	α	4.31 (1H, m)	4.31 (m)
	β	1.86 (1H, m)	1.86 (m)
	γ_1	0.80 (3H, d, 7.2)	0.78 (3H, d, 7)
	γ_2	0.67 (3H, d, 7.4)	0.63 (3H, d, 7)
Phe ⁶	NH	7.98 (1H, m)	7.90 (m)
	α	4.45 (1H, m)	4.36 (m)
	β	2.98 (1H, m)/3.16 (1H, m)	3.01 (m)/3.06 (m)
	H2	7.22 (1H, m)	7.22 (1H, m)
	H3	7.22 (1H, m)	7.22 (1H, m)
	H4	7.22 (1H, m)	7.22 (1H, m)
	H5	7.22 (1H, m)	7.22 (1H, m)
	H6	7.22 (1H, m)	7.22 (1H, m)
Ser ⁷	NH	8.15 (1H, d, 5.9)	8.30 (d, 7)
	α	4.09 (1H, m)	4.16 (m)
	β	3.59 (2H, m)	3.65 (2H, m)
Trp ⁸	NH	7.94 (1H, d, 5.7)	7.85 (d, 7)
	α	4.60 (1H, m)	4.42 (m)
	β	3.16 (1H, m)/3.22 (1H, m)	3.01 (m)/3.09 (m)
	H2	7.16 (1H, s)	7.09 (s)
	H4	7.53 (1H, d, 7.9)	7.51 (d, 8)
	H5	7.07 (1H, t, 7.5)	7.11 (t, 8)
	H6	7.17 (1H, m)	7.17 (t, 8)
	H7	7.41 (1H, d, 8.4)	7.35 (d, 8)
NH	7.75 (1H, s)	7.75 (d, 7)	

[a] ¹H NMR data of isolated lyciumin C in DMSO-d6. Multiplicity m (s=singlet, d=doublet, t=triplet, dd=double doublet, m=multiplet), intensity int, coupling constants J in Hertz (Figure S12). [b] ¹H NMR data of lyciumin C in DMSO-d6 from reference 9.

Table S7 | NMR analysis of lyciumin I from *Glycine max* (600 MHz, DMSO-d₆).

Residue	C	$\delta(^{13}\text{C})$ [ppm] [a]	H	$\delta(^1\text{H})$ (int, m, J) [ppm] [b]	COSY [c]	ROESY [d]	HMBC [e]	
PyroGlu ¹	α	53.6	α	4.35 (1H, m)	PyroGlu ¹ : H β 1/2, Hy, NH	PyroGlu ¹ : H β 1/2, Hy, NH, Pro ² : H δ 1/2	PyroGlu ¹ : C β , Cy, C δ , C=O	
	β	23.6	β 1	1.85 (1H, m)	PyroGlu ¹ : Ha, H β 2, Hy	PyroGlu ¹ : Ha, H β 2, Hy	PyroGlu ¹ : Ca, Cy, C δ , C=O	
	γ	29.0	β 2	2.25 (1H, m)	PyroGlu ¹ : Ha, H β 1, Hy	PyroGlu ¹ : Ha, H β 1, Hy	PyroGlu ¹ : Ca, Cy, C δ , C=O	
	δ	177.2	γ	2.10 (2H, m)	PyroGlu ¹ : H β 1/2	PyroGlu ¹ : Ha, H β 1/2	PyroGlu ¹ : Ca, C β , C δ	
	C=O	171.8	NH	7.75 (1H, s)	PyroGlu ¹ : Ha	PyroGlu ¹ : Ha, Hy, Pro ² : H δ 2	PyroGlu ¹ : Ca, C β , Cy, C δ	
Pro ²	α	59.0	α	4.34 (1H, m)	Pro ² : H β , Hy1/2	Pro ² : H β , Hy1/2, H δ 2	PyroGlu ¹ : C=O, Pro ² : C β , Cy, C δ , C=O	
	β	28.4	β	1.77 (2H, m)	Pro ² : Ha, Hy1/2, H δ 1/2	Pro ² : Ha, Hy1/2, H δ 1/2	Pro ² : Ca, Cy, C δ	
	γ	24.4	γ 1	1.79 (1H, m)	Pro ² : Ha, H β , Hy2, H δ 1/2	Pro ² : Ha, H β , Hy2, H δ 1/2, Val ⁵ : Hy1/2	Pro ² : C β , C δ	
	δ	46.0	γ 2	1.83 (1H, m)	Pro ² : Ha, H β , Hy1, H δ 1/2	Pro ² : Ha, H β , Hy1, H δ 2	Pro ² : C β , C δ	
		C=O	171.4	δ 1	3.38 (1H, m)	Pro ² : H β , Hy1/2, H δ 2	PyroGlu ¹ : Ha, H β 2, Pro ² : H β , Hy1, H δ 2	Pro ² : C β , Cy
			δ 2	3.58 (1H, m)	Pro ² : H β , Hy1/2, H δ 1	PyroGlu ¹ : Ha, NH, Pro ² : Ha, H β , Hy1/2, H δ 1	Pro ² : C β , Cy	
Tyr ³	α	54.5	α	4.35 (1H, m)	Tyr ³ : H β 1/2, NH	Tyr ³ : H β 1/2, H2/6, NH, Gly ⁴ : NH	Pro ² : C=O, Tyr ³ : C β , C=O	
	β	35.8	β 1	2.60 (1H, m)	Tyr ³ : Ha, H β 2	Tyr ³ : Ha, H2/6, NH	Tyr ³ : Ca, C1, C2/6, C=O	
	C1	126.5	β 2	2.70 (1H, m)	Tyr ³ : Ha, H β 1	Tyr ³ : Ha, H2/6	Tyr ³ : Ca, C1, C2/6, C=O	
	C2	129.6	H2	6.68 (1H, d, 8.5)	Tyr ³ : H3	Tyr ³ : Ha, H β , H3/5	Tyr ³ : C β , C3/5, C4, C6	
	C3	114.4	H3	6.35 (1H, d, 8.5)	Tyr ³ : H2	Tyr ³ : H2/6	Tyr ³ : C1, C4, C5	
	C4	155.8	OH	9.18 (1H, br s)	n/a	n/a	n/a	
	C5	114.4	H5	6.35 (1H, d, 8.5)	Tyr ³ : H6	Tyr ³ : H2/6	Tyr ³ : C1, C3, C4	
	C6	129.6	H6	6.68 (1H, d, 8.5)	Tyr ³ : H5	Tyr ³ : Ha, H β , H3/5	Tyr ³ : C β , C2, C3/5, C4	
		C=O	171.4	NH	7.90 (1H, m)	Tyr ³ : Ha	Tyr ³ : Ha, H β 1, Gly ⁴ : NH	Pro ² : C=O
Gly ⁴	α	61.0	α	6.64 (1H, d, 8.3)	Gly ⁴ : NH	Gly ⁴ : NH, Val ⁵ : NH, Trp ⁸ : H2, H4	Tyr ³ : C=O, Gly ⁴ : C=O, Trp ⁸ : C2, C3	
		C=O	166.5	NH	9.28 (1H, d, 8.1)	Gly ⁴ : Ha	Tyr ³ : Ha, NH, Gly ⁴ : Ha, Trp ⁸ : H2, H4	Tyr ³ : C=O
Val ⁵	α	61.4	α	3.68 (1H, t, 7.7)	Val ⁵ : H β , NH	Val ⁵ : H β , Hy1/2, Tyr ⁶ : NH	Gly ⁴ : C=O, Val ⁵ : C β , Cy1/2, C=O	
	β	28.5	β	2.00 (1H, m)	Val ⁵ : Ha, Hy1/2	Val ⁵ : Ha, Hy1/2, Tyr ⁶ : NH, H2/6	Val ⁵ : Ca, Cy1/2, C=O	
	γ 1	19.0	γ 1	0.67 (3H, d, 7.0)	Val ⁵ : H β , Hy2	Pro ² : Hy1, Val ⁵ : Ha, H β , Hy2, Tyr ⁶ : H2/6, H3/5	Val ⁵ : Ca, C β , Cy2	
	γ 2	18.4	γ 2	0.79 (3H, d, 7.0)	Val ⁵ : H β , Hy1	Pro ² : Hy1, Val ⁵ : Ha, H β , Hy1, NH, Tyr ⁶ : H2/6, H3/5, Trp ⁸ : H4	Val ⁵ : Ca, C β , Cy1	
		C=O	170.7	NH	7.91 (1H, d, 6.2)	Val ⁵ : Ha	Gly ⁴ : Ha, Val ⁵ : Ha, H β , Hy2, Tyr ⁶ : Ha	n/a
Tyr ⁶	α	55.7	α	4.31 (1H, m)	Tyr ⁶ : H β 1/2, NH	Val ⁵ : NH, Tyr ⁶ : H β 1/2, H2/6, NH, Thr ⁷ : NH	Tyr ⁶ : C β , C=O	
	β	35.6	β 1	2.91 (1H, m)	Tyr ⁶ : Ha, H β 2	Tyr ⁶ : Ha, H β 2, H2/6, NH, Thr ⁷ : Hy, NH	Tyr ⁶ : Ca, C1, C2/6	
	C1	126.4	β 2	3.12 (1H, m)	Tyr ⁶ : Ha, H β 1	Tyr ⁶ : Ha, H β 1, H2/6, NH, Thr ⁷ : Hy, NH	Tyr ⁶ : Ca, C1, C2/6	
	C2	129.7	H2	7.01 (1H, d, 8.5)	Tyr ⁶ : H3	Val ⁵ : H β , Hy1/2, Tyr ⁶ : Ha, H β 1/2, H3	Tyr ⁶ : C β , C3/5, C4, C6	
	C3	114.7	H3	6.63 (1H, d, 8.5)	Tyr ⁶ : H2	Val ⁵ : Hy1/2, Tyr ⁶ : H2	Tyr ⁶ : C5, C4	
	C4	155.6	OH	9.18 (1H, br s)	n/a	n/a	n/a	
	C5	114.7	H5	6.63 (1H, d, 8.5)	Tyr ⁶ : H6	Val ⁵ : Hy1/2, Tyr ⁶ : H6	Tyr ⁶ : C3, C4	
	C6	129.7	H6	7.01 (1H, d, 8.5)	Tyr ⁶ : H5	Val ⁵ : H β , Hy1/2, Tyr ⁶ : Ha, H β 1/2, H5	Tyr ⁶ : C β , C2, C3/5, C4	
		C=O	171.7	NH	8.02 (1H, d, 7.7)	Tyr ⁶ : Ha	Val ⁵ : Ha, H β , Tyr ⁶ : Ha, H β 1, Trp ⁸ : H4	Val ⁵ : C=O
Thr ⁷	α	60.0	α	4.00 (1H, m)	Thr ⁷ : H β , Hy, NH	Thr ⁷ : H β , Hy, NH, Trp ⁸ : NH	Tyr ⁶ : C=O, Thr ⁷ : C β , Cy, C=O	
	β	66.5	β	4.02 (1H, m)	Thr ⁷ : Ha, Hy, NH	Tyr ⁶ : NH, Thr ⁷ : Ha, Hy, NH	Thr ⁷ : Ca, Cy, C=O	
	γ	19.6	OH	4.84 (1H, m)	n/a	n/a	n/a	
		C=O	169.4	γ	1.10 (3H, d, 6.0)	Thr ⁷ : Ha, H β	Tyr ⁶ : H β 1/2, H2/6, Thr ⁷ : Ha, H β , NH, Trp ⁸ : NH	Thr ⁷ : Ca, C β , C=O
				NH	7.84 (1H, d, 5.0)	Thr ⁷ : Ha, H β	Tyr ⁶ : Ha, H β 1/2, NH, Thr ⁷ : Ha, H β , Hy, Trp ⁸ : H2, NH	Tyr ⁶ : Ca, C=O, Thr ⁷ : C=O
Trp ⁸	α	51.4	α	4.57 (1H, m)	Trp ⁸ : H β 1/2, NH	Trp ⁸ : H β 1/2, H2, H7, NH	Thr ⁷ : C=O, Trp ⁸ : C β , C1, C=O	
	β	26.1	β 1	3.12 (1H, m)	Trp ⁸ : Ha, H β 2	Trp ⁸ : Ha, H7, NH	Trp ⁸ : Ca, C1, C2, C=O	
	C1	111.0	β 2	3.20 (1H, m)	Trp ⁸ : Ha, H β 1	Trp ⁸ : Ha, H7, NH	Trp ⁸ : Ca, C1, C2, C=O	
	C2	125.0	H2	7.33 (1H, s)	Trp ⁸ : H7	Gly ⁴ : Ha, NH, Thr ⁷ : Ha, NH, Trp ⁸ : Ha, H β , NH	Gly ⁴ : Ca, Trp ⁸ : C1, C3, C8	
	C3	135.8	H4	7.40 (1H, d, 8.3)	Trp ⁸ : H2, H4, H5, H6	Gly ⁴ : Ha, NH, Val ⁵ : Hy2, Tyr ⁶ : NH, Trp ⁸ : H5, H6	Trp ⁸ : C1, C3, C6, C8	
	C4	109.6	H5	7.07 (1H, t, 7.5)	Trp ⁸ : H4, H5, H7	Trp ⁸ : H4, H6, H7	Trp ⁸ : C4, C7, C8	
	C5	119.2	H6	7.14 (1H, t, 7.5)	Trp ⁸ : H6, H7	Trp ⁸ : H4, H5, H7	Trp ⁸ : C3, C4, C7	
	C6	121.3	H7	7.52 (1H, d, 7.9)	Trp ⁸ : H6, H7	Trp ⁸ : Ha, H β 1/2, H5, H6	Trp ⁸ : C1, C3, C5, C6, C7, C8	
	C7	118.1	NH	8.10 (1H, d, 7.5)	Trp ⁸ : Ha	Thr ⁷ : Ha, Hy, NH, Trp ⁸ : Ha, H β 1/2, H2	Thr ⁷ : C=O	
		C8	128.0					
		C=O	172.9					

[a] ¹³C NMR data of major conformer of isolated lyciumin I in DMSO-d₆. Values were derived from HSQC and HMBC NMR analyses (Figure S19 & S20), [b] ¹H NMR data of major conformer of isolated lyciumin I in DMSO-d₆. Multiplicity m (s=singlet, d=doublet, t=triplet, dd=double doublet, m=multiplet), intensity int, coupling constants J in Hertz (Figure S16), [c] ¹H-¹H COSY correlations of major conformer of lyciumin I in DMSO-d₆ (Figure S17), [d] ROESY correlations of major conformer of lyciumin I in DMSO-d₆ (Figure S21), [e] HMBC correlations of major conformer of lyciumin I in DMSO-d₆ (Figure S20)

Table S8 | Bioinformatic analysis of lyciumin precursor genes and co-clustered glutamine cyclotransferase genes in genomes of *Beta vulgaris* and *Chenopodium quinoa* (Figure 3C).

Gene	Predicted function	Reference	Gene product length [aa]	Closest functional blastp homolog (organism) [Similarity/Identity, %/ %]
<i>Chenopodium quinoa</i> (v1.0) locus				
AUR62017095-RA (<i>CquBURP1</i>)	BURP domain lyciumin precursor	XP_021740703.1	619	XP_010675925.1 PREDICTED: BURP domain protein USPL1 [<i>Beta vulgaris subsp. vulgaris</i>] [68/57]
AUR62017096-RA	Glutamine cyclotransferase	XP_021740704.1	286	XP_010675927.1 PREDICTED: glutaminyl-peptide cyclotransferase isoform X1 [<i>Beta vulgaris subsp. vulgaris</i>] [80/71]
<i>Beta vulgaris</i> locus (RefBeet-1.2.2)				
LOC104891851 (<i>BvuBURP2</i>)	BURP domain lyciumin precursor	XP_010675925.1	446	XP_010676059.1 PREDICTED: BURP domain protein USPL1-like (<i>Beta vulgaris subsp. vulgaris</i>) [93/89]
LOC104891854	Glutamine cyclotransferase	XP_010675927.1	306	XP_021771347.1 glutaminyl-peptide cyclotransferase-like isoform X1 [<i>Chenopodium quinoa</i>]
LOC104891968 (<i>BvuBURP1</i>)	BURP domain lyciumin precursor	XP_010676059.1	404	XP_010675925.1 PREDICTED: BURP domain protein USPL1 (<i>Beta vulgaris subsp. vulgaris</i>) [93/89]
LOC104891853	Glutamine cyclotransferase	XP_010675926.1	201	XP_021740704.1 glutaminyl-peptide cyclotransferase-like (<i>Chenopodium quinoa</i>) [73/68]

Table S9 | LC-MS dataset accessions (MassIVE, GNPS) (21)

Dataset	Figure	MassIVE dataset accession
Amaranth_grain	Figure S11, S27	MSV000082522
beet_root	Figure S13, S27	MSV000082523
Chenopodium-quinoa-flower	Figure S14, S27	MSV000082525
Eggplant-stem	Figure S22	MSV000082526
Lycium-barbarum-root (LB-root)	Figure 1, S1, S4, S6, S29, S31	MSV000082527
Medicago_truncatula_seed	Figure S23	MSV000082528
Potato_tuber_sprout	Figure S26	MSV000082529
Russett-potato-sprout	Figure S26	MSV000082530
Soy-root	Figure S15	MSV000082532
NB-At-LBA4404-pEAQ-6d	Figure 1, 3	MSV000082533
NB-At-LBA4404-pEAQ-Sali3-2-6d	Figure 4	MSV000082534
NB-LbaLycA-6d	Figure 1, S29, S31	MSV000082536
NB-Sali3-2-QAYGVYTW-6d	Figure 4, S32	MSV000082537
NB-Sali3-2-QGVYTW-6d	Figure 4	MSV000082538
NB-Sali3-2-QPAGVYTW	Figure S33	MSV000082539
NB-Sali3-2-QPFGFFSW	Figure S43	MSV000082540
NB-Sali3-2-QPFGVYTW	Figure S42	MSV000082541
NB-Sali3-2-QPWVGAW	Figure S40	MSV000082542
NB-Sali3-2-QPWVGVTW	Figure S39	MSV000082543
NB-Sali3-2-QPWGVYSW	Figure S44	MSV000082544
NB-Sali3-2-QPWGVYTW	Figure S42	MSV000082545
NB-Sali3-2-QPYAVYTW	Figure S34	MSV000082546
NB-Sali3-2-QPYGAYTW	Figure S35	MSV000082547
NB-Sali3-2-QPYGVATW	Figure S36	MSV000082548
NB-Sali3-2-QPYGVYAW	Figure S37	MSV000082549
NB-Sali3-2-QPYGVYFW	Figure S45	MSV000082550
NB-Sali3-2-QPYGVYTA	Figure 4	MSV000082552
NB-Sali3-2-QPYGVYTAW	Figure 4	MSV000082553
NB-Sali3-2-QPYTVYTW	Figure S38	MSV000082555
NB-Sali3-2-QYGVYTW	Figure 4	MSV000082556
NB-StuBURP-6d	Figure S26	MSV000082557

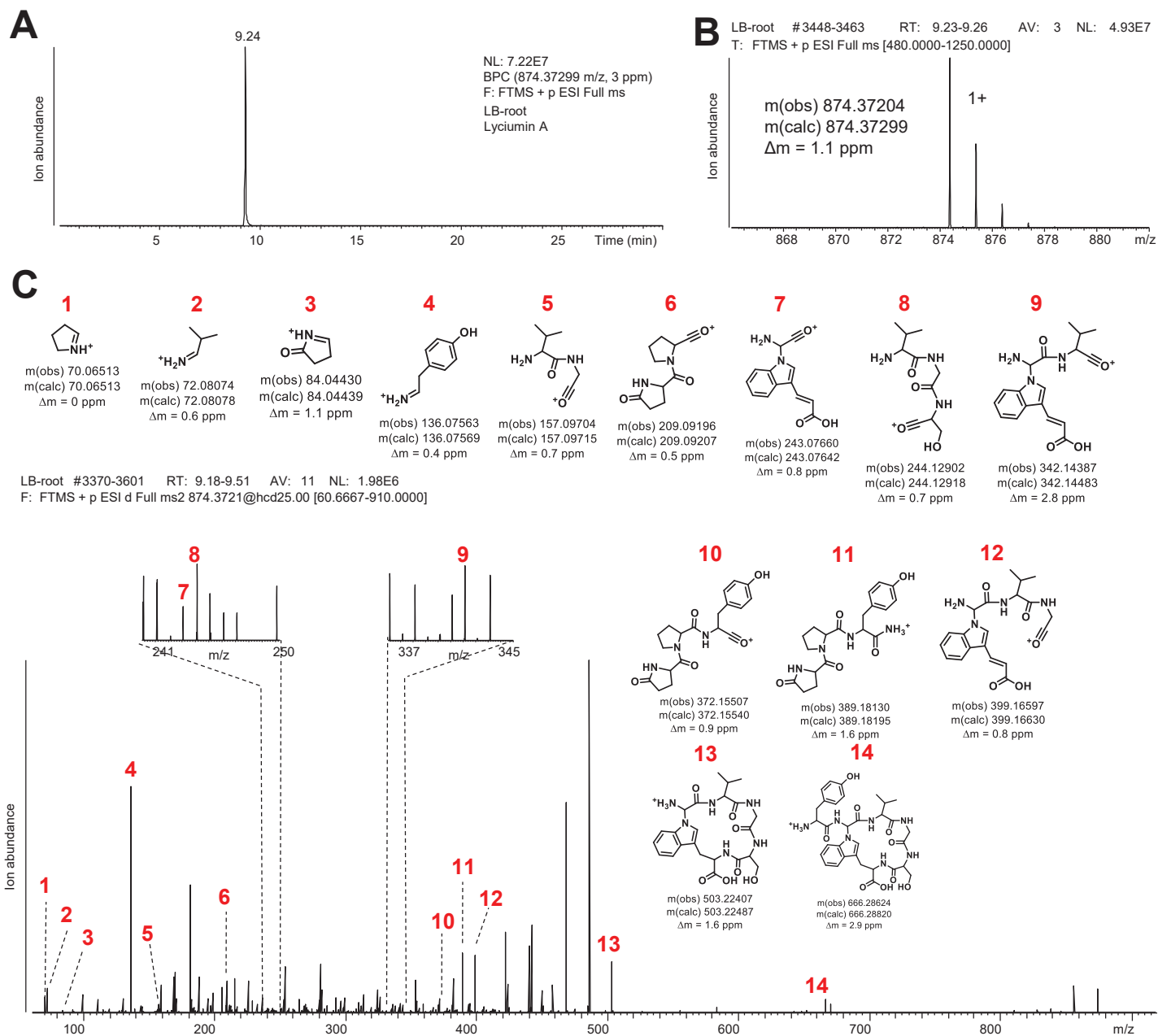
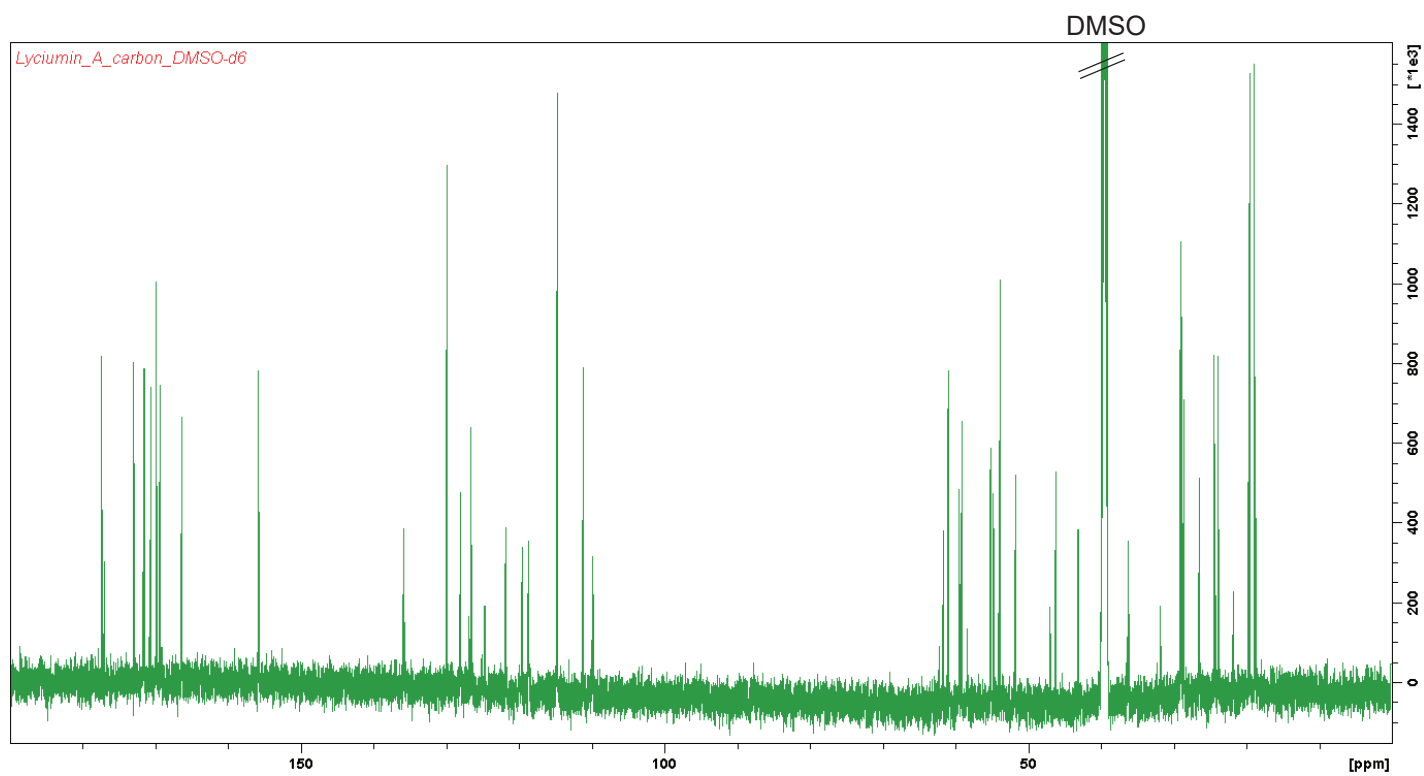
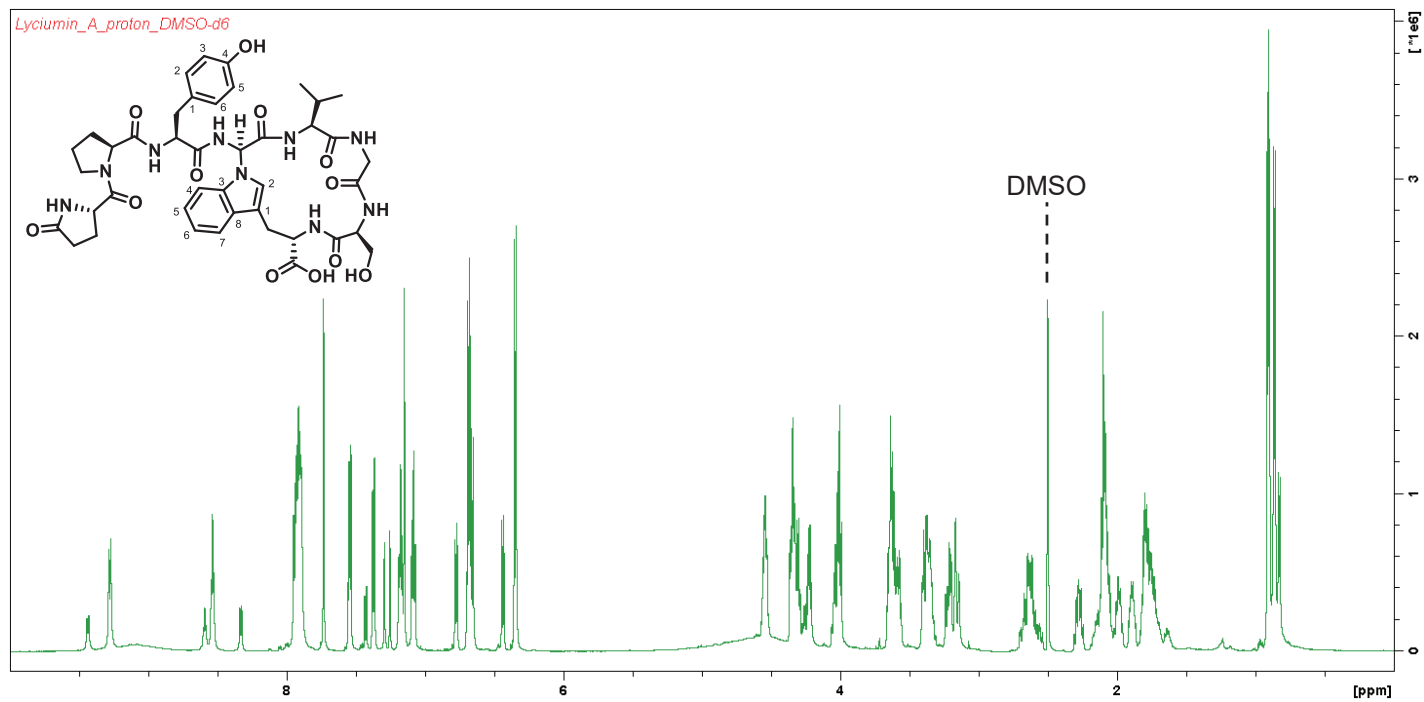


Figure S1 | MS analysis of lyciumin A. (A) LC-MS chemotyping of predicted lyciumin A in peptide extract of *Lycium barbarum* root. **(B)** MS analysis of lyciumin A. **(C)** MS/MS analysis of lyciumin A.



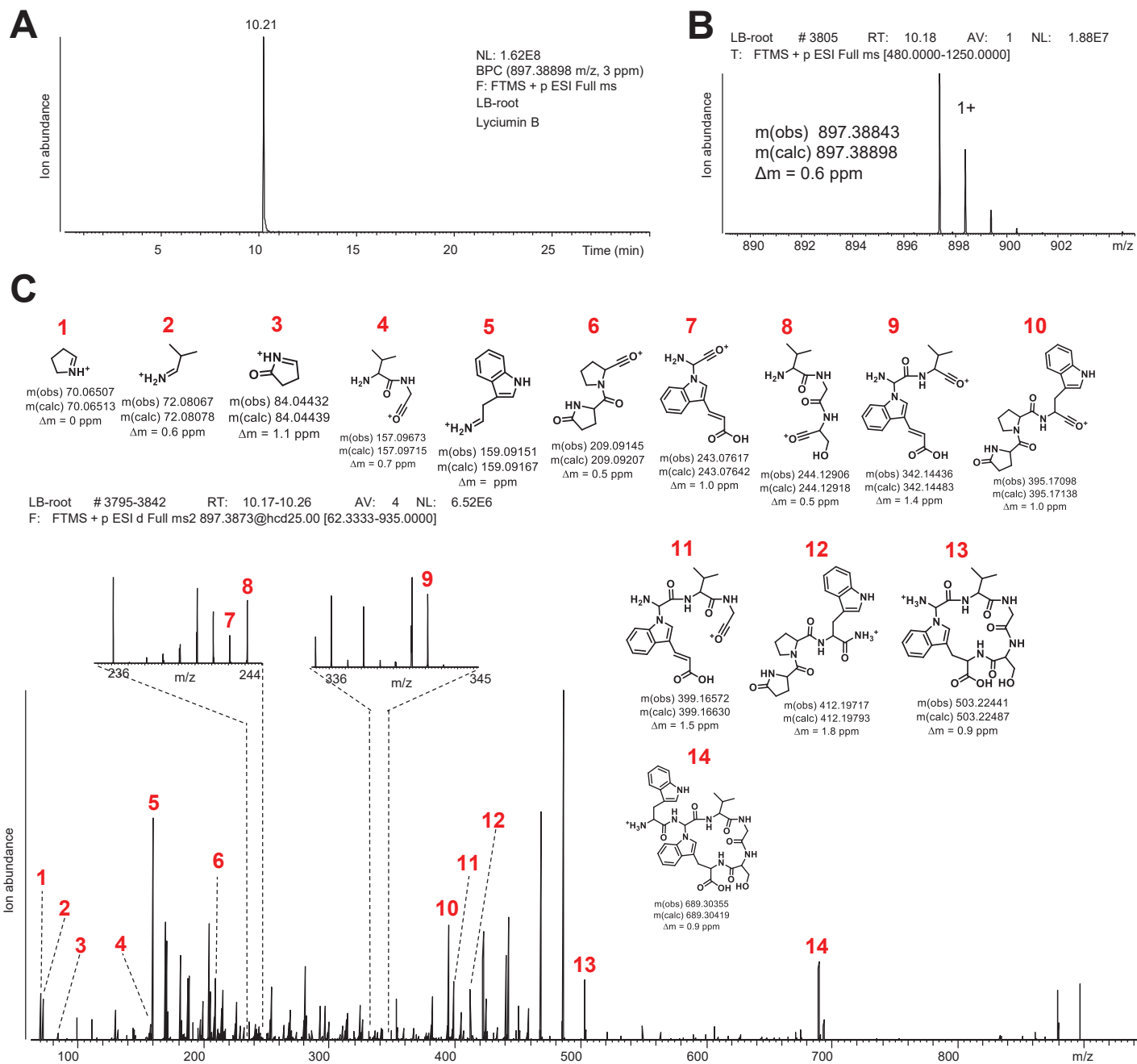


Figure S4 | MS analysis of lyciumin B. (A) LC-MS chemotyping of predicted lyciumin B in peptide extract of *Lycium barbarum* root. (C) MS analysis of lyciumin B. (D) MS/MS analysis of lyciumin B.

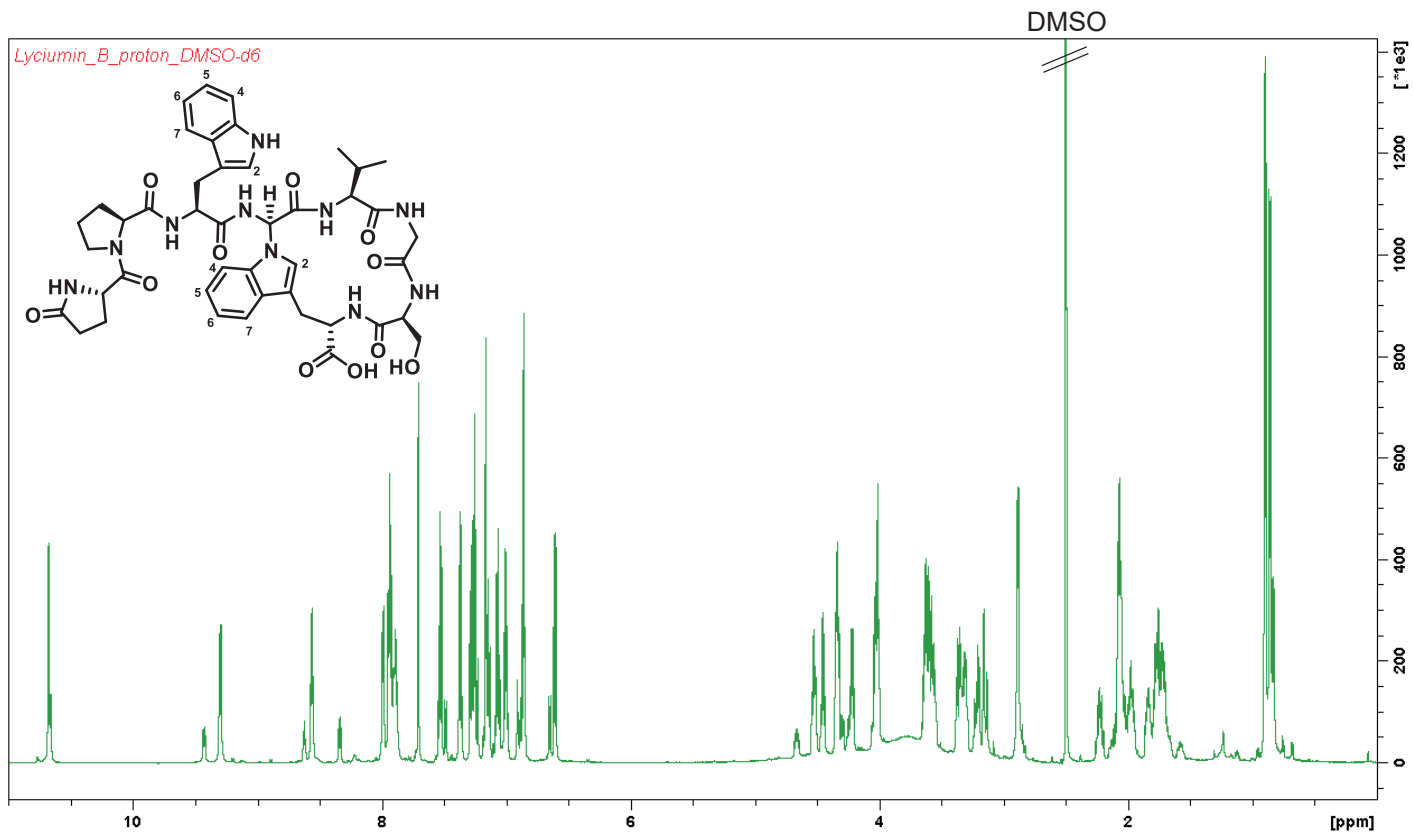


Figure S5 | ^1H NMR spectrum of lyciumin B in DMSO-d₆ (600 MHz).

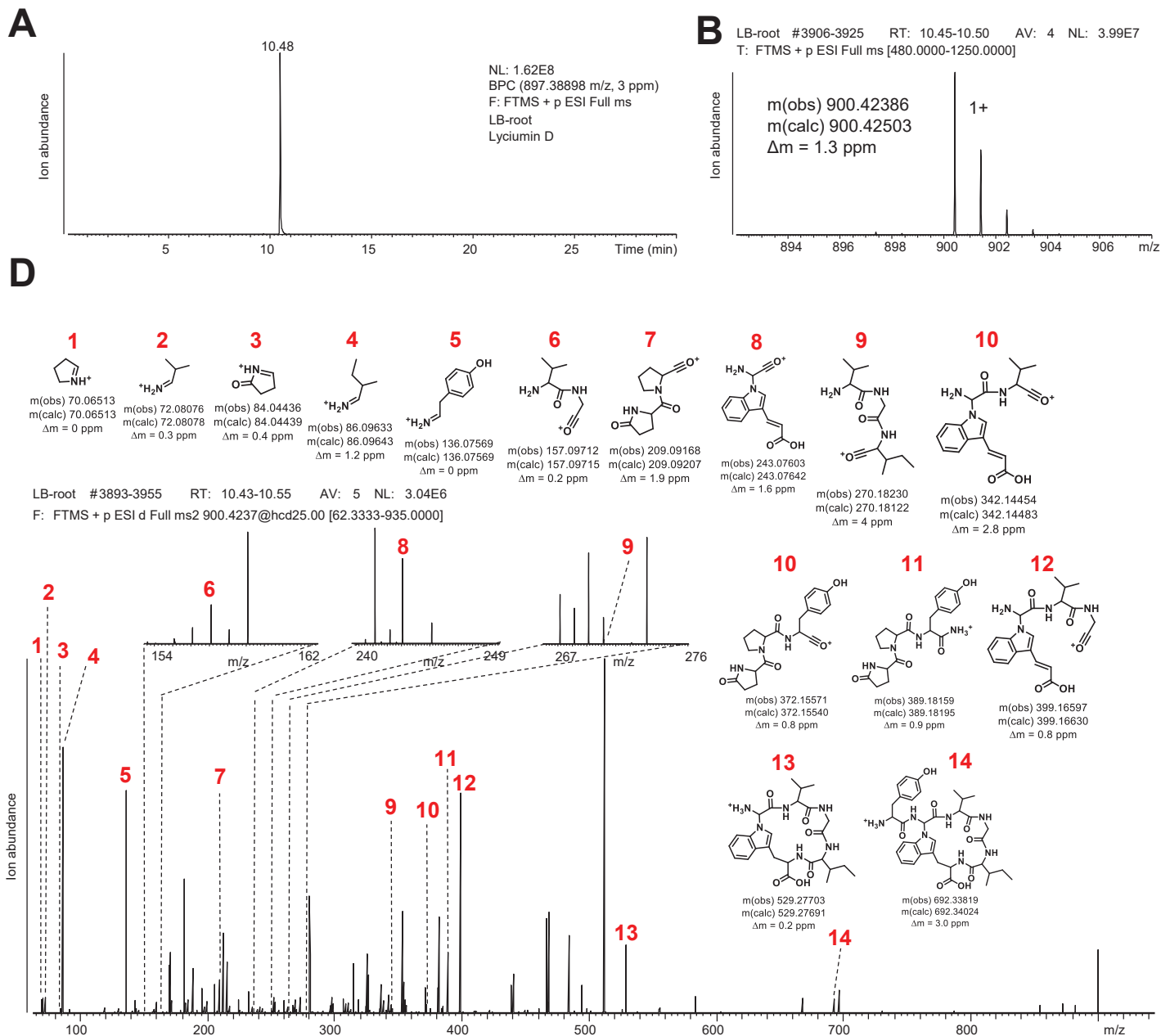


Figure S6 | MS analysis of lyciumin D. (A) Lycium D planar structure. **(B)** LC-MS chemotyping of predicted lyciumin D in peptide extract of *Lycium barbarum* root. **(C)** MS analysis of lyciumin D. **(D)** MS/MS analysis of lyciumin D.

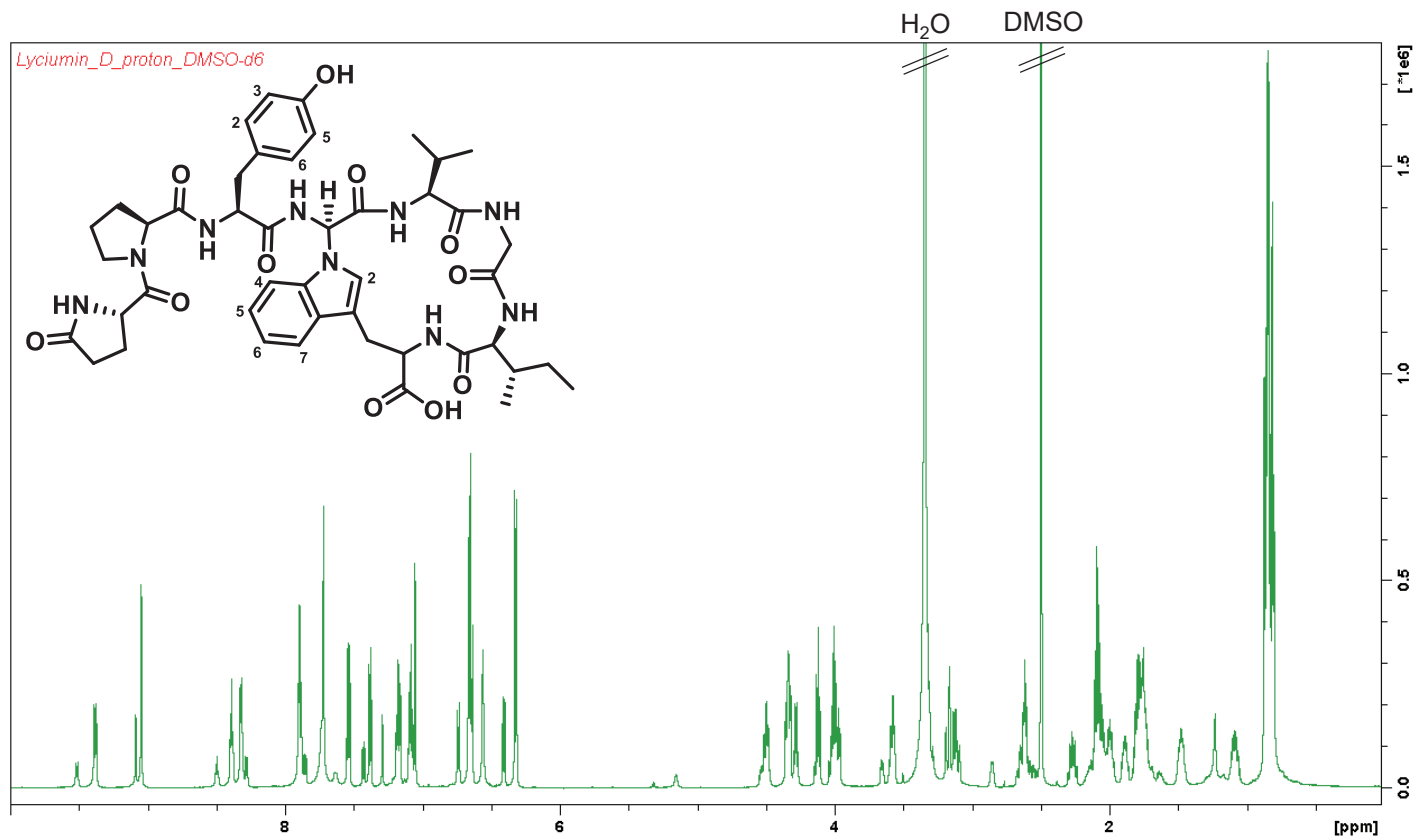


Figure S7 | ¹H NMR spectrum of lyciumin D in DMSO-d₆ (600 MHz).

```

>TRINITY_DN33942_c2_g1_i2|m.67 TRINITY_DN33942_c2_g1_i2|g.67 type:5prime_partial len:297
gc:universal TRINITY_DN33942_c2_g1_i2:2-892(+)
EGDVKKLFPWGVGSWYQAANEGDVKKLRQPYGVGIWYEAANEGQVKKLRQPYGVGSWYNTATKKDVNENLPVTPYFFETDLHQGKKMNLPSL
KNYNPAPILPRKVADSI PFSSDKIEEILKHFSIDKDSEGAKMIKKTIKMCEEQAGNGEKKYCATSLESMDVFTSSYLGTNNIIALSTLVEKET
PEVQIYTIIEVKEKANGKGVICHKVAYPYAIHYCHSVGSTRTFMVMVMSDGTQVNAVSECHEDTAPMNPALPFQLLNVPKPGDKPICHFIELD
DQIALVPSQDATQVSEN
>TRINITY_DN32732_c0_g2_i1|m.98 TRINITY_DN32732_c0_g2_i1|g.98 type:internal len:130
gc:universal TRINITY_DN32732_c0_g2_i1:389-3(-)
GIKQQTRVMLKNYANHGEWVPGIKQQTRVMLKNYTNHGEWVPGIKQQTRVMLKNYPNHGEWVPGIKQQTRVMLKNYANHMELVYGMKQQTRVK
LKKLRQPYGVGSWYQAANEGDVKKIRQPYGVGSWYQ
>TRINITY_DN32732_c0_g2_i3|m.101 TRINITY_DN32732_c0_g2_i3|g.101 type:5prime_partial len:345
gc:universal TRINITY_DN32732_c0_g2_i3:1216-182(-)
WYQAANEGDVKKLRQPYGVGSWYQAANEGDVKKLHQPYGVGSWYQAANEGDVKKLRQPYGVGSWYQAANEGDVKKLRQPYGVGIWYEAANEGQ
VKKLRQPYGVGSWYNTATKKDVNENLPVTPYFFETDLRQGKKMNLPSLKNYNPAPILPRKVADSI PFSSDKIEEILKHFSIDKDSEGAKMIK
TIKMCEEQAGNGEKKYCATSLESMDVFTSSYLGTNNIIALSTLVEKETPEVQIYTIIEVKEKANGKGVICHKVAYPYAIHYCHSVGSTRTFMV
SMVMSDGTQVNAVSECHEDTAPMNPALPFQLLNVPKPGDKPICHFILDDQIALVPSQDATQVSEN

```

Figure S8 | Candidate transcripts of lyciumin precursor peptide gene from *Lycium barbarum* root transcriptome. Predicted lyciumin core peptides are highlighted in green (lyciumin A), blue (lyciumin B) and red (lyciumin D).

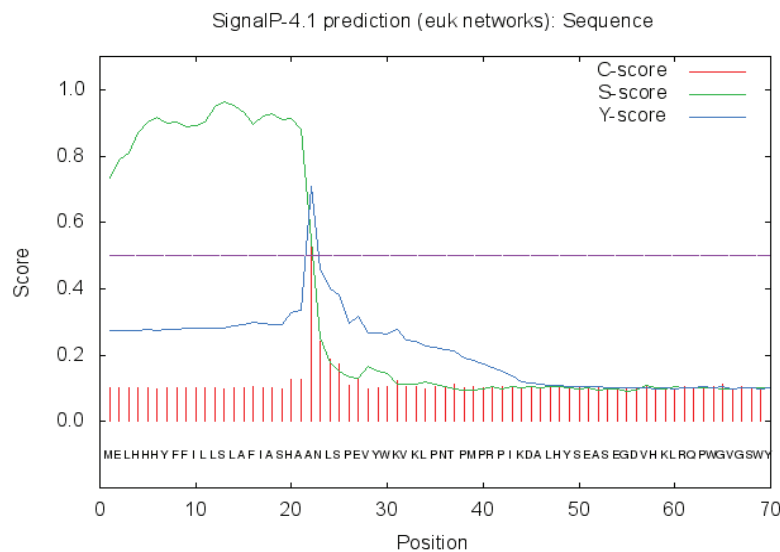


Figure S9 | Signal peptide prediction of LbaLycA with SignalP-4.1.

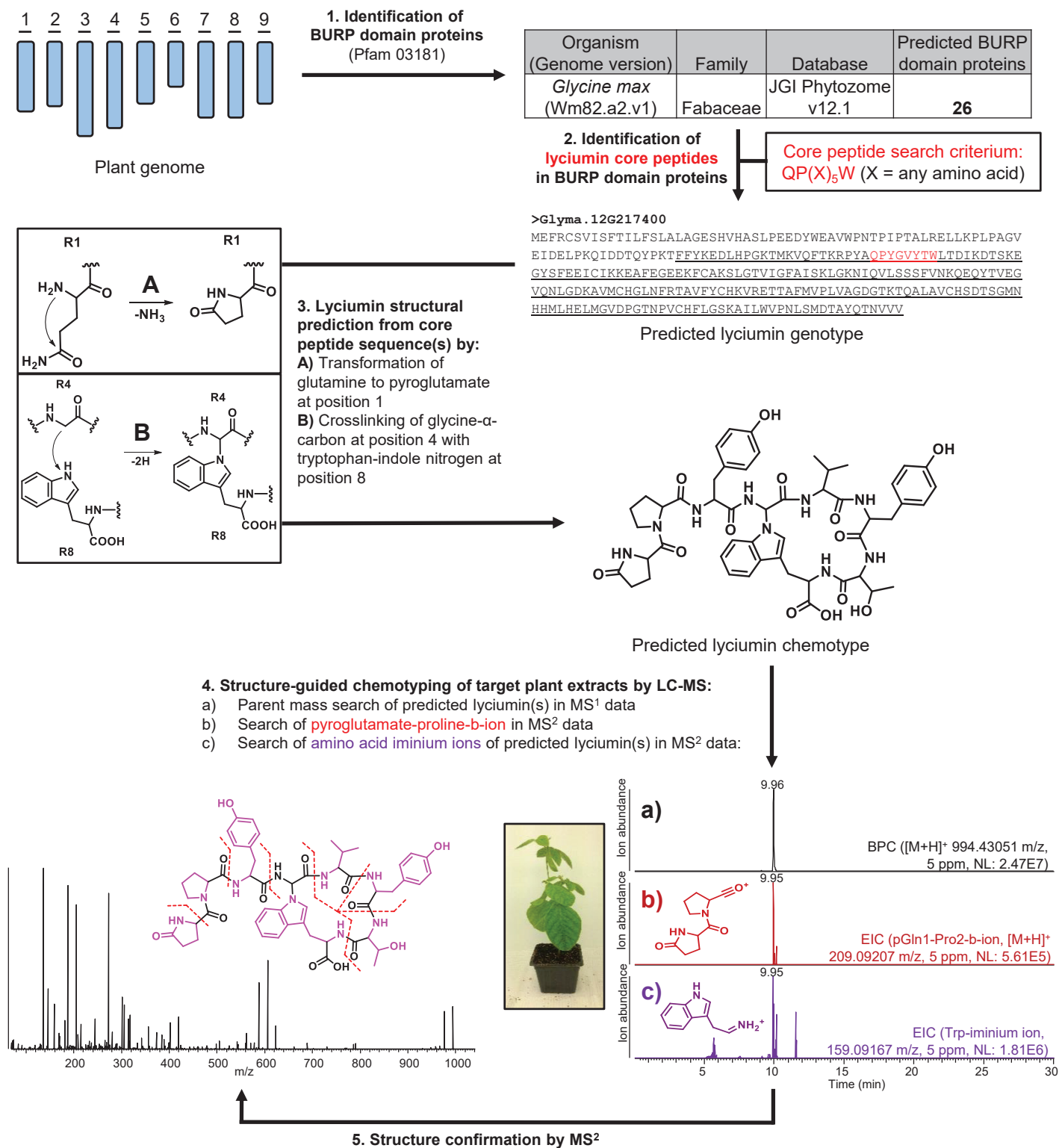


Figure S10 | Precursor gene-guided genome mining workflow for lyciumin discovery.

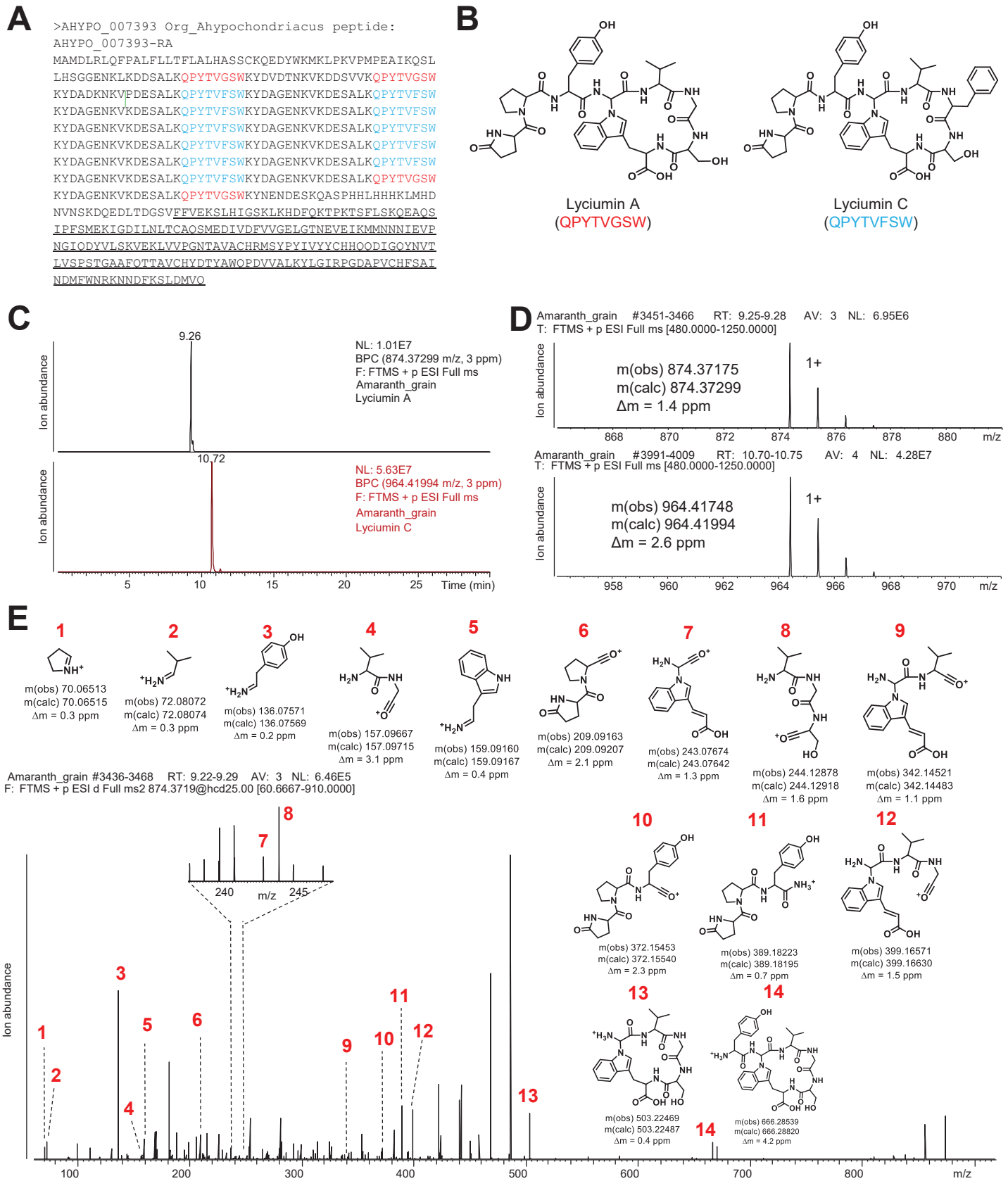


Figure S11 | Genome mining of lyciumins from *Amaranthus hypochondriacus*. (A) *Amaranthus hypochondriacus* lyciumin precursor peptide (BURP domain underlined, core peptides highlighted in blue and red). (B) Predicted lyciumin chemotypes. (C) LC-MS chemotyping of predicted lyciumin chemotypes in peptide extract of *Amaranthus hypochondriacus* seeds. (D) MS analysis of predicted lyciumin chemotypes of *Amaranthus hypochondriacus*. (E) MS/MS analysis of predicted lyciumin chemotypes of *Amaranthus hypochondriacus*.

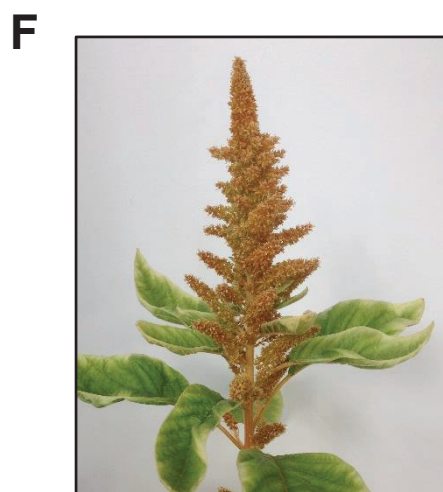
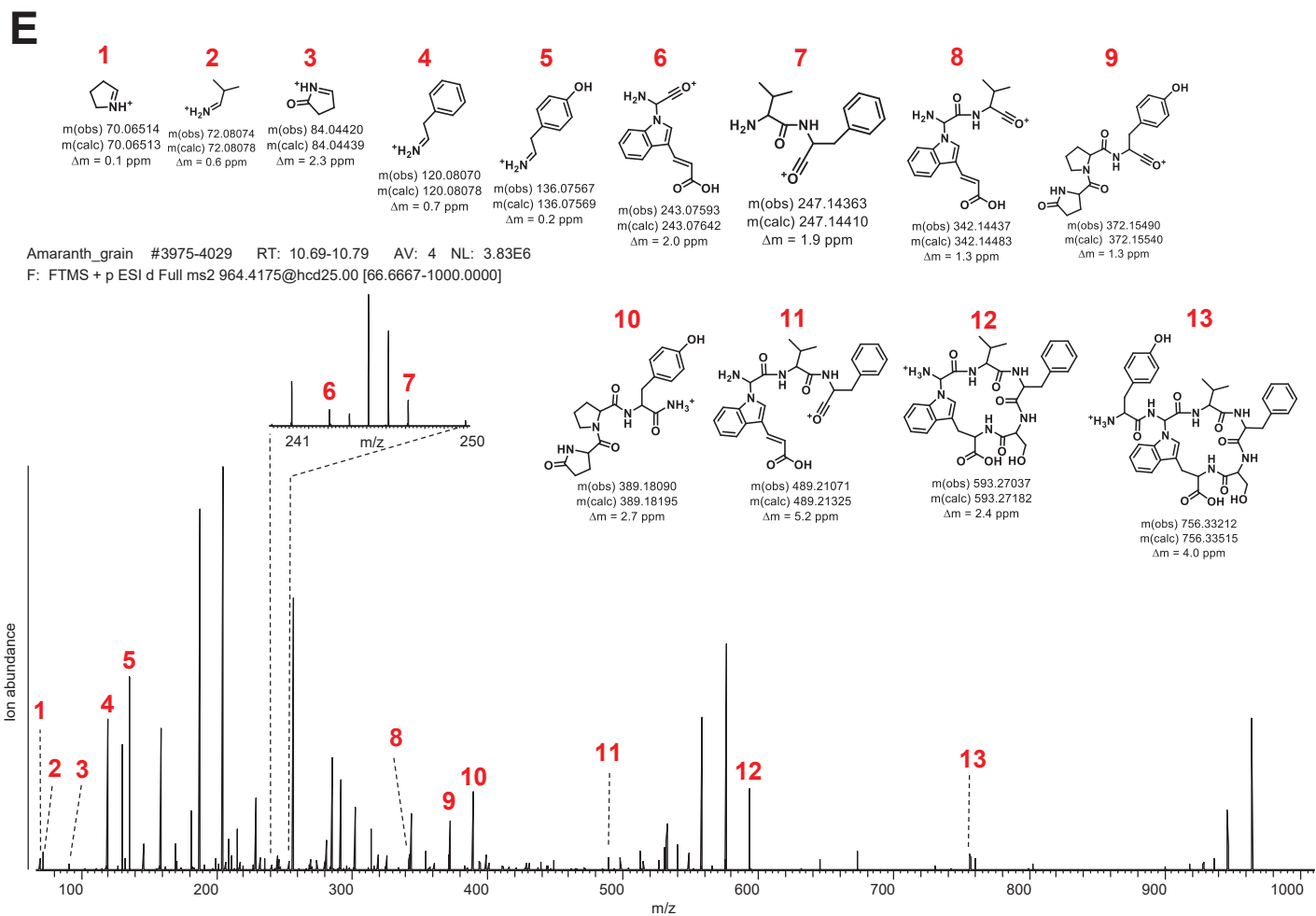


Figure S11 | Genome mining of lyciumins from *Amaranthus hypochondriacus*. (E) MS/MS analysis of predicted lyciumin chemotypes of *Amaranthus hypochondriacus*. (F) *Amaranthus hypochondriacus* plant.

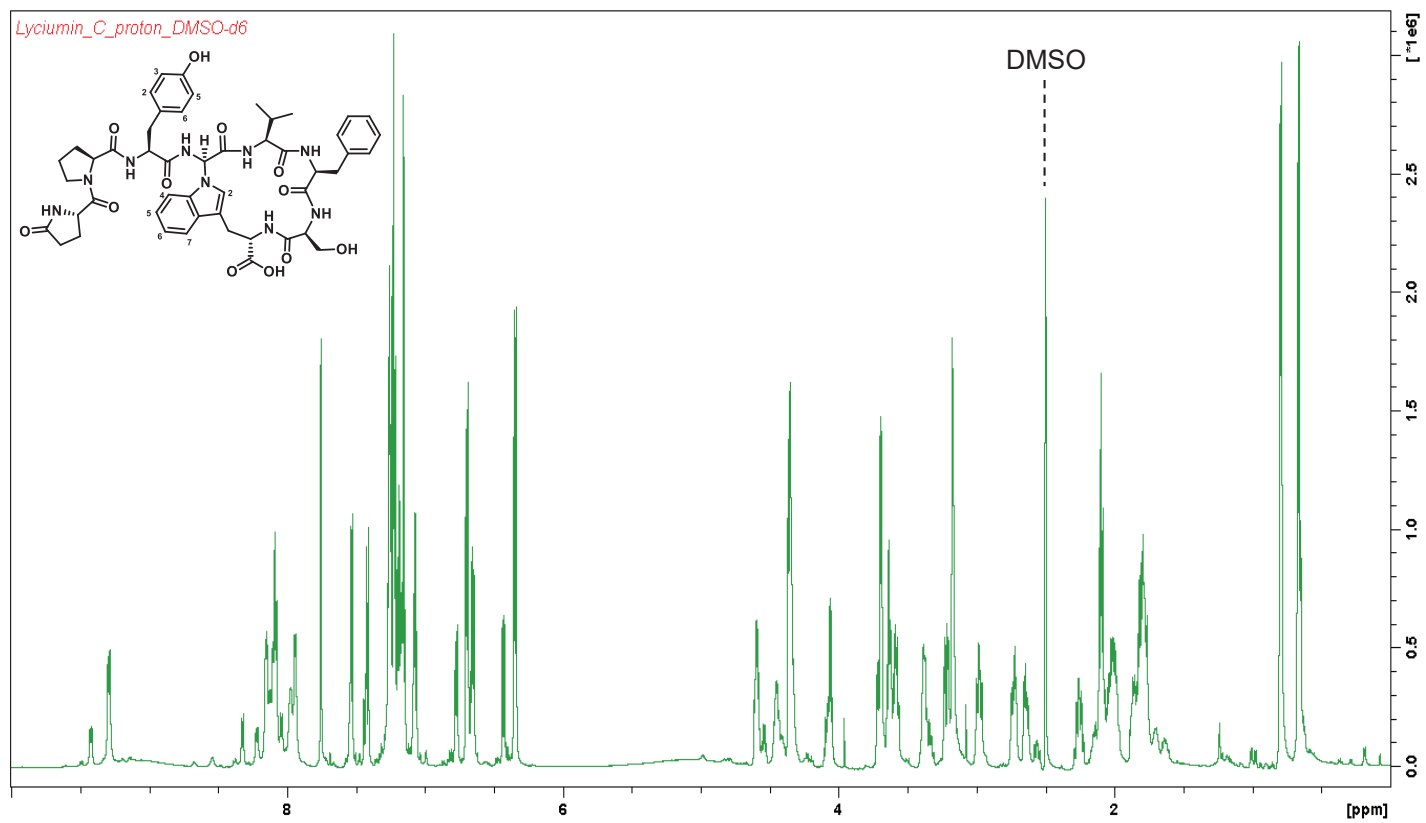


Figure S12 | ^1H NMR spectrum of lyciumin C in DMSO- d_6 (600 MHz).

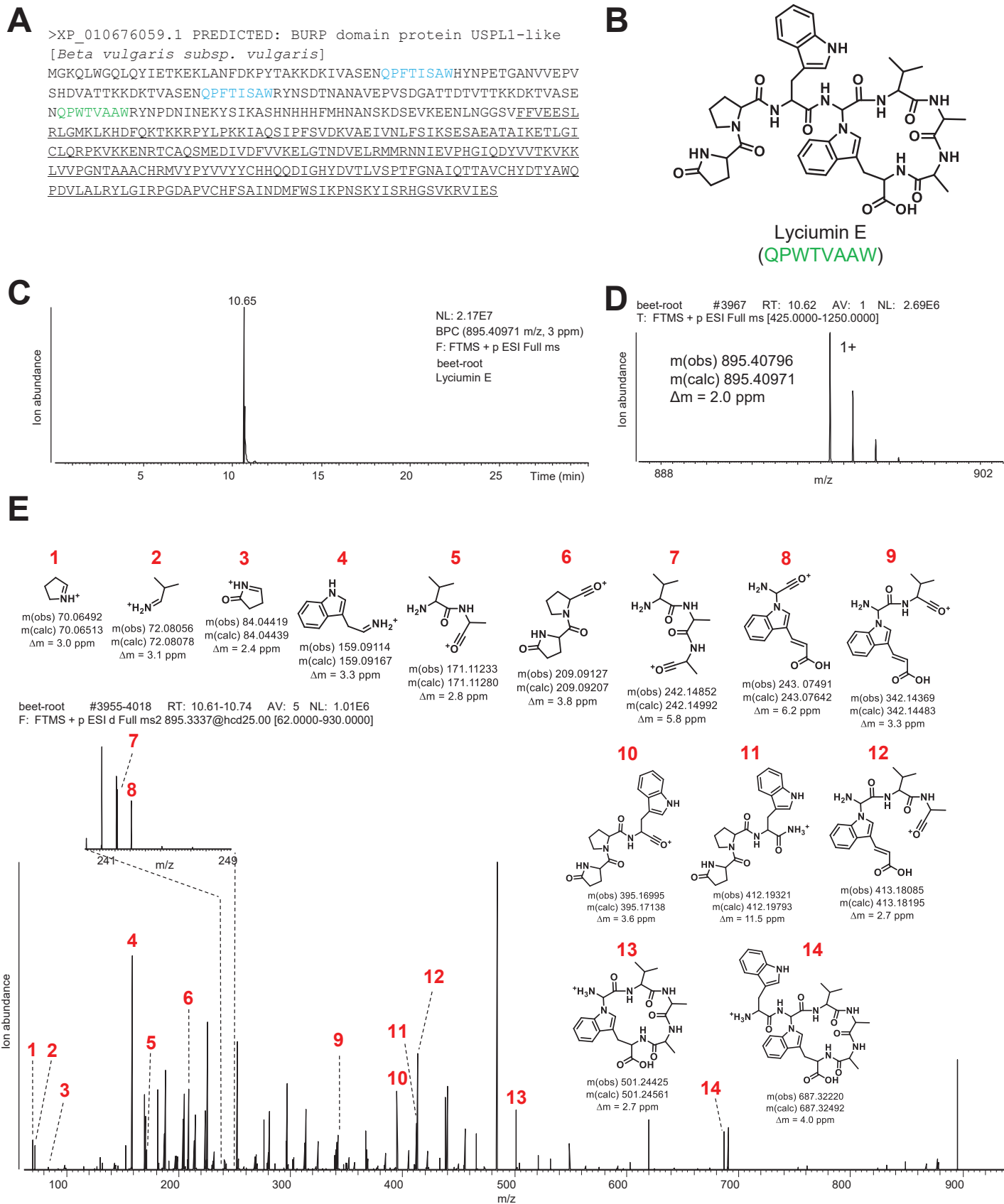


Figure S13 | Genome mining of lyciumins from *Beta vulgaris*. (A) *Beta vulgaris* lyciumin precursor peptide (BURP domain underlined, core peptides highlighted in blue and green). (B) Predicted lyciumin chemotype. (C) LC-MS chemotyping of predicted lyciumin chemotype in peptide extract of *Beta vulgaris* root. (D) MS analysis of predicted lyciumin chemotype of *Beta vulgaris*. (E) MS/MS analysis of predicted lyciumin chemotype of *Beta vulgaris*.

F



Figure S13 | Genome mining of lyciumins from *Beta vulgaris*. (F) *Beta vulgaris* plant.

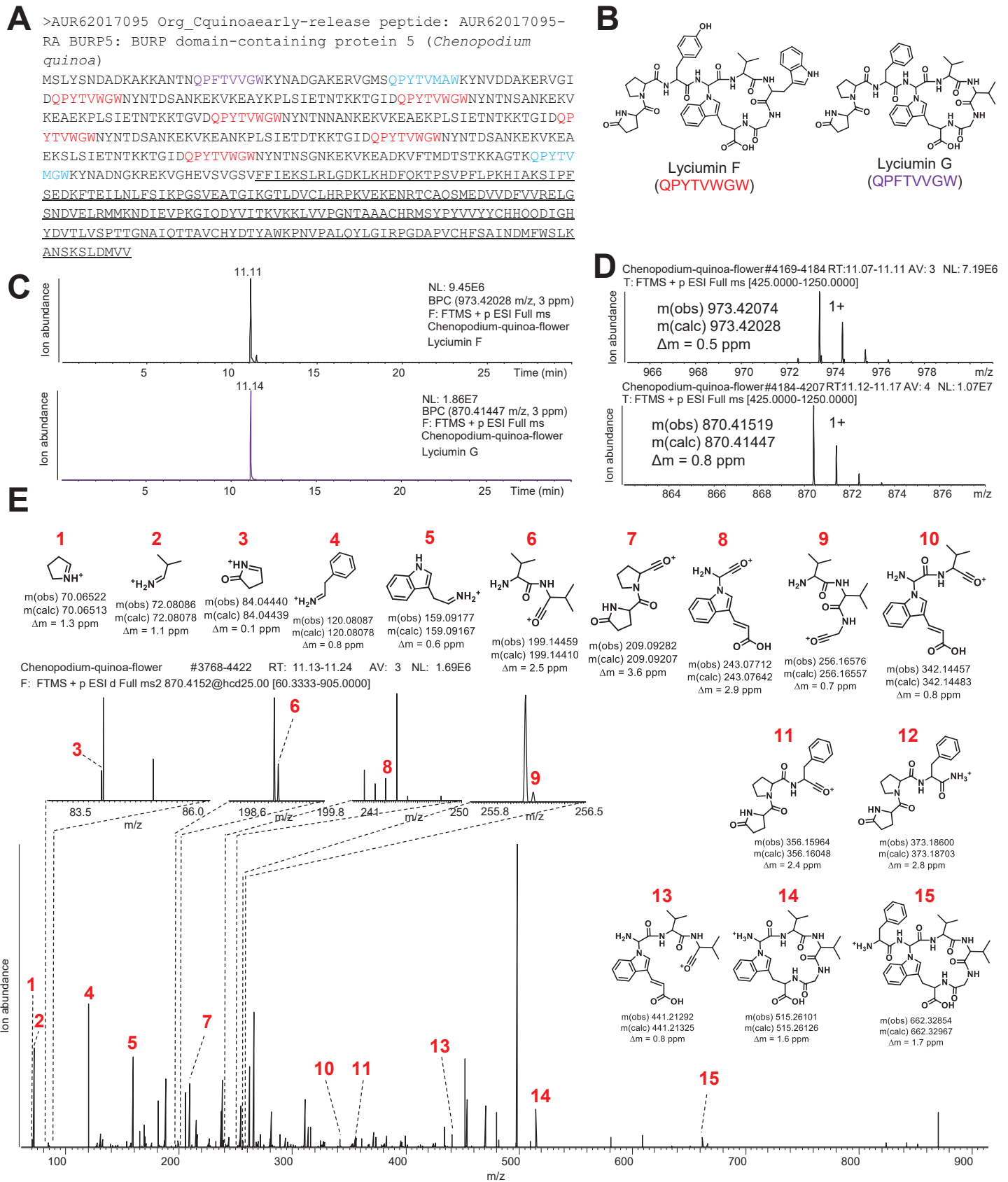


Figure S14 | Genome mining of lyciumins from *Chenopodium quinoa*. (A) *Chenopodium quinoa* lyciumin precursor peptide (BURP domain underlined, core peptides highlighted in blue, red and purple). (B) Predicted lyciumin chemotypes. (C) LC-MS chemotyping of predicted lyciumin chemotypes in peptide extract of *Chenopodium quinoa* flower. (D) MS analysis of predicted lyciumin chemotypes of *Chenopodium quinoa*. (E) MS/MS analysis of predicted lyciumin chemotypes of *Chenopodium quinoa*.

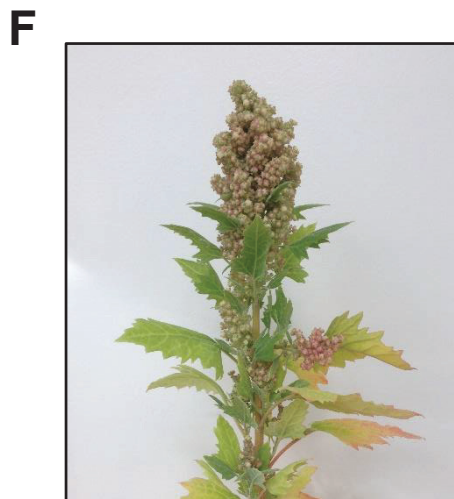
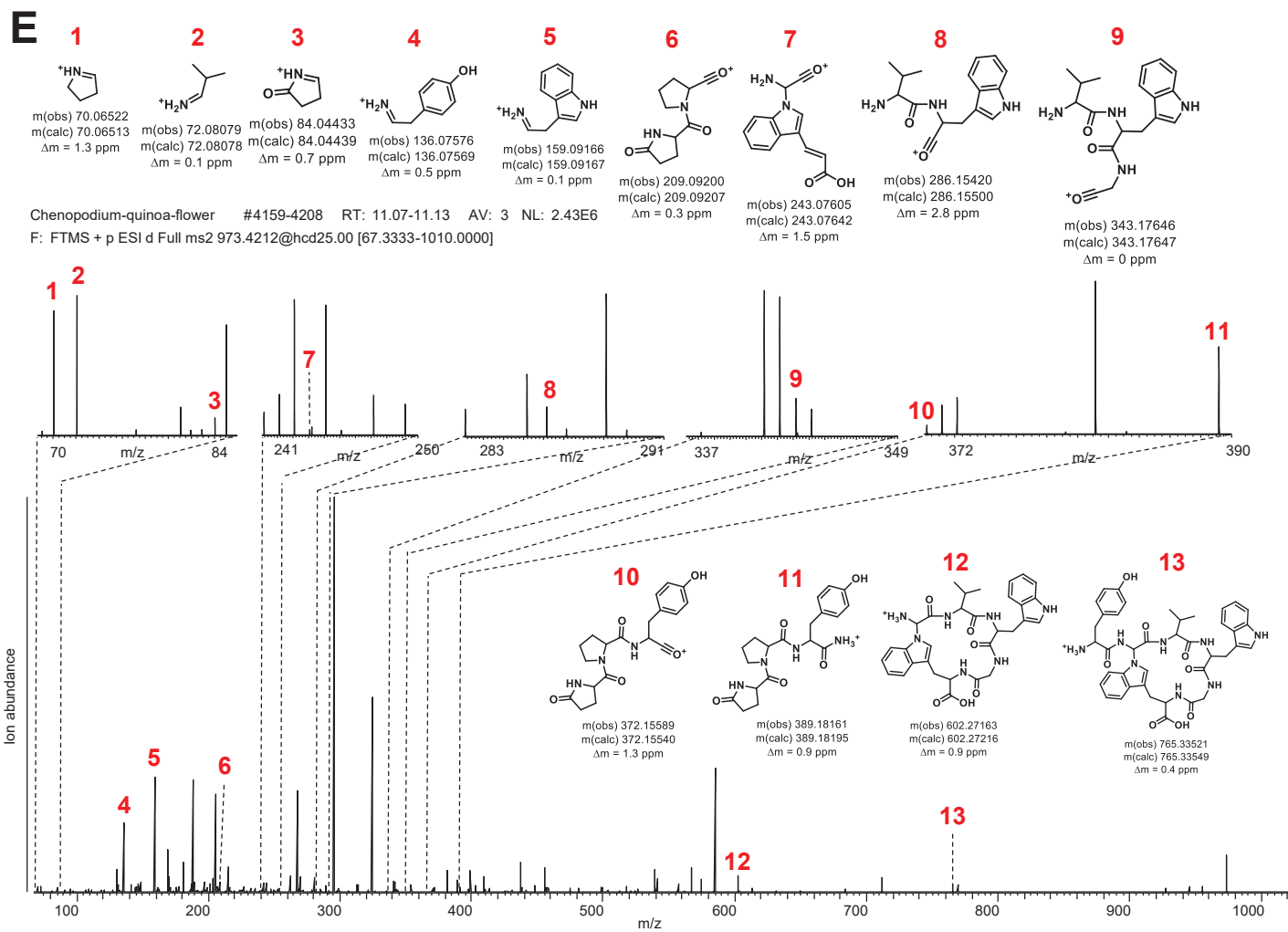


Figure S14 | Genome mining of lyciumins from *Chenopodium quinoa*. (E) MS/MS analysis of predicted lyciumin chemotypes of *Chenopodium quinoa*. (F) *Chenopodium quinoa* plant.

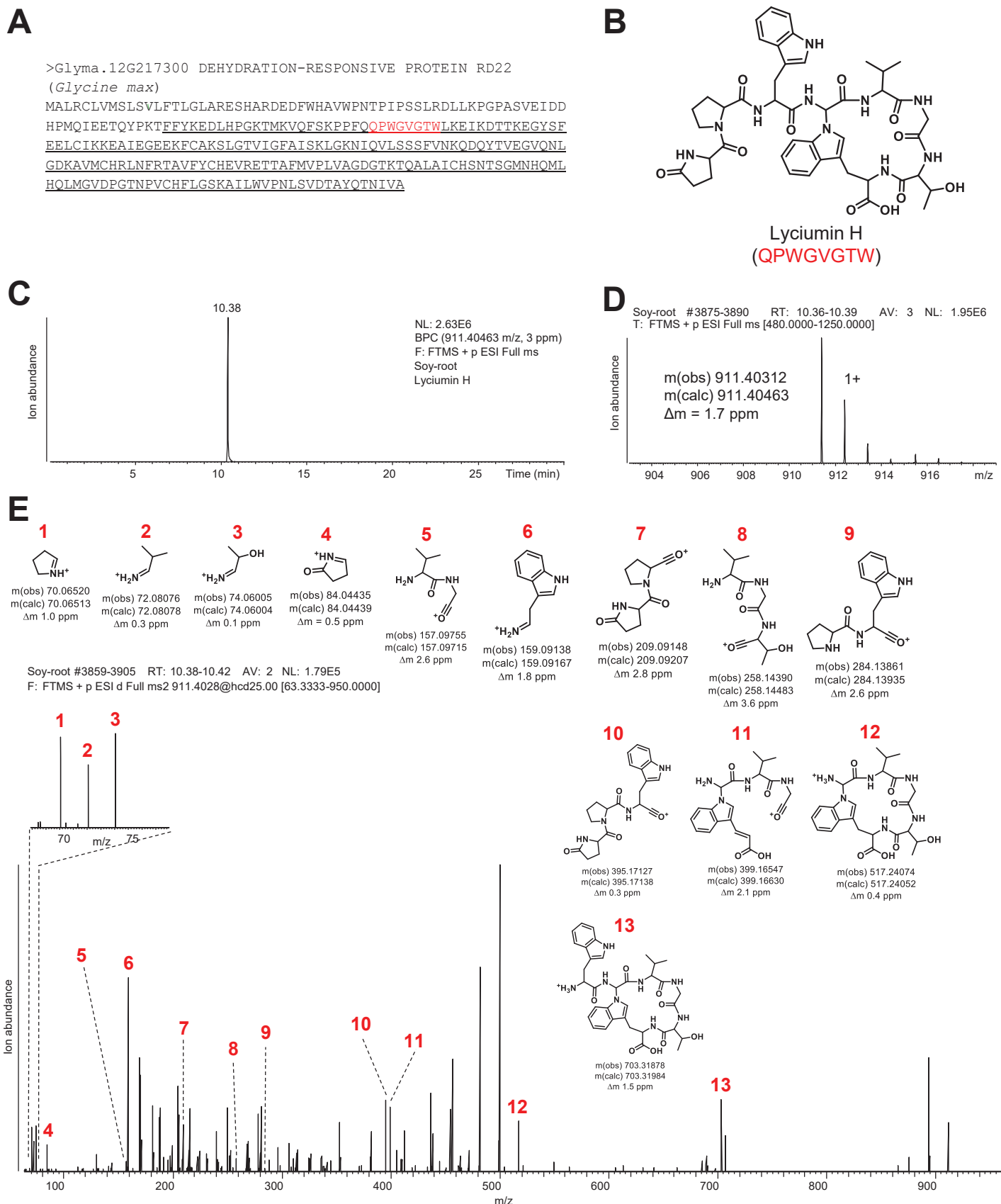


Figure S15 | Genome mining of lyciumins from *Glycine max*. (A) *Glycine max* lyciumin H precursor peptide (BURP domain underlined, core peptide highlighted in red). (B) Predicted lyciumin H chemotype. (C) LC-MS chemotyping of predicted lyciumin H chemotype in peptide extract of *Glycine max* root. (D) MS analysis of predicted lyciumin H chemotype of *Glycine max* root. (E) MS/MS analysis of predicted lyciumin H chemotype of *Glycine max* root.

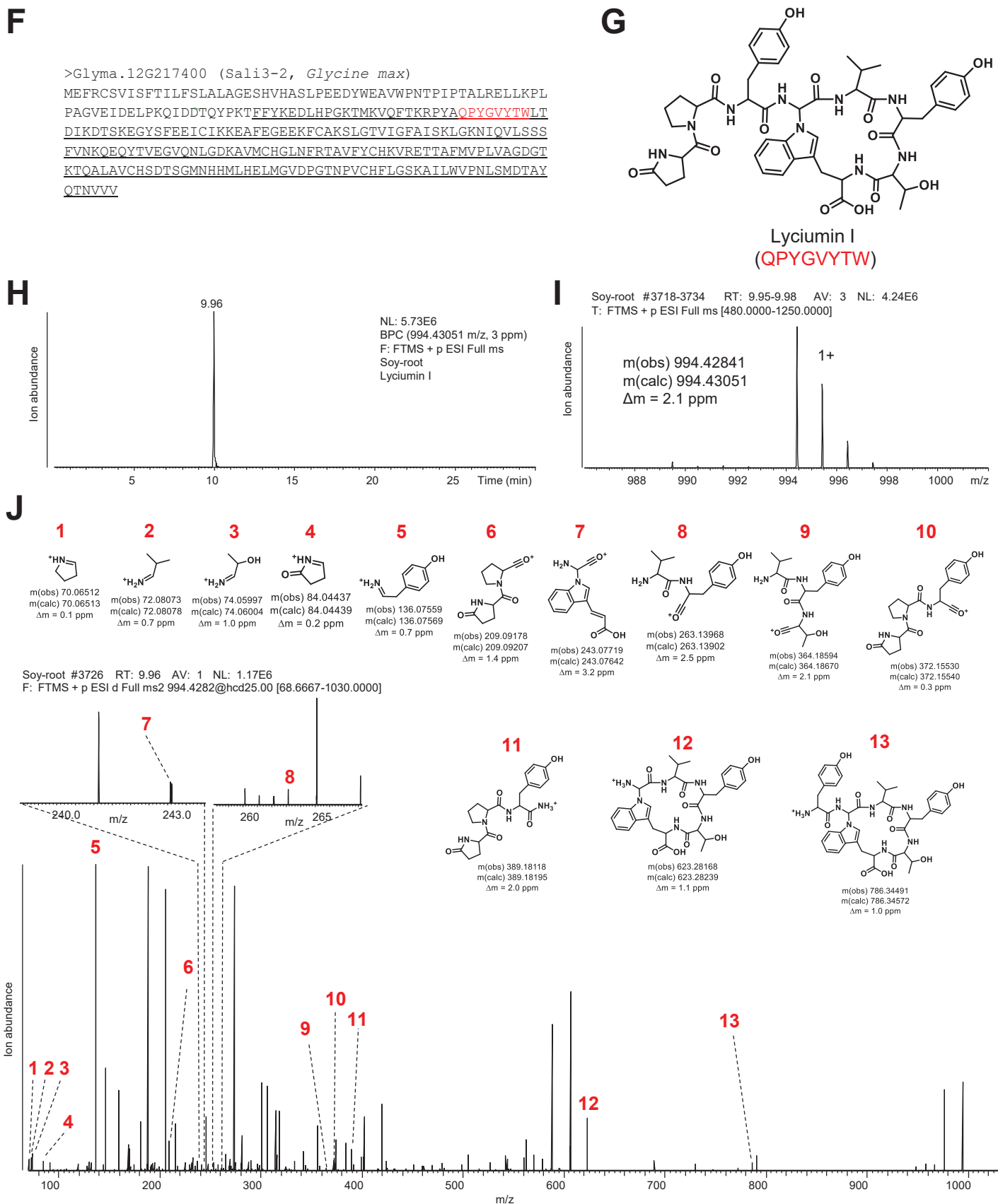


Figure S15 | Genome mining of lyciumins from *Glycine max*. (F) *Glycine max* lyciumin I precursor peptide (BURP domain underlined, core peptide highlighted in red). (G) Predicted lyciumin I chemotype. (H) LC-MS chemotyping of predicted lyciumin I chemotype in peptide extract of *Glycine max* root. (I) MS analysis of predicted lyciumin I chemotype of *Glycine max* root. (J) MS/MS analysis of predicted lyciumin I chemotype of *Glycine max* root.

K



Figure S15 | Genome mining of lyciumins from *Glycine max*. (K) *Glycine max* plant.

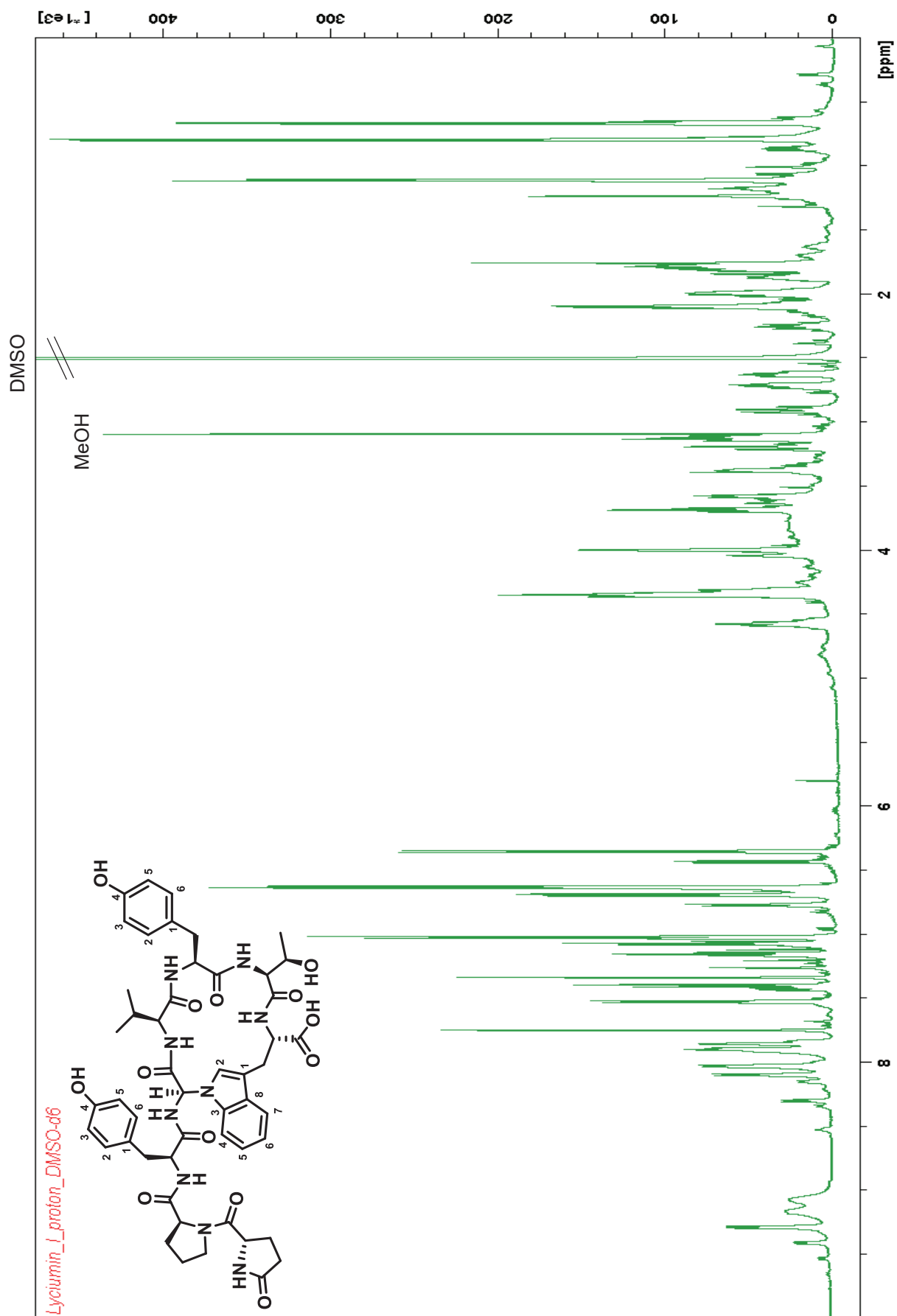


Figure S16 | ¹H NMR spectrum of lyciumin I in DMSO-d₆ (600 MHz).

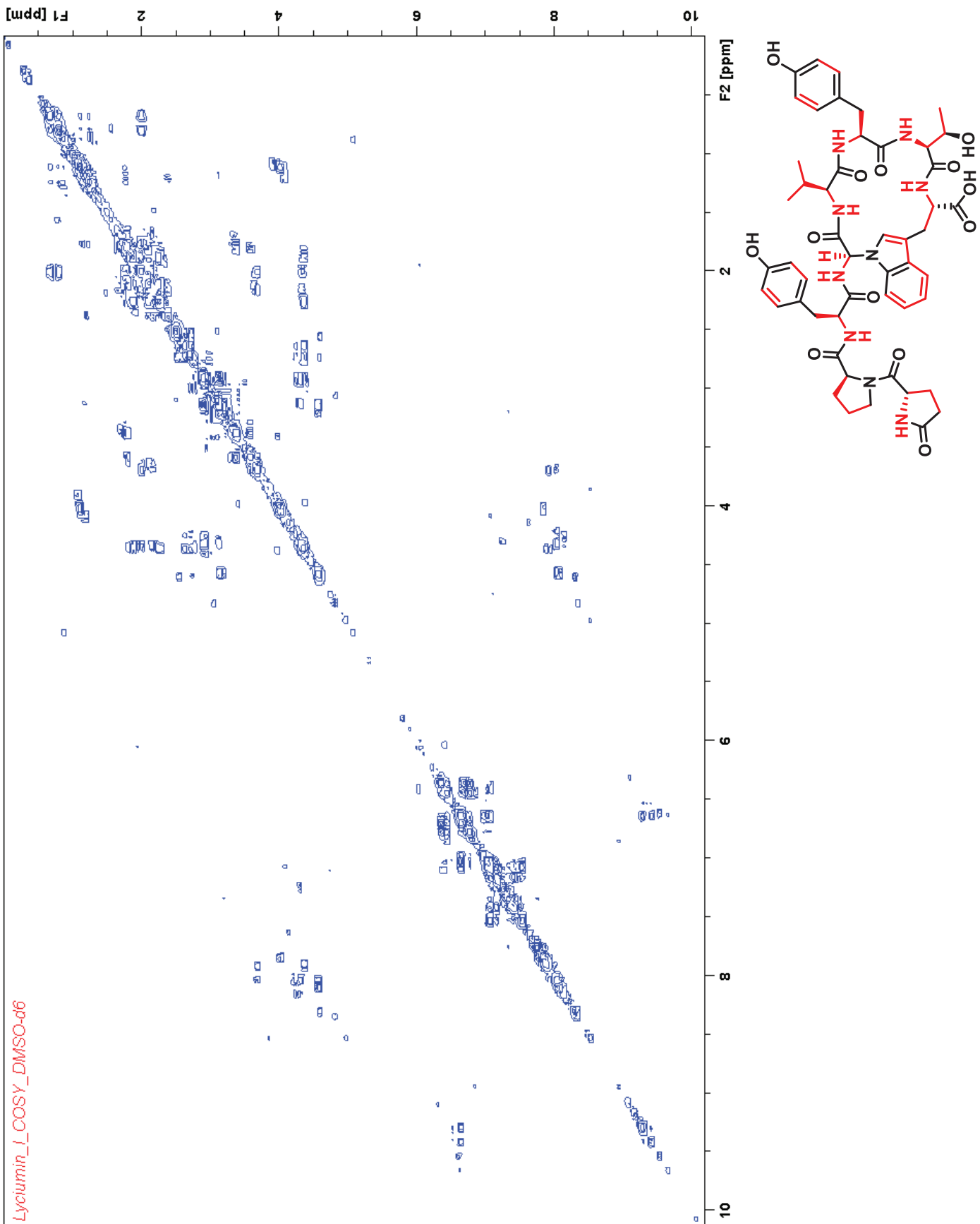


Figure S17 | ^1H - ^1H COSY NMR spectrum of lyciumin I in DMSO- d_6 (600 MHz).

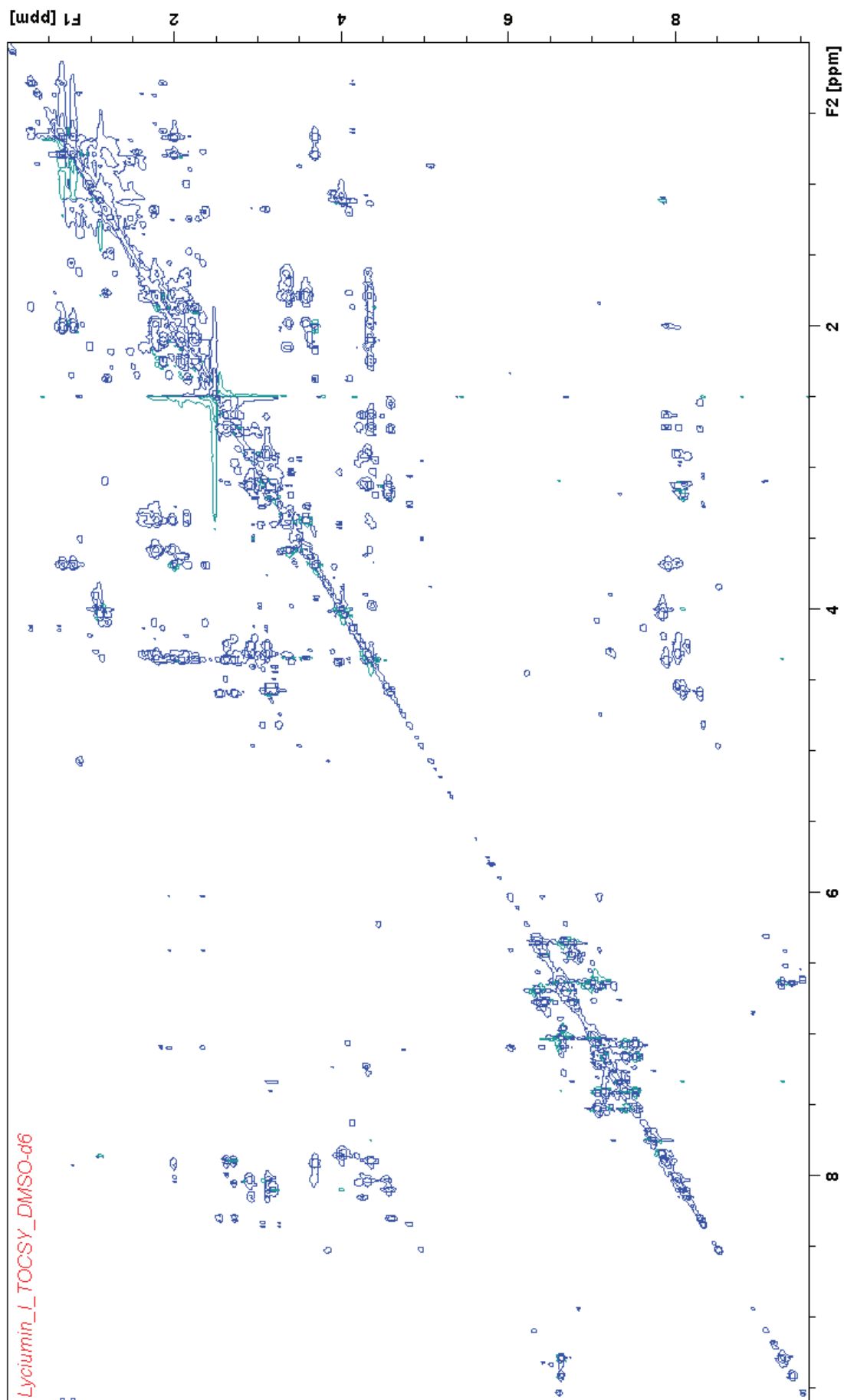


Figure S18 | ^1H - ^1H TOCSY NMR spectrum of lyciumin I in DMSO- d_6 (600 MHz).

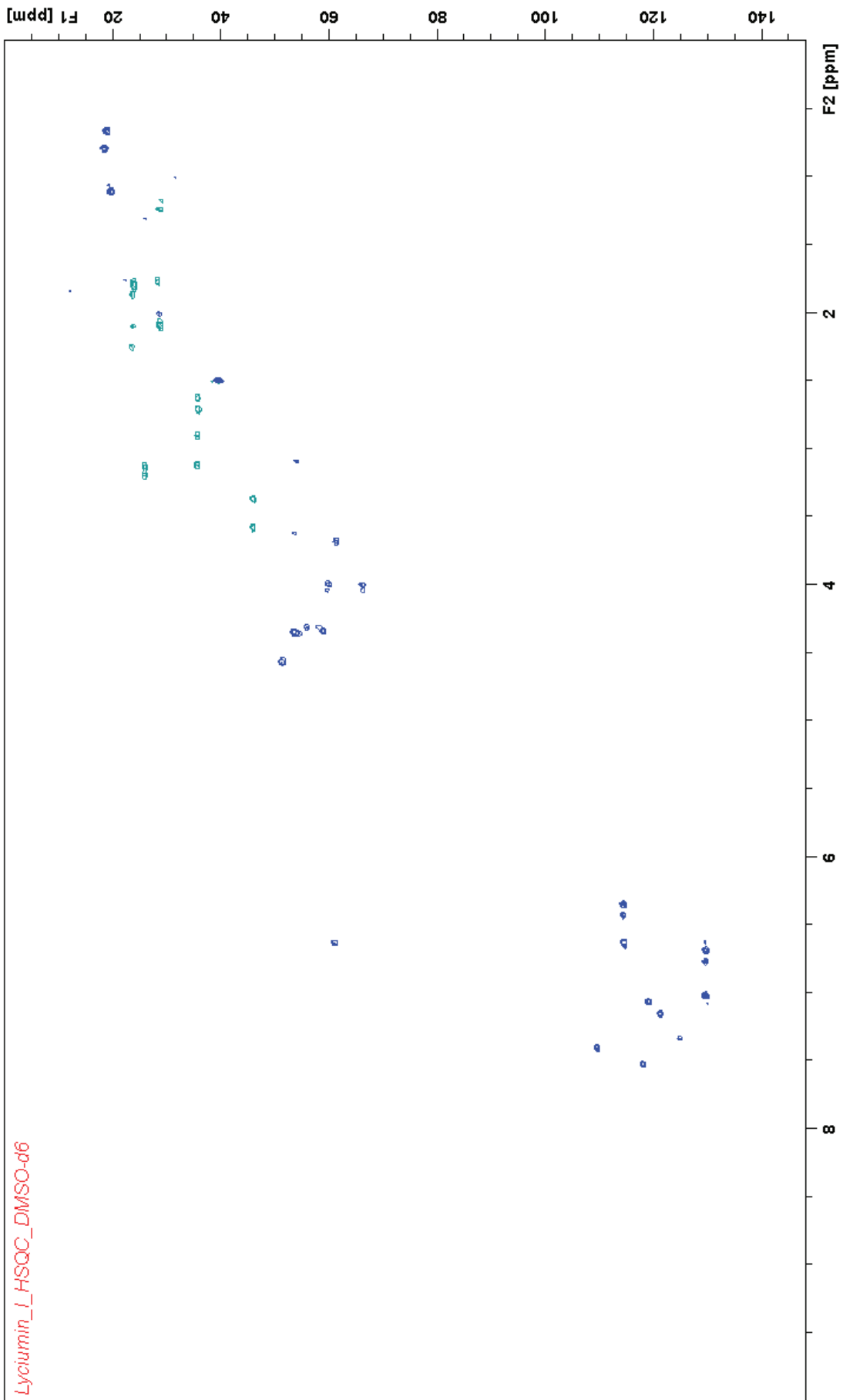


Figure S19 | ^1H - ^{13}C HSQC NMR spectrum of lyciumin I in DMSO- d_6 (600 MHz).

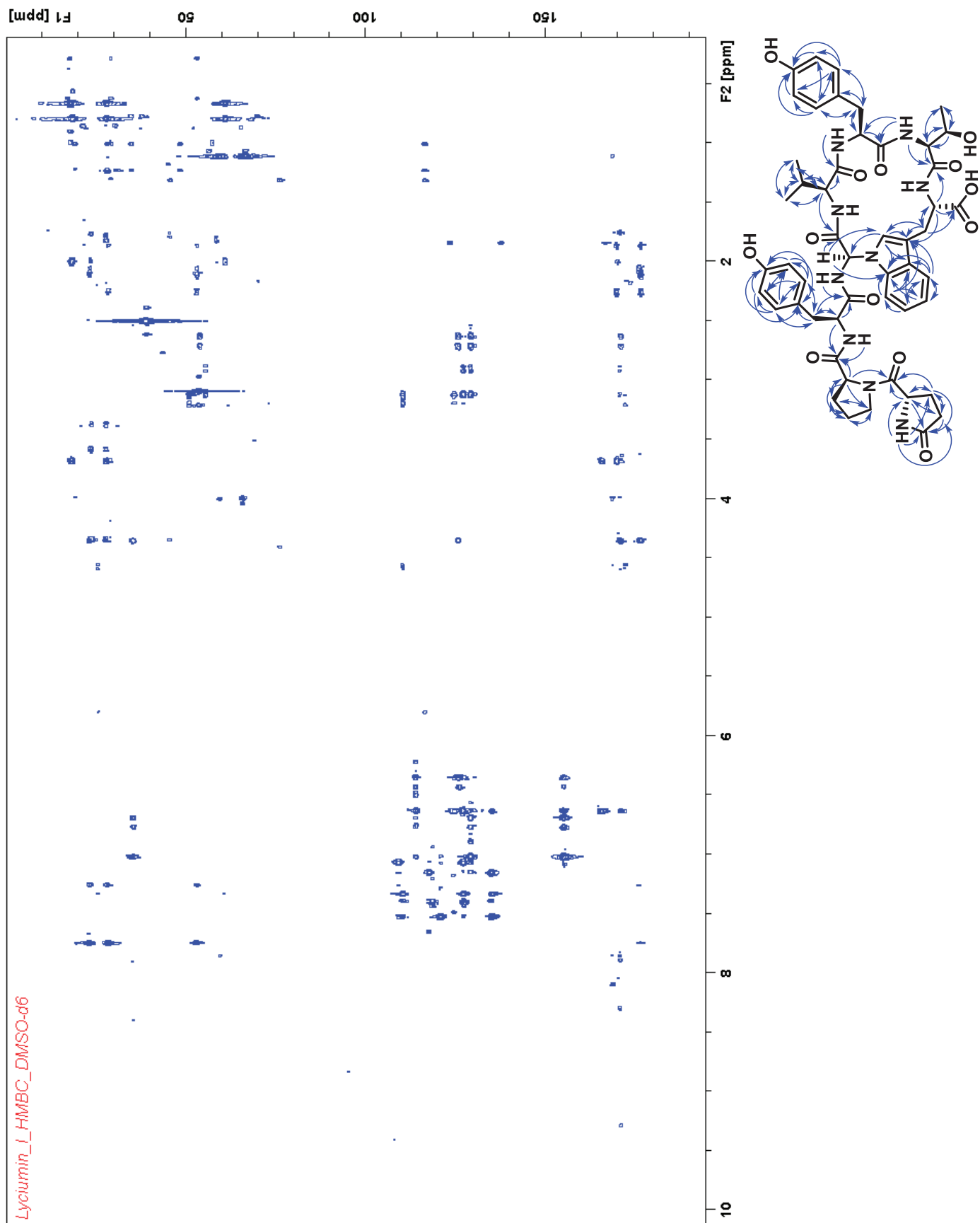


Figure S20 | ^1H - ^{13}C HMBC NMR spectrum of lyciumin I in DMSO- d_6 (600 MHz).

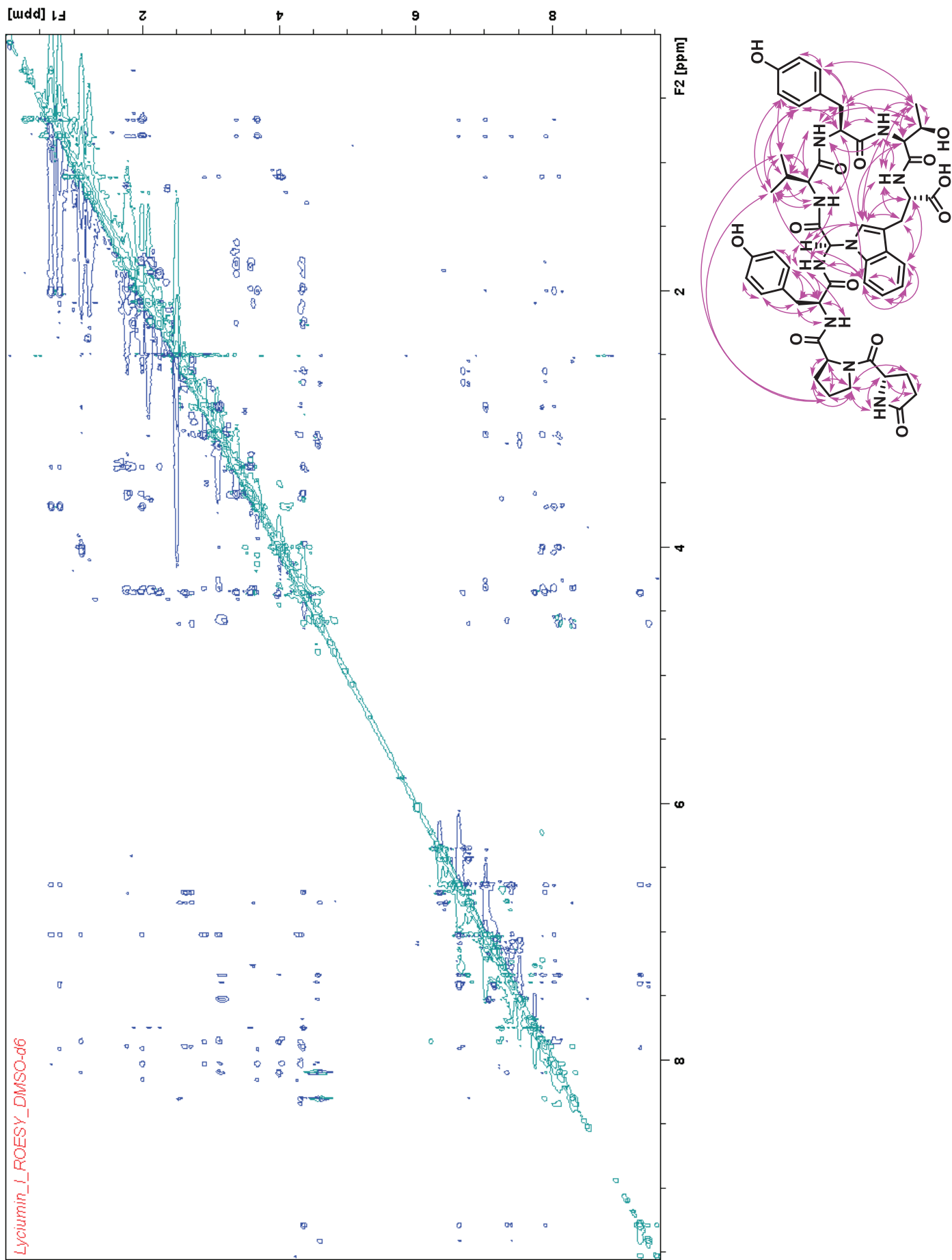


Figure S21 | ^1H - ^1H ROESY NMR spectrum of lyciumin I in DMSO-d_6 (600 MHz).

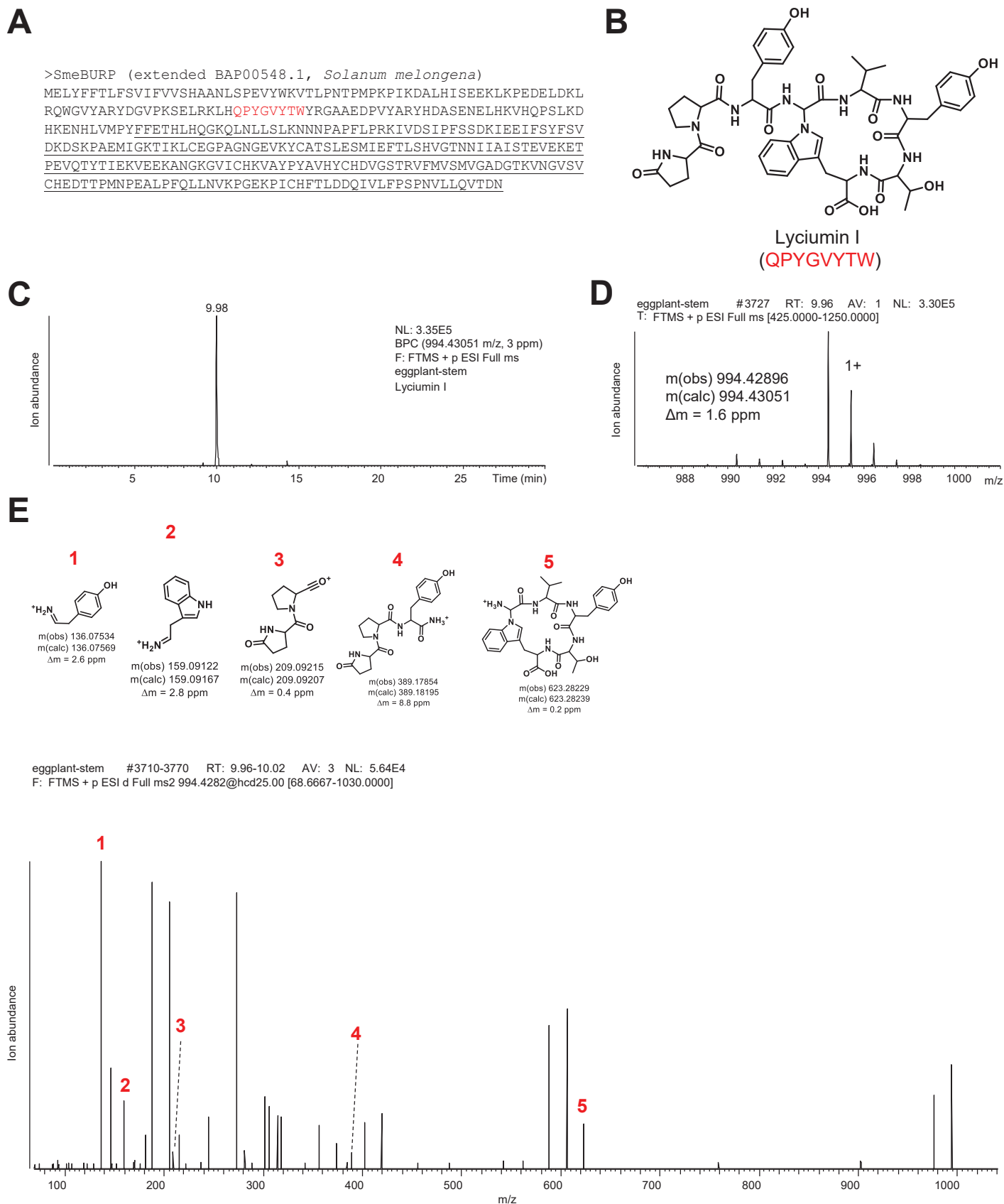


Figure S22 | Genome mining of lyciumins from *Solanum melongena*. (A) *Solanum melongena* lyciumin I precursor peptide (BURP domain underlined, core peptide highlighted in red). (B) Predicted lyciumin I chemotype. (C) LC-MS chemotyping of predicted lyciumin I chemotype in peptide extract of *Solanum melongena* stem. (D) MS analysis of predicted lyciumin I chemotype of *Solanum melongena* stem. (E) MS/MS analysis of predicted lyciumin I chemotype of *Solanum melongena* stem.

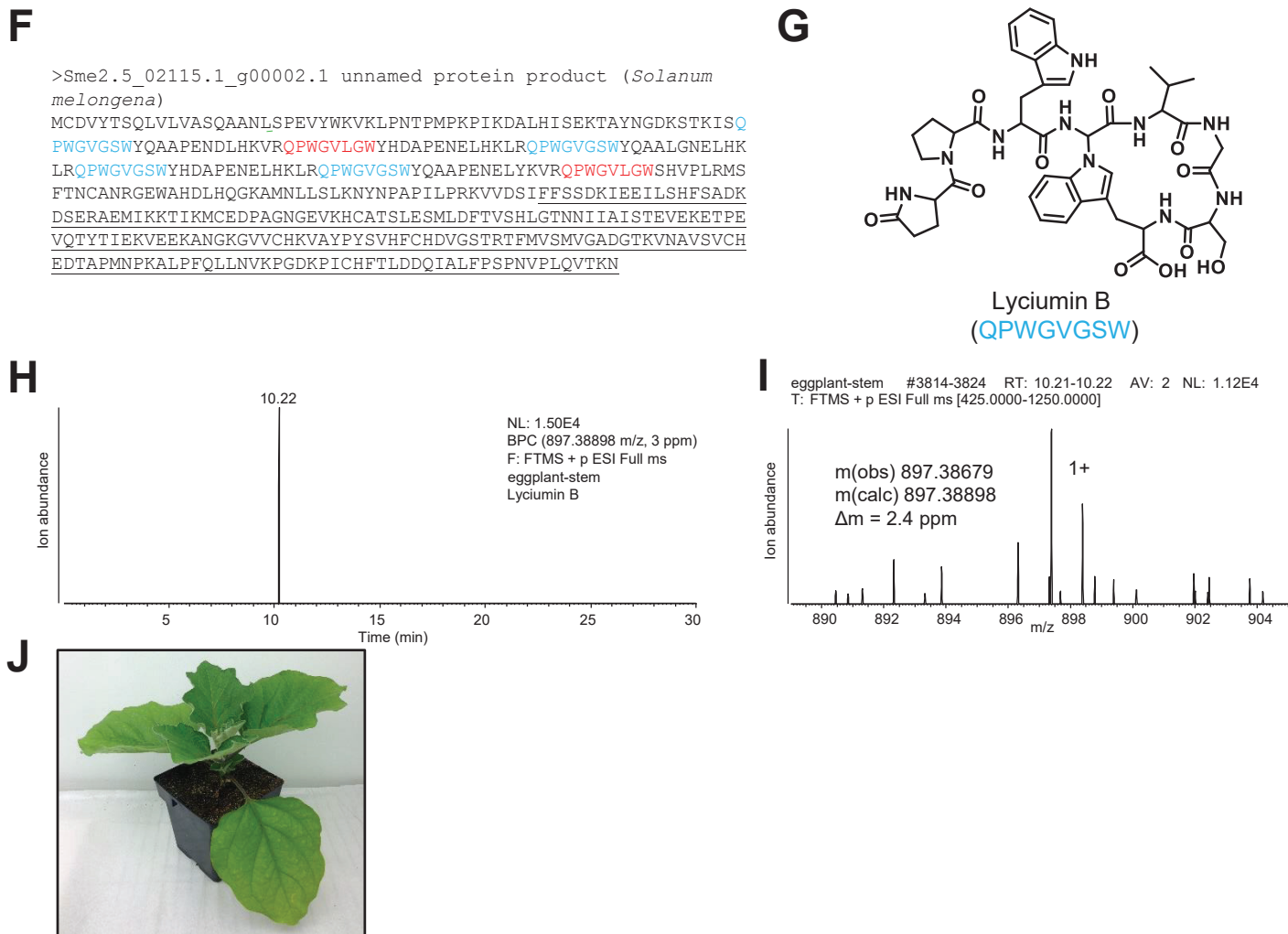


Figure S22 | Genome mining of lyciumins from *Solanum melongena*. (F) *Solanum melongena* lyciumin B precursor peptide (BURP domain underlined, core peptides highlighted in blue and red). (G) Predicted lyciumin B chemotype. (H) LC-MS chemotyping of predicted lyciumin B chemotype in peptide extract of *Solanum melongena* stem. (I) MS analysis of predicted lyciumin B chemotype of *Solanum melongena* stem. (J) *Solanum melongena* plant.

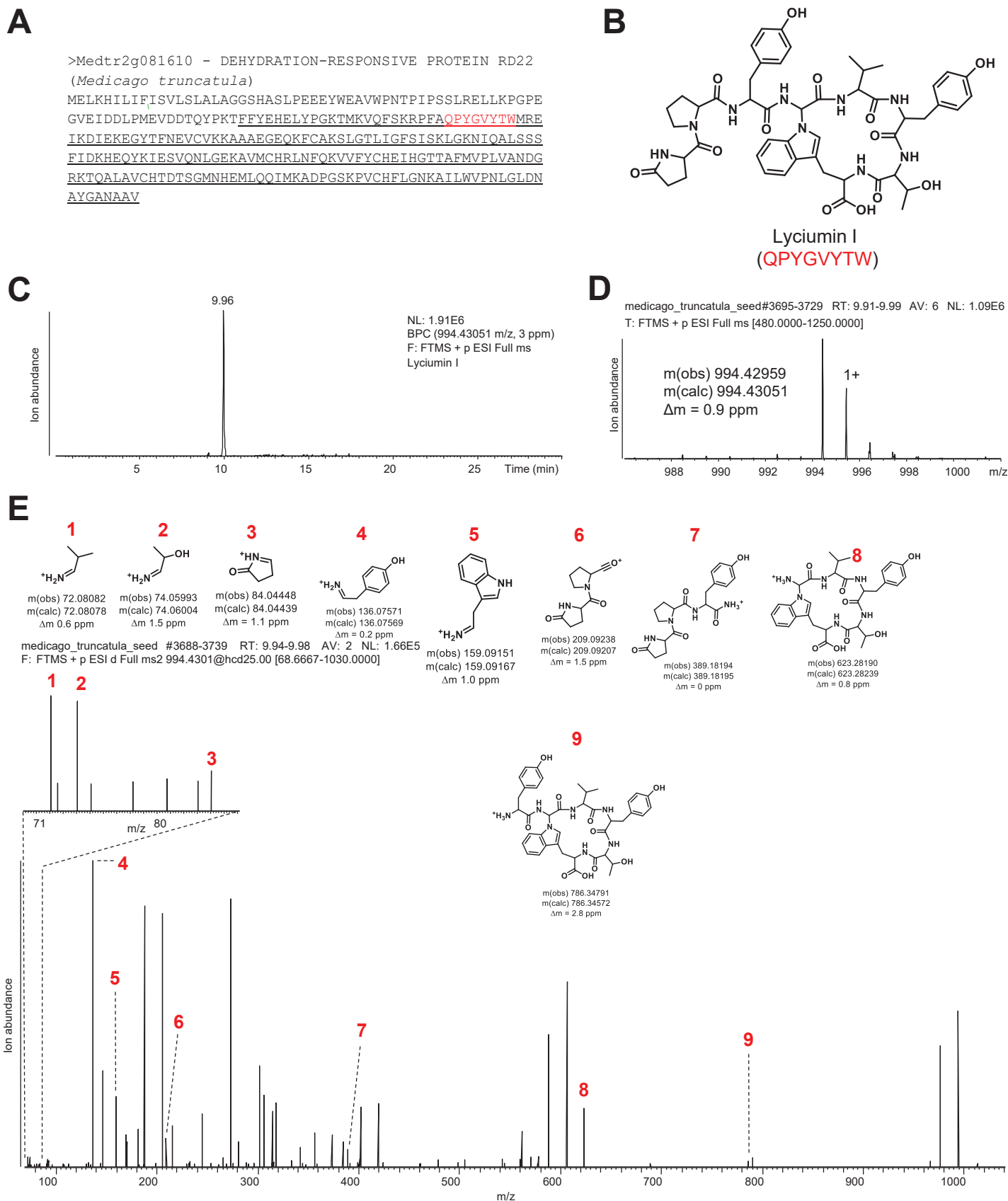
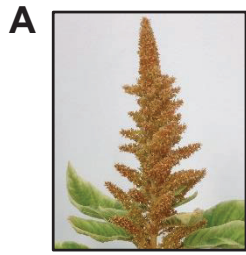


Figure S23 | Genome mining of lyciumins from *Medicago truncatula*. (A) *Medicago truncatula* lyciumin I precursor peptide (BURP domain underlined, core peptide highlighted in red). (B) Predicted lyciumin I chemotype. (C) LC-MS chemotyping of predicted lyciumin I chemotype in peptide extract of *Medicago truncatula* seeds. (D) MS analysis of predicted lyciumin I chemotype of *Medicago truncatula* seeds. (E) MS/MS analysis of predicted lyciumin I chemotype of *Medicago truncatula* seeds.



Amaranthus hypochondriacus

Gene expression (RSEM, [TPM]) in tissues/conditions									
Transcript	Lyciumin chemotype	Cotyledon	Developing embryo	Drought	Leaf	Mature seed	Root	Stem	Flower
AHYPO_007393-RA	Lyciumin A & C	37338	2055	60460	7236	66366	77877	15572	13250
	References (SRA)	SRR1598915	SRR1598909	SRR1598914	SRR1598912	SRR1598916	SRR1598913	SRR1598910	SRR1598911



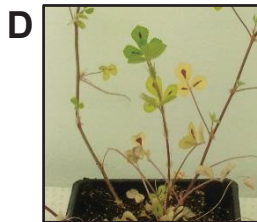
Chenopodium quinoa

Gene expression (RSEM, [TPM]) in tissues/conditions																									
Transcript	Lyciumin chemotype	Flower 1	Flower 2	Flower 3	Leaf 1	Leaf 2	Leaf 3	Seed 1	Seed 2	Seed 3	Stem 1	Stem 2	Stem 3	Seedling 1	Seedling 2	Seedling 3									
AUR62017095	Lyciumin F & G	1227.05	1334.44	1095.61	270.1	355.2	207.5	77.2	58.82	71.32	1196.8	2195.5	1938	154.87	183.16	122.36									
	Reference (SRA)	Flower 1	SRR5974430	Seed 1	SRR5974426	Seedling 1	SRR5974428	Flower 2	SRR5974427	Seed 2	SRR5974424	Seedling 2	SRR5974429	Flower 3	SRR5974436	Seed 3	SRR5974431	Seedling 3	SRR5974434						
		Flower 2	SRR5974427	Seed 2	SRR5974424	Seedling 2	SRR5974429	Flower 3	SRR5974436	Seed 3	SRR5974431	Seedling 3	SRR5974434	Leaf 1	SRR5974438	Stem 1	SRR5974432	Leaf 2	SRR5974437	Stem 2	SRR5974433	Leaf 3	SRR5974435	Stem 3	SRR5974425

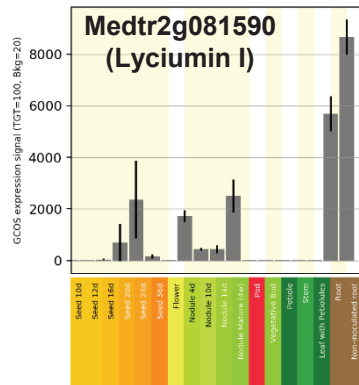


Glycine max

Gene expression (bar.utoronto.ca, [RPKM]) in tissues/conditions																	
Transcript	Lyciumin chemotype	Flower	Leaves	Green Pods	Nodule	Root	Root tip	Root Hair 12HAI	Root Hair 24HAI	Root Hair 48HAI	Root Hair 84HAI	Root Hair 108HAI	Root Hair 144HAI	Root Hair 180HAI	Root Hair 216HAI	Root Hair 252HAI	SAM
Glyma.12G217300	Lyciumin H	247.58	33.73	3505.92	1959.25	2072.86	6.48	508.24	709.11	720.55	999.91	782.47	931.26	6611.09	259.63		
Glyma.12G217400 (Sal3-2)	Lyciumin I	330.31	154.83	681.91	3770.9	4154.42	1.54	399.73	513.62	688.9	1066.59	760.96	1386.26	1757	648.96		
	Reference	Libault, M., Farmer, A., Brechenmacher, L., et al. <i>Plant Physiol.</i> 2010, 152, 541-555. Libault, M. et al. <i>The Plant Journal</i> 2010, 63, 85-99.															
Transcript	Lyciumin chemotype	Flower	Young Leaf	One CM Pod	Pod Shell (10-13 DAF)	Pod Shell (14-17 DAF)	Nodule	Root	Seed 10-13 DAF	Seed 14-17 DAF	Seed 21 DAF	Seed 25 DAF	Seed 28 DAF	Seed 35 DAF	Seed 42 DAF		
Glyma.12G217300	Lyciumin H	317	10	458	379	877	231	489	12	24	40	24	17	19	15		
Glyma.12G217400 (Sal3-2)	Lyciumin I	104	23	141	120	95	220	790	4	3	4	36	68	332	399		
	Reference	Severin, et al. <i>BMC Plant Biology</i> 2010, 10, 160.															



Medicago truncatula



Solanum tuberosum

Gene expression (RSEM, [TPM]) in tissues/conditions																	
Transcript	Lyciumin chemotype	Flower	Leaf	Leaf 2	Petiole	Root	Whole plant	Shoot apex	Stamen	Stem	Stolon	Tuber	Tuber 2	Tuber cortex	Tuber peel	Tuber pith	Tuber sprout
PGSC0003DMG400047074	Lyciumin B, K, L, M, N, O	4.56	17.03	2.86	10.71	1190.71	324.87	474.98	2.26	118.65	491.75	718.27	411.05	91.6	606.46	38.04	3599.35
	Reference	ERR029903	ERR029910	ERR029919	ERR029911	ERR029917	ERR029922	ERR029912	ERR029918	ERR029913	ERR029914	ERR029915	ERR029916	ERR029924	ERR029921	ERR029920	ERR029923

Figure S24 | Lyciumin precursor gene expression in (A) *Amaranthus hypochondriacus*, (B) *Chenopodium quinoa*, (C) *Glycine max*, (D) *Medicago truncatula*¹⁵ and (E) *Solanum tuberosum*.

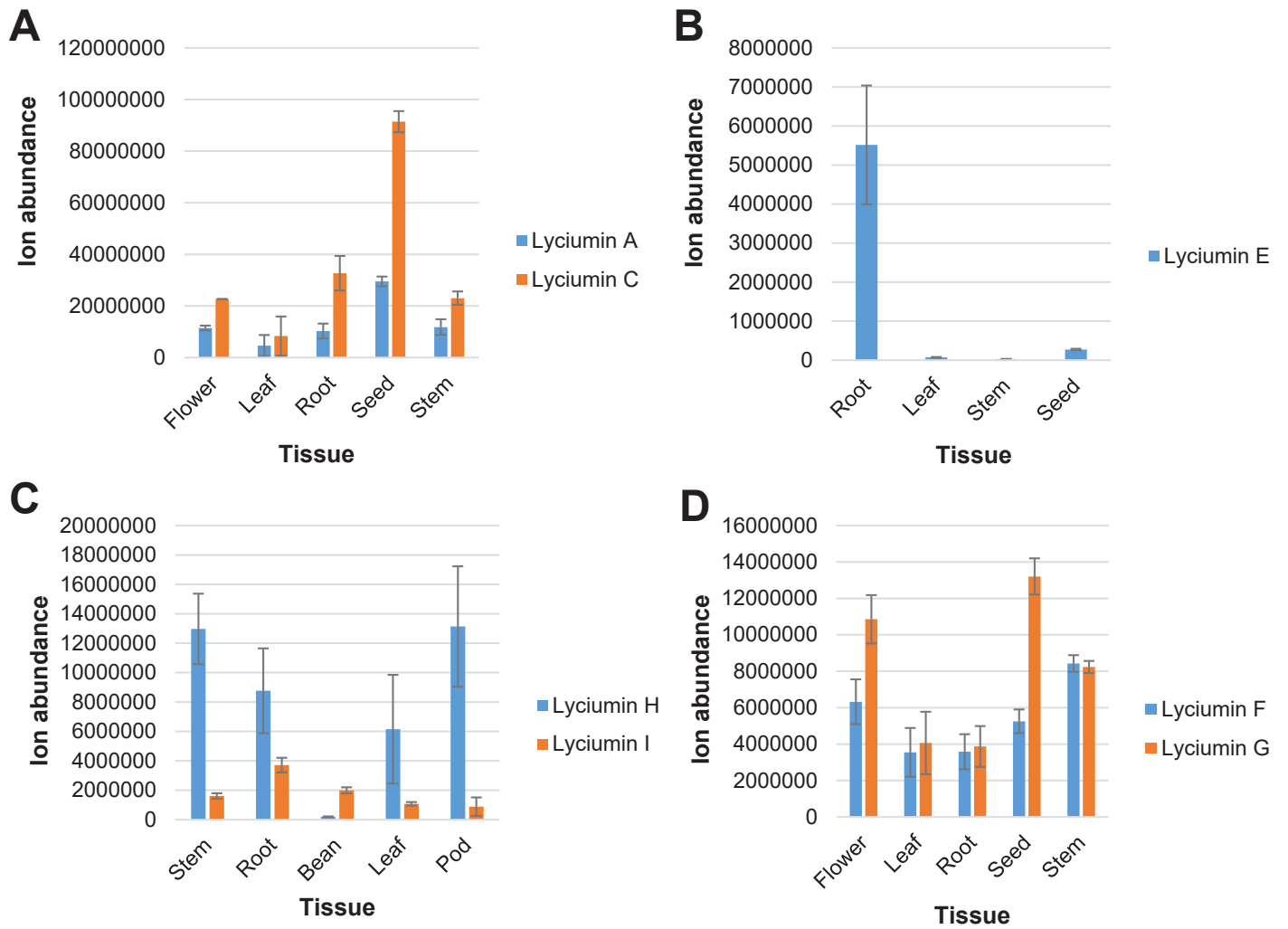


Figure S25 | Lyciumin chemotyping in source plant tissues. (A) *Amaranthus hypochondriacus*. (B) *Beta vulgaris*. (C) *Glycine max*. (D) *Chenopodium quinoa*.

A Predicted precursor peptide from *Solanum tuberosum* genome (JGI Phytozome, v4.03)

>PGSC0003DMG400047074 Org_Stuberosum peptide: PGSC0003DMP400069178 BURP domain-containing protein (PAC:37467747)
MELHHQYYFFTFVSVIFVVSAAANLSPEVYWRVKLPNTMPMTPPIKDALHISDGIPLRSTFTKYANHGGEVWDGIRLPFENELHKVR**QPWGVDSWYQAAPENELHKVRQPYGVGVWYN**
DAAKKDLNDNHVPVTPYFFETDLHOGKKMNLOS LKYNPAPILPRKVVDSTAFSSDKIEEILNHFSVDKDSERAKDIKKTIKTCEEPAGNGEVKHCATSLES MIDFTLSHLGTNNIIAM
STEVEKETPEVQOAYTIEKVEEKANGKGVVCHKVAYPYAVHFCHDVGSTRTFMVSMVGADGTKVNAVSVCHEDTASMNPKALPFOLLNVKPGDKPICHFTLDDOIALFPSONAVLQVAE
N

B LbaLycA blastp hits of Trinity (v2.4) *de novo* transcriptome assembly:

>lcl|Potato_tuber|TRINITY_DN47721_c0_g1_i1 (5' partial)
VR**QPFVGRWYN**DAASENELHKVR**QPFVGVWYQAASENELHKVRQPYGVGVWYN**DAAKKDLNDNHVPVTPYFFETDLHOGKKMNLES LKYNPAPILPRKVVDSTAFSSDKIEEILNHFS
VDKDSERAKDIKKTIKMCEDPAGNGEVKHCATSLES MIDFTLSHLGTNNIIAMSTEVEKETPEVQTYTIEKVEEKANGKGVVCHKVAYPYAVHFCHDVGSTRTFMVSMVGADGTKVNAVSVCHEDTASMNPKALPFOLLNVKPGDKPICHFTLDDOIALFPSONALAEN

>lcl|Potato_tuber|TRINITY_DN47721_c1_g2_i3 (5' partial)
APENELQKVR**QPFVGRWYN**DAAPENELQKVR**QPFVGRWYN**DAAPENELYKVR**QPFVGRWYN**DAAKKDLNDNHVPVTPYFFETDLHOGKQMNLOS LKYNPAPILPRKVVDSTAFSSDKIEEILNHFS
VKHCATSLES MIDFTLSHLGTNNIIAMSTEVEKETPEVQTYTIEKVEEKANGKGVVCHKVAYPYAVHFCHDVGSTRTFMVSMVGADGTKVNAVSVCHEDTASMNPKALPFOLLNVKPGDKPICHFTLDDOIALFPSONALAEN

>lcl|Potato_tuber|TRINITY_DN47721_c1_g2_i4 (5' partial)
MGSWYQAAPENELHKVH**QPFVGVAVYN**DAAKKDLNDNHVPVTPYFFETDLHOGKKMNLOS LKYNPAPILPRKVVDSTAFSSDKIEEILNHFSVDKDSERAKDIKKTIKMCEDPAGNGE
VKHCATSLES MIDFTLSHLGTNNIIAMSTEVEKETPEVQTYTIEKVEEKANGKGVVCHKVAYPYAVHFCHDVGSTRTFMVSMVGADGTKVNAVSVCHEDTASMNPKALPFOLLNVKPGDKPICHFTLDDOIALFPSONALAEN

>lcl|Potato_tuber|TRINITY_DN48305_c1_g2_i2 (3' partial)
MELHHQYYFFTFVSVIFVVSAAANLSPEVYWRVKLPNTMPMTPPIKDALHISEKTAYNGDGNTKIS**QPYGVFAWYKAATENELHKVRQPYGVFAWYKAASENVLHKVRQPYG**

C LbaLycA hits of rnaSPAdes (v1.0) *de novo* transcriptome assembly (kmer 25,75):

>lcl|Potato_tuber|NODE_10739_length_1460_cov_677.901_ID_21479
MELHHQYYFFTLFVSVIFLVSAAANLSPEVYWRVKLPNTMPMTPPIKDALHISENELHKVR**QPYGVLAWYQAASENELHKVRQPYGVLAHQAAASENELHKVRQPYGVLAHQAAAPENEL**
HKVRQPYGVYRWYQAASENELHKVRQPYGVYRWYQAASENELHKVRQPYGVYRWYQAAPENELHKVRQPYGVSRWYNDAATKDLNDNHVPVTPYFFETDLHOGKKMNLOS LKYNPAPIL
LPRKVVDSTAFSSDKIEEILNHFSVDKDSERAKDIKKTIKMCEDPAGNGEVKHCATSLES MIDFTLSHLGTNNIIAMSTEVEKETPEVQTYTIEKVEEKANGKGVVCHKVAYPYAVHF
CHDVGSTRTFMVSMVGADGTKVNAVSVCHEDTASMNPKALPFOLLNVKPGDKPICHFTLDDOIALFPSONALAE*

>lcl|Potato_tuber|NODE_29201_length_620_cov_26.9761_ID_58407
MELHHQYYFFTLFVSVIFVVSAAANLSPEVYWRVKLPNTMPMTPPIKDALHISEKTAYNGDGNTKIS**QPWGVGAWYQDAPENELHKVRQPWGVGSWYQASPENLHKVRQPWGVVAVYQA**
ASENKLHKVRQPWGVGSWYQAAPENELHKVRQPYGVFRWYQAASENELHKVRQPWGVGSWYQDASENELHKVRQPWG

>lcl|Potato_tuber|NODE_26964_length_666_cov_44.9932_ID_53933
MELHHQYYFFTFVSVIFVVSAAANLSPEVYWRVKLPNTMPMTPPIKDALHISEKTAYNGDGNTKIS**QPYGVFAWYQAASENELHKVRQPYGVGDWYQAASENELHKVRQPYGVFAWYKA**
ITENELHKVRQPYGVFAWYKAATENELHKVRQPYGVFAWYKAASENELHKVRQPYGVFAWYNDAAKKDLNDNHVPVTPYFFETDLHOGKKM

>lcl|Potato_tuber|NODE_40653_length_459_cov_9.7474_ID_81309
IKDALHISEKTAYNGDGNTKIS**QPWGVGAWYQDAPENELHKVRQPWGVGSWYQASPENLHKVRQPWGVGAWYQAAPENELHKVRQPWGVGSWYQAAPENELHKVRQPYGVFRWYQA**
ASENELHKVRQPWGVGSWYQDASENELHKVRQPWG

D Core peptides from BURP domain precursor peptide genes:
Genome sequence (v4.03): QPWGVDSW, QPYGVGVW
Trinity transcriptome assembly: QPFVGRW, QPFVGVW, QPYGVGVW, QPWGVGRW, QPFVGVAV, **QPYGVFAW**
rnaSPAdes assembly: **QPYGVLAW, QPYGVYRW, QPYGVSRW, QPWGVGAW, QPWGVVAV, QPWGVGSW, QPYGVFRW, QPYGVFAW, QPYGVGDW**

Figure S26 | Genome and transcriptome mining of lyciumins from *Solanum tuberosum*. (A) Lyciumin precursor peptide derived from *Solanum tuberosum* genome (BURP domain underlined, core peptides highlighted in red). (B) Lyciumin precursor peptide transcripts derived from *Solanum tuberosum* tuber transcriptome (SRR5970148) *de novo* assembled with Trinity (v2.4, BURP domain underlined, core peptides highlighted in red). (C) Lyciumin precursor peptide transcripts derived from *Solanum tuberosum* tuber transcriptome (SRR5970148) *de novo* assembled with rnaSPAdes (v1.0, BURP domain underlined, core peptides highlighted in red). (D) Predicted lyciumin core peptides derived from genome mining and transcriptome mining of *Solanum tuberosum*. Bold core peptides indicate detected lyciumin chemotypes.

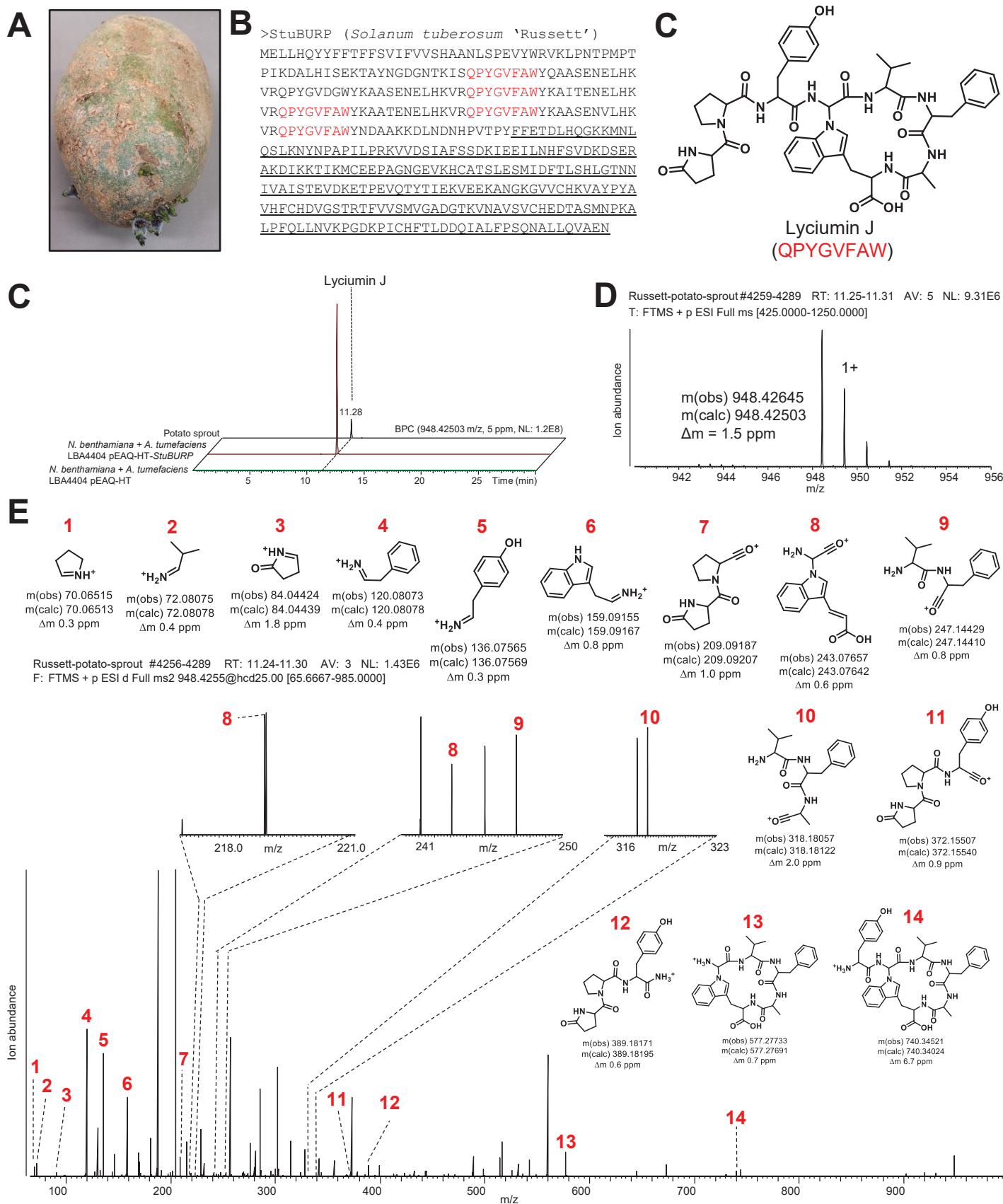


Figure S26 | Genome and transcriptome mining of lyciumins from *Solanum tuberosum*. (A) *Solanum tuberosum* 'Russett' – sprouting tuber. (B) *Solanum tuberosum* lyciumin J precursor peptide (BURP domain underlined, core peptide highlighted in red). (C) Predicted lyciumin J chemotype. (D) LC-MS chemotyping of predicted lyciumin J chemotype in peptide extract of *Solanum tuberosum* sprout and of *N. benthamiana* six days after infiltration with *A. tumefaciens* LBA4404 pEAQ-HT-*StuBURP*. (E) MS analysis of predicted lyciumin J chemotype of *Solanum tuberosum* sprout. (F) MS/MS analysis of predicted lyciumin J chemotype of *Solanum tuberosum* sprout.

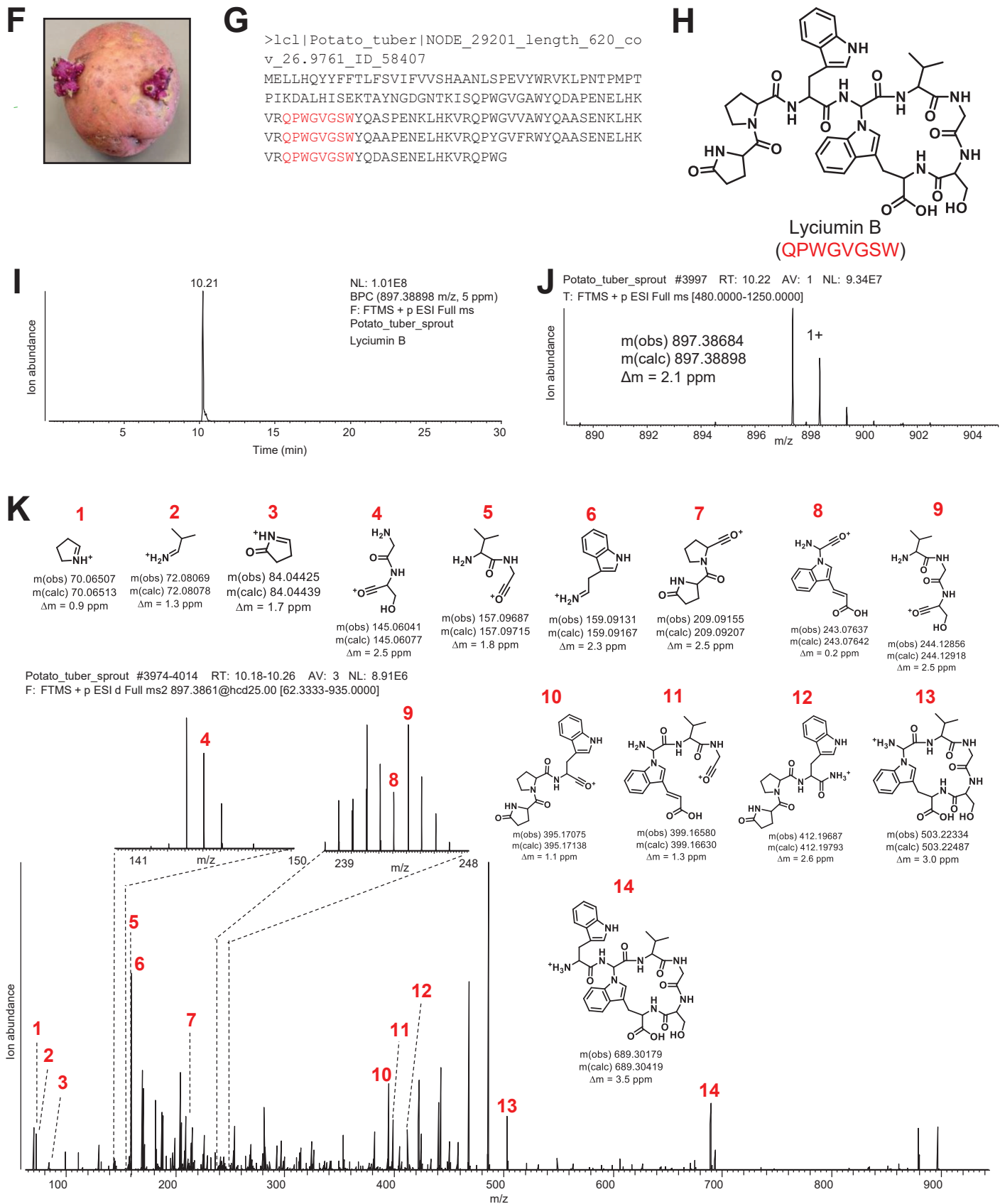


Figure S26 | Genome and transcriptome mining of lyciumins from *Solanum tuberosum*. (F) *Solanum tuberosum* 'Red potato' - sprouting tuber. (G) *Solanum tuberosum* lyciumin B precursor peptide transcript (BURP domain underlined, core peptides highlighted in red). (H) Predicted lyciumin B chemotype. (I) LC-MS chemotyping of predicted lyciumin B chemotype in peptide extract of *Solanum tuberosum* sprout. (J) MS analysis of predicted lyciumin B chemotype of *Solanum tuberosum* sprout. (K) MS/MS analysis of predicted lyciumin B chemotype of *Solanum tuberosum* sprout.

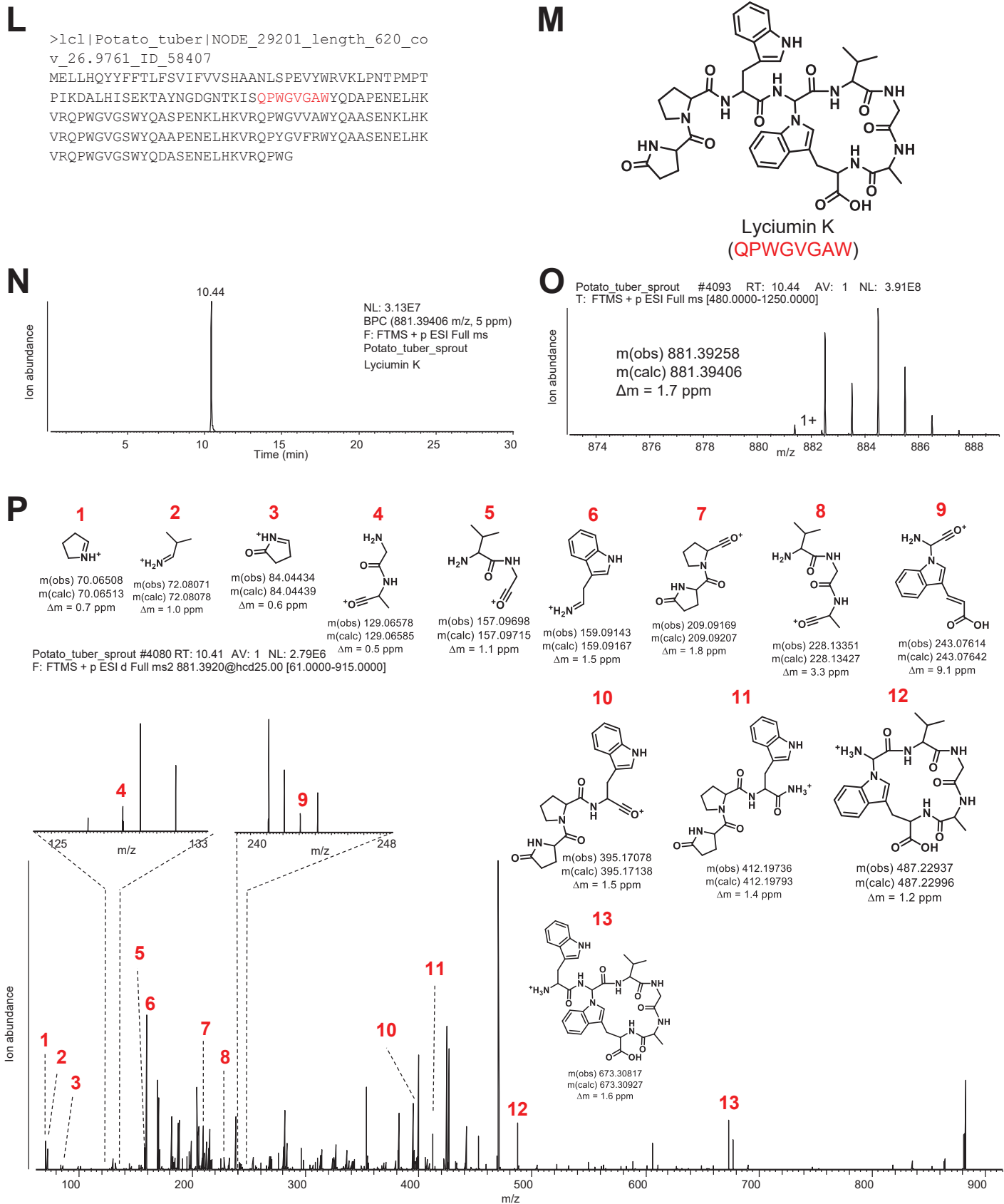


Figure S26 | Genome and transcriptome mining of lyciumins from *Solanum tuberosum*. (L) *Solanum tuberosum* lyciumin K precursor peptide transcript (BURP domain underlined, core peptides highlighted in red). (M) Predicted lyciumin K chemotype. (N) LC-MS chemotyping of predicted lyciumin K chemotype in peptide extract of *Solanum tuberosum* sprout. (O) MS analysis of predicted lyciumin K chemotype of *Solanum tuberosum* sprout. (P) MS/MS analysis of predicted lyciumin K chemotype of *Solanum tuberosum* sprout.

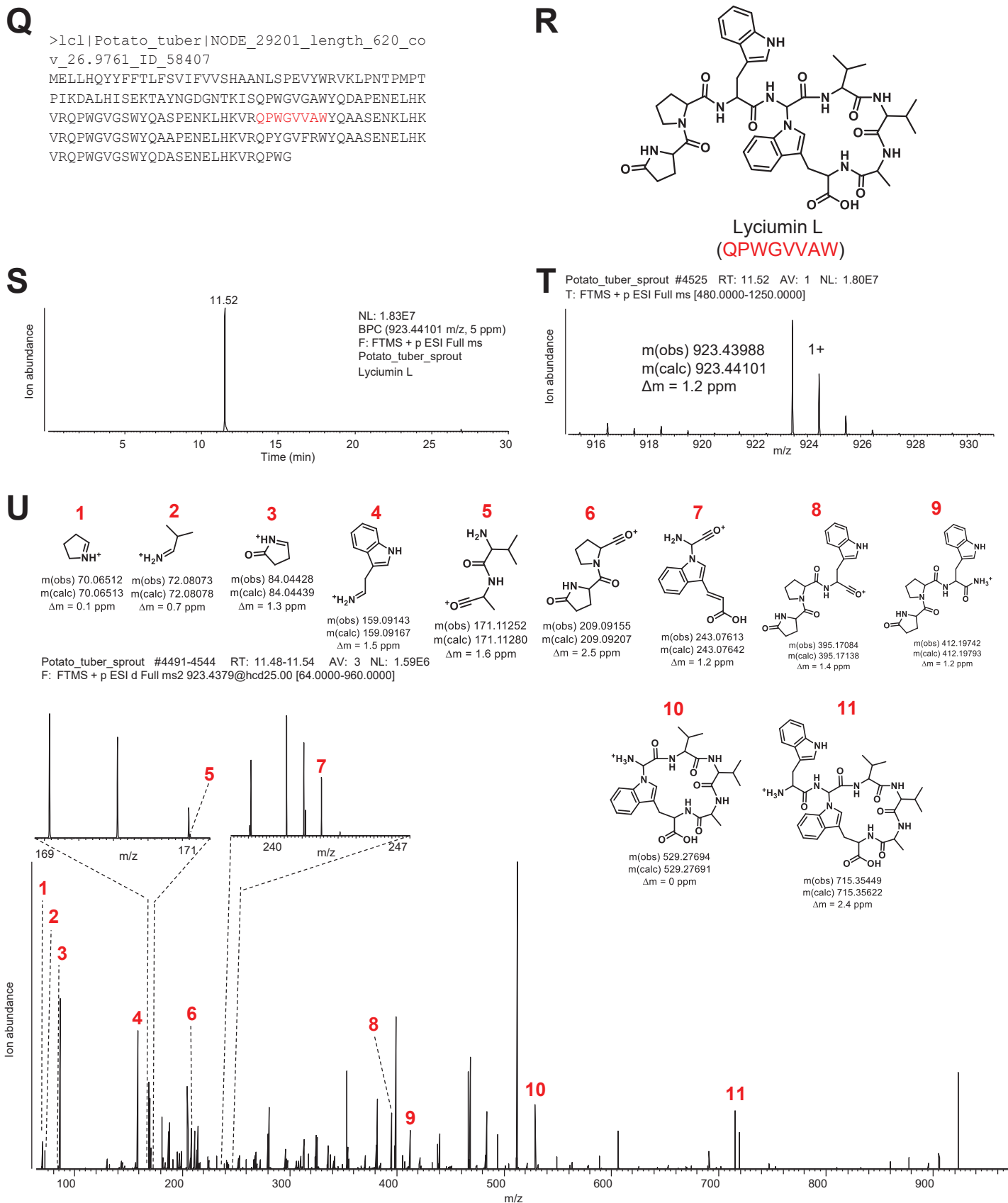


Figure S26 | Genome and transcriptome mining of lyciumins from *Solanum tuberosum*. (Q) *Solanum tuberosum* lyciumin L precursor peptide transcript (BURP domain underlined, core peptides highlighted in red). (R) Predicted lyciumin L chemotype. (S) LC-MS chemotyping of predicted lyciumin L chemotype in peptide extract of *Solanum tuberosum* sprout. (T) MS analysis of predicted lyciumin L chemotype of *Solanum tuberosum* sprout. (U) MS/MS analysis of predicted lyciumin L chemotype of *Solanum tuberosum* sprout.

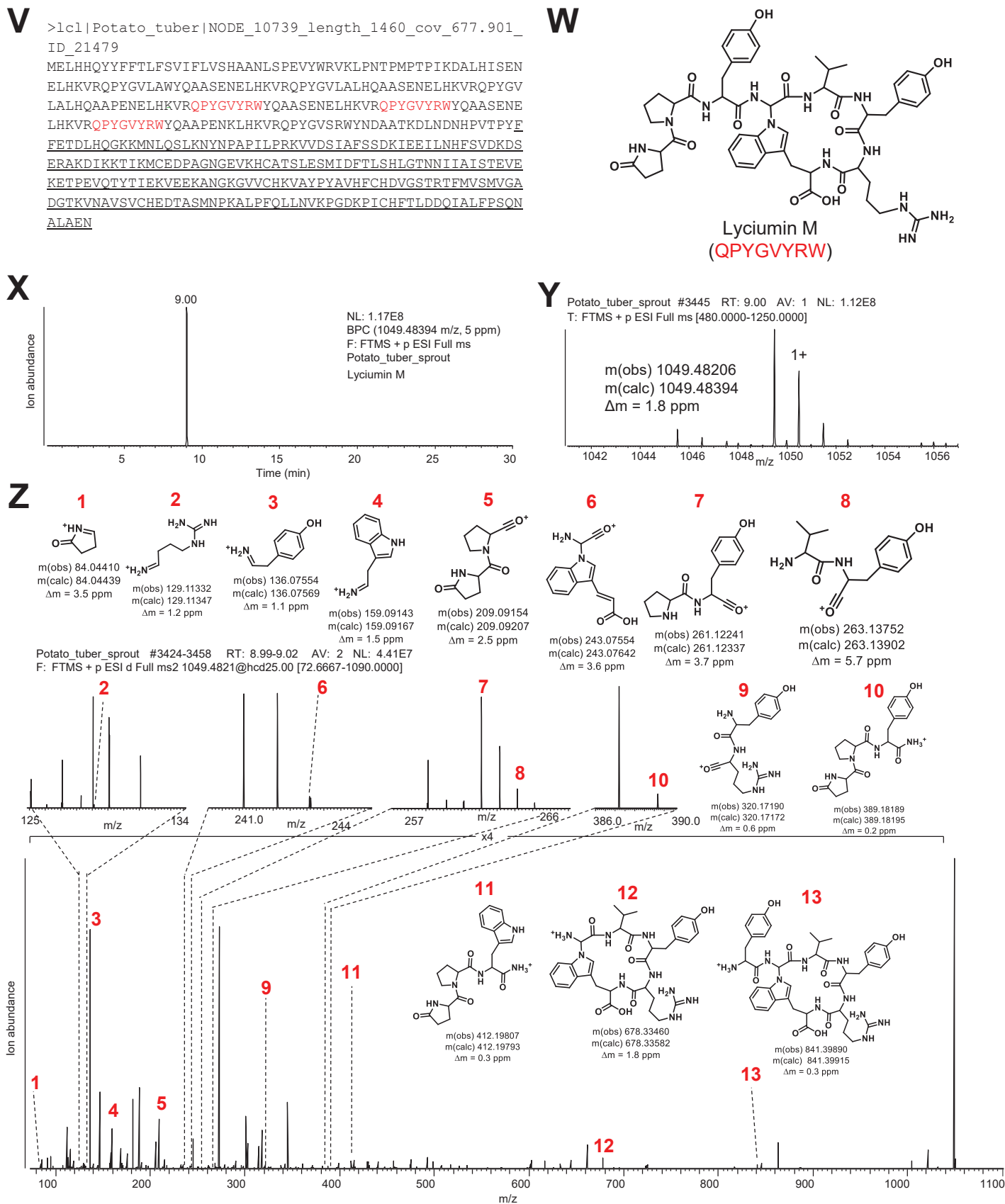


Figure S26 | Genome and transcriptome mining of lyciumins from *Solanum tuberosum*. (V) *Solanum tuberosum* lyciumin M precursor peptide transcript (BURP domain underlined, core peptides highlighted in red). (W) Predicted lyciumin M chemotype. (X) LC-MS chemotyping of predicted lyciumin M chemotype in peptide extract of *Solanum tuberosum* sprout. (Y) MS analysis of predicted lyciumin M chemotype of *Solanum tuberosum* sprout. (Z) MS/MS analysis of predicted lyciumin M chemotype of *Solanum tuberosum* sprout.

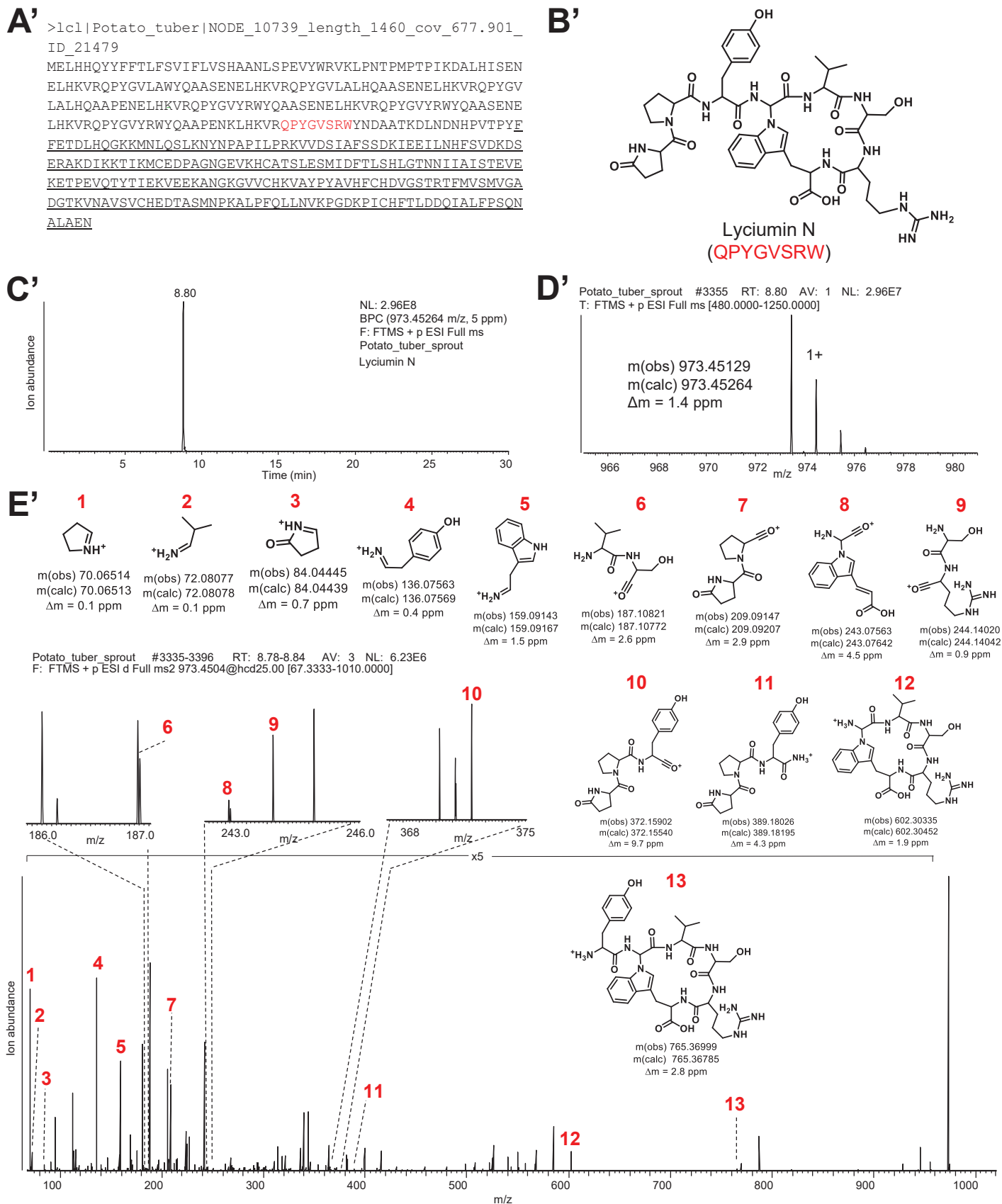


Figure S26 | Genome and transcriptome mining of lyciumins from *Solanum tuberosum*. (A') *Solanum tuberosum* lyciumin N precursor peptide transcript (BURP domain underlined, core peptides highlighted in red). (B') Predicted lyciumin N chemotype. (C') LC-MS chemotyping of predicted lyciumin N chemotype in peptide extract of *Solanum tuberosum* sprout. (D') MS analysis of predicted lyciumin N chemotype of *Solanum tuberosum* sprout. (E') MS/MS analysis of predicted lyciumin N chemotype of *Solanum tuberosum* sprout.

F'

```
>lcl|Potato_tuber|NODE_10739_length_1460_cov_677.901_
ID_21479
MELHHQYYFFTLFSVIFLVSHAANLSPEVYWRVKLPNTMPPTPIKDALHISEN
ELHKVRQPYGVLAWYQAASENELHKVRQPYGVLALHQAASENELHKVRQPYGV
LALHQAAPENELHKVRQPYGVRWYQAASENELHKVRQPYGVRWYQAASEN
LHKVRQPYGVRWYQAASENELHKVRQPYGVSRWYNDAATKDLNDNHPVTPYF
FETDLHQGKKMNLQSLKKNYPAPILPRKVVDSIAFSSDKIEILNHFSVDKDS
ERAKDIKKTIKMCEDPAGNGEVKHCATSLESMDIFTLSHLGTNNIIAISTEVE
KETPEVQTYTIEKVEEKANGKGVVCHKVAVPYAVHFCHDVGSTRTFMVSMVGA
DGTKVNAVSVCHEDTASMNPKALPFOLLNVKPGDKPICHFTLDDOIALFPSON
ALAEN
```

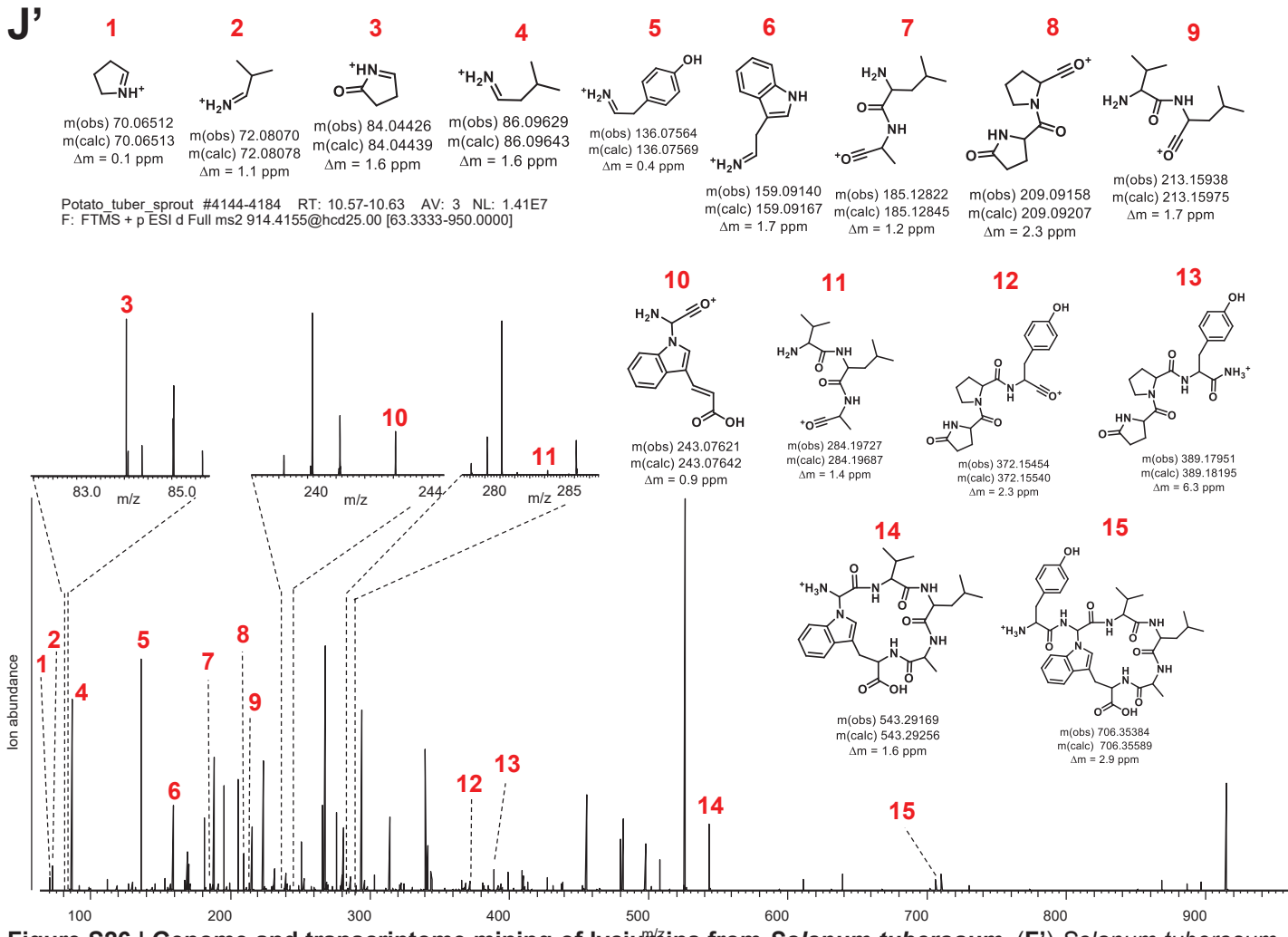
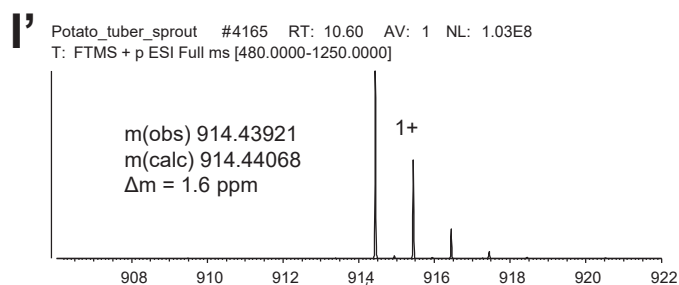
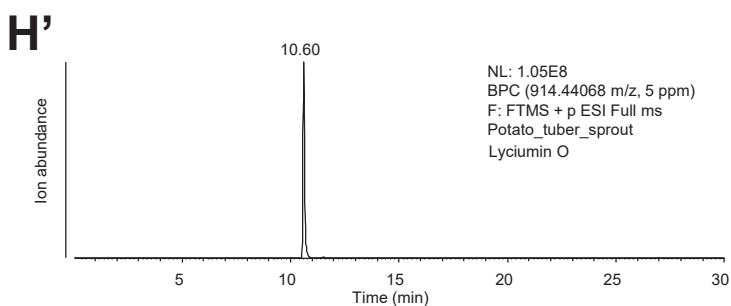
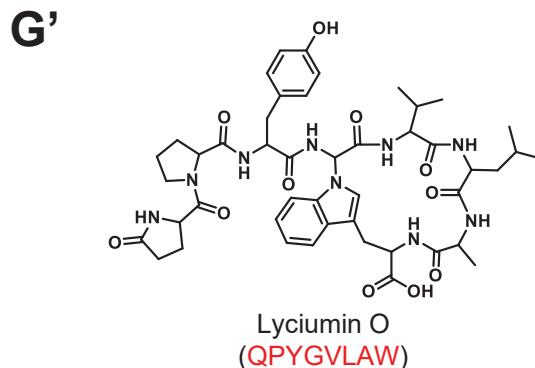


Figure S26 | Genome and transcriptome mining of lyciumins from *Solanum tuberosum*. (F') *Solanum tuberosum* lyciumin O precursor peptide transcript (BURP domain underlined, core peptides highlighted in red). (G') Predicted lyciumin O chemotype. (H') LC-MS chemotyping of predicted lyciumin O chemotype in peptide extract of *Solanum tuberosum* sprout. (I') MS analysis of predicted lyciumin O chemotype of *Solanum tuberosum* sprout. (J') MS/MS analysis of predicted lyciumin O chemotype of *Solanum tuberosum* sprout.

K'

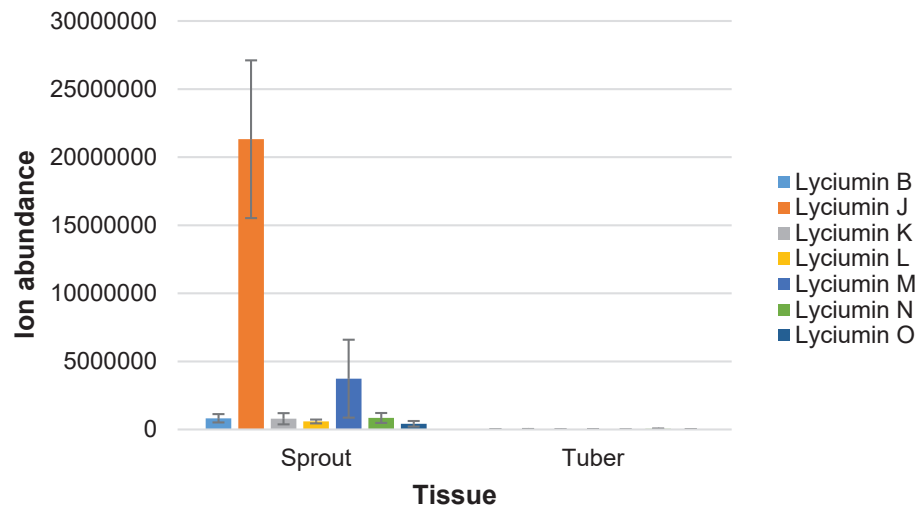


Figure S26 | Genome and transcriptome mining of lyciumins from *Solanum tuberosum*. (K') Chemotyping of lyciumins in sprout and tuber tissues of *Solanum tuberosum* ('red potato').

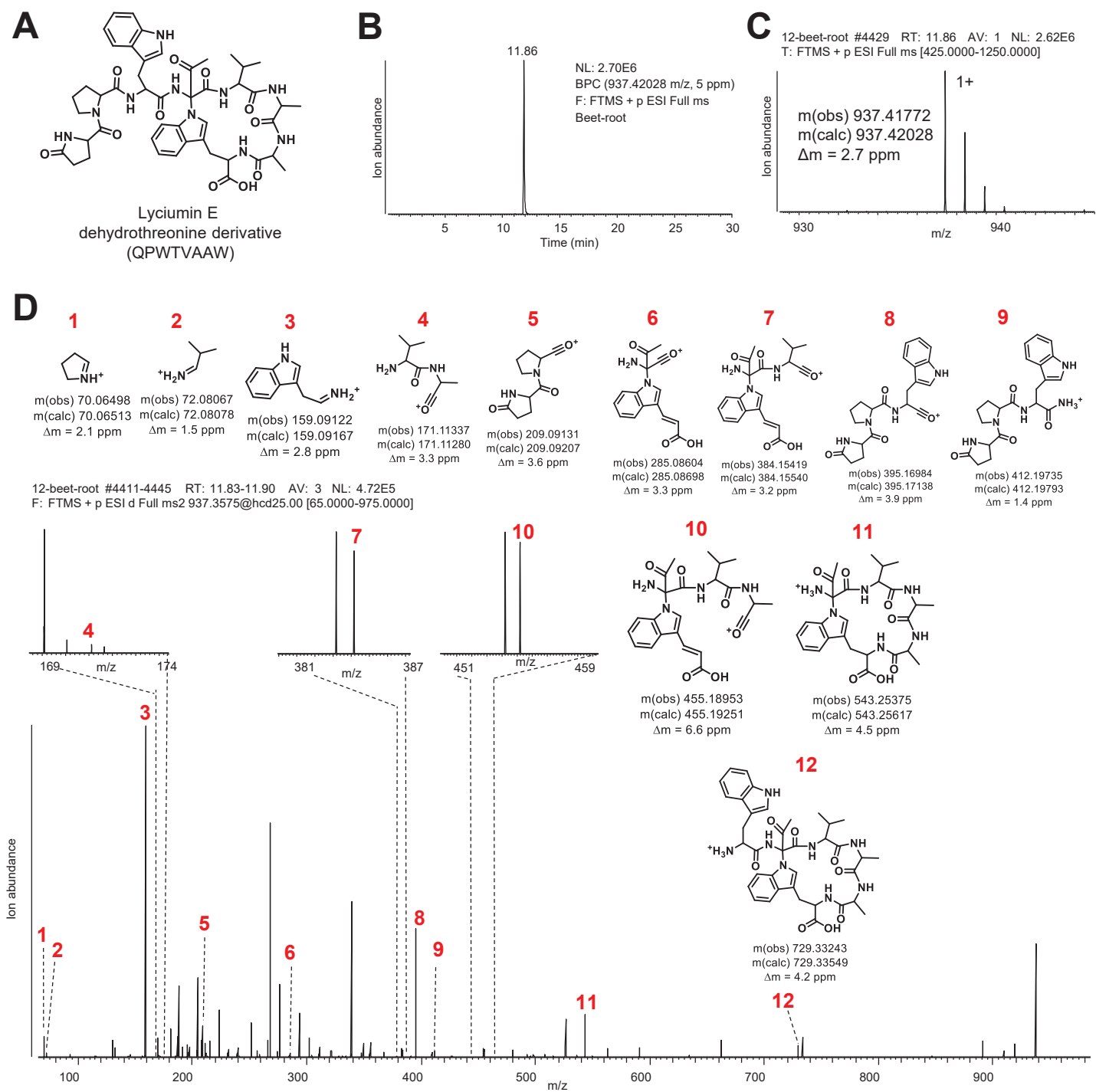


Figure S27 | Detection of candidate dehydrothreonine-lyciumin derivatives in Amaranthaceae. (A) Predicted *Beta vulgaris* lyciumin E dehydrothreonine derivative chemotype (core peptide). **(B)** LC-MS chemotyping of predicted lyciumin E dehydrothreonine derivative chemotype in peptide extract of *Beta vulgaris* root. **(C)** MS analysis of predicted lyciumin E dehydrothreonine derivative chemotype of *Beta vulgaris*. **(D)** MS/MS analysis of predicted lyciumin E dehydrothreonine derivative chemotype of *Beta vulgaris*.

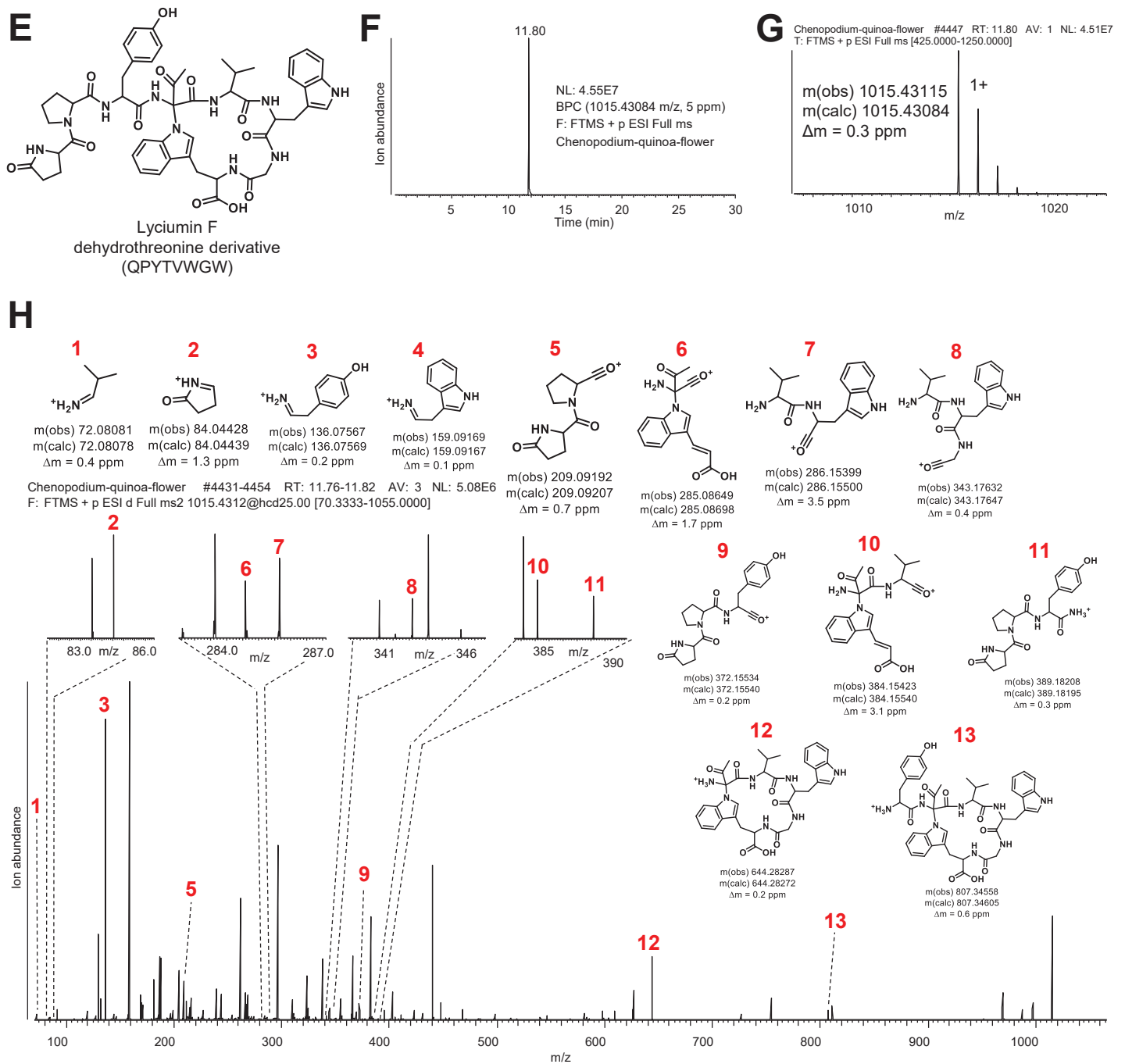


Figure S27 | Detection of candidate dehydrothreonine-lyciumin derivatives in Amaranthaceae. (E) Predicted *Chenopodium quinoa* lyciumin F dehydrothreonine derivative chemotype (core peptide). **(F)** LC-MS chemotyping of predicted lyciumin F dehydrothreonine derivative chemotype in peptide extract of *Chenopodium quinoa* flower. **(G)** MS analysis of predicted lyciumin F dehydrothreonine derivative chemotype of *Chenopodium quinoa*. **(H)** MS/MS analysis of predicted lyciumin F dehydrothreonine derivative chemotype of *Chenopodium quinoa*.

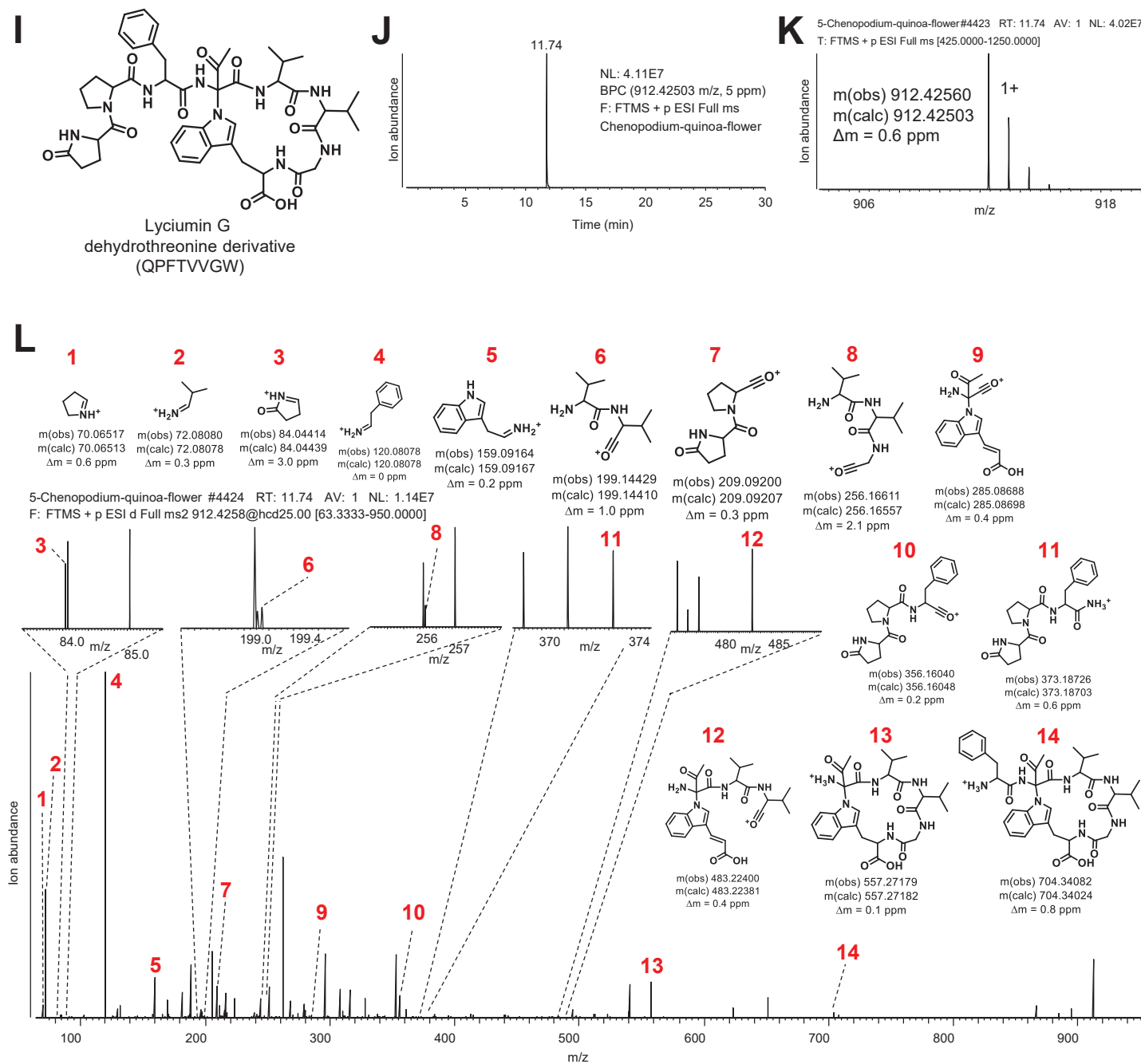


Figure S27 | Detection of candidate dehydrothreonine-lyciumin derivatives in Amaranthaceae. (I) Predicted *Chenopodium quinoa* lyciumin G dehydrothreonine derivative chemotype (core peptide). (J) LC-MS chemotyping of predicted lyciumin G dehydrothreonine derivative chemotype in peptide extract of *Chenopodium quinoa* flower. (K) MS analysis of predicted lyciumin G dehydrothreonine derivative chemotype of *Chenopodium quinoa*. (L) MS/MS analysis of predicted lyciumin G dehydrothreonine derivative chemotype of *Chenopodium quinoa*.

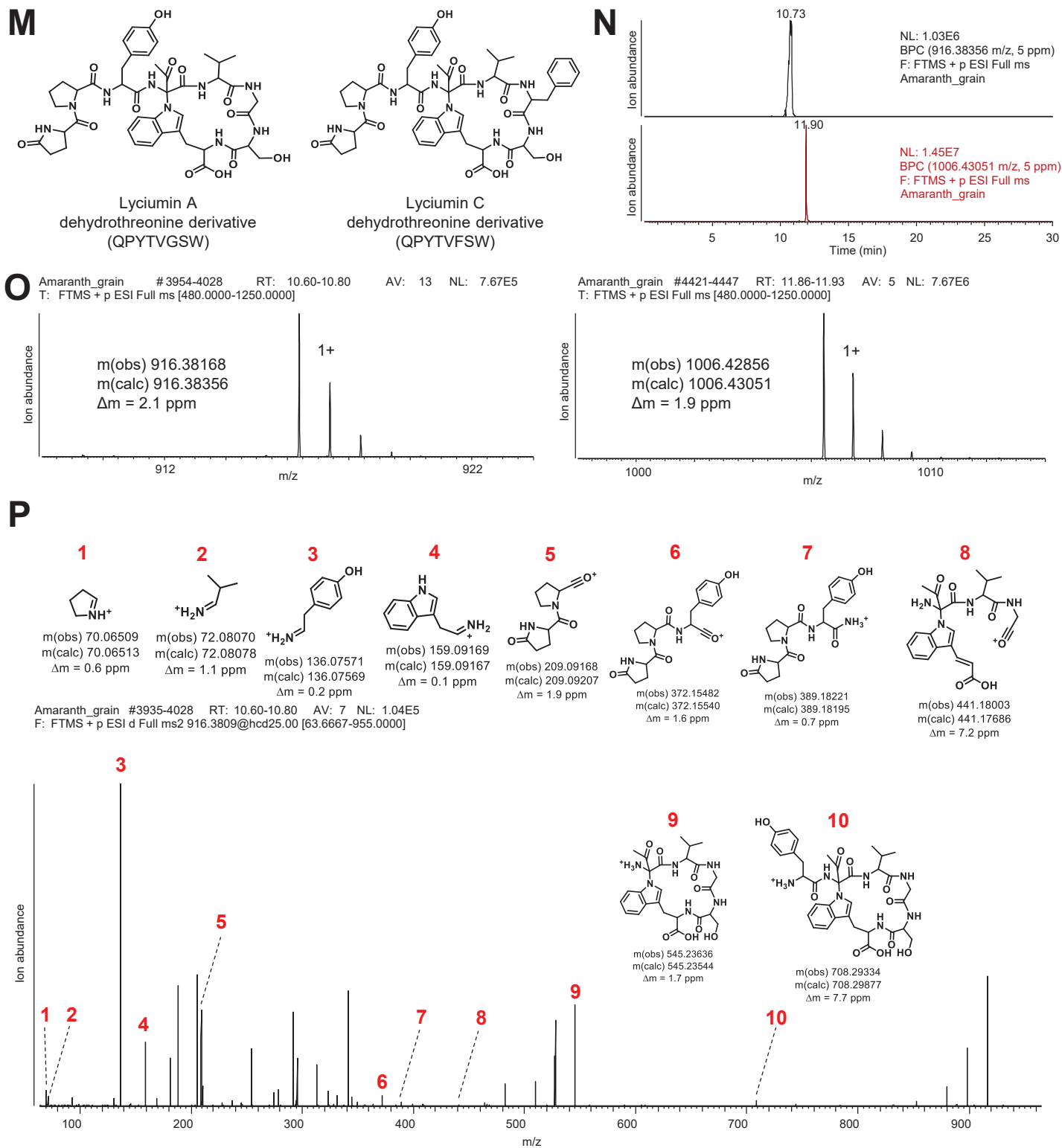


Figure S27 | Detection of candidate dehydrothreonine-lyciumin derivatives in Amaranthaceae. (M) Predicted *Amaranthus hypochondriacus* lyciumin A and C dehydrothreonine derivatives chemotypes (core peptide). **(N)** LC-MS chemotyping of predicted lyciumin A and C dehydrothreonine derivative chemotypes in peptide extract of *Amaranthus hypochondriacus* seeds. **(O)** MS analysis of predicted lyciumin A and C dehydrothreonine derivative chemotypes of *Amaranthus hypochondriacus*. **(P)** MS/MS analysis of predicted lyciumin A and C dehydrothreonine derivative chemotypes of *Amaranthus hypochondriacus*.

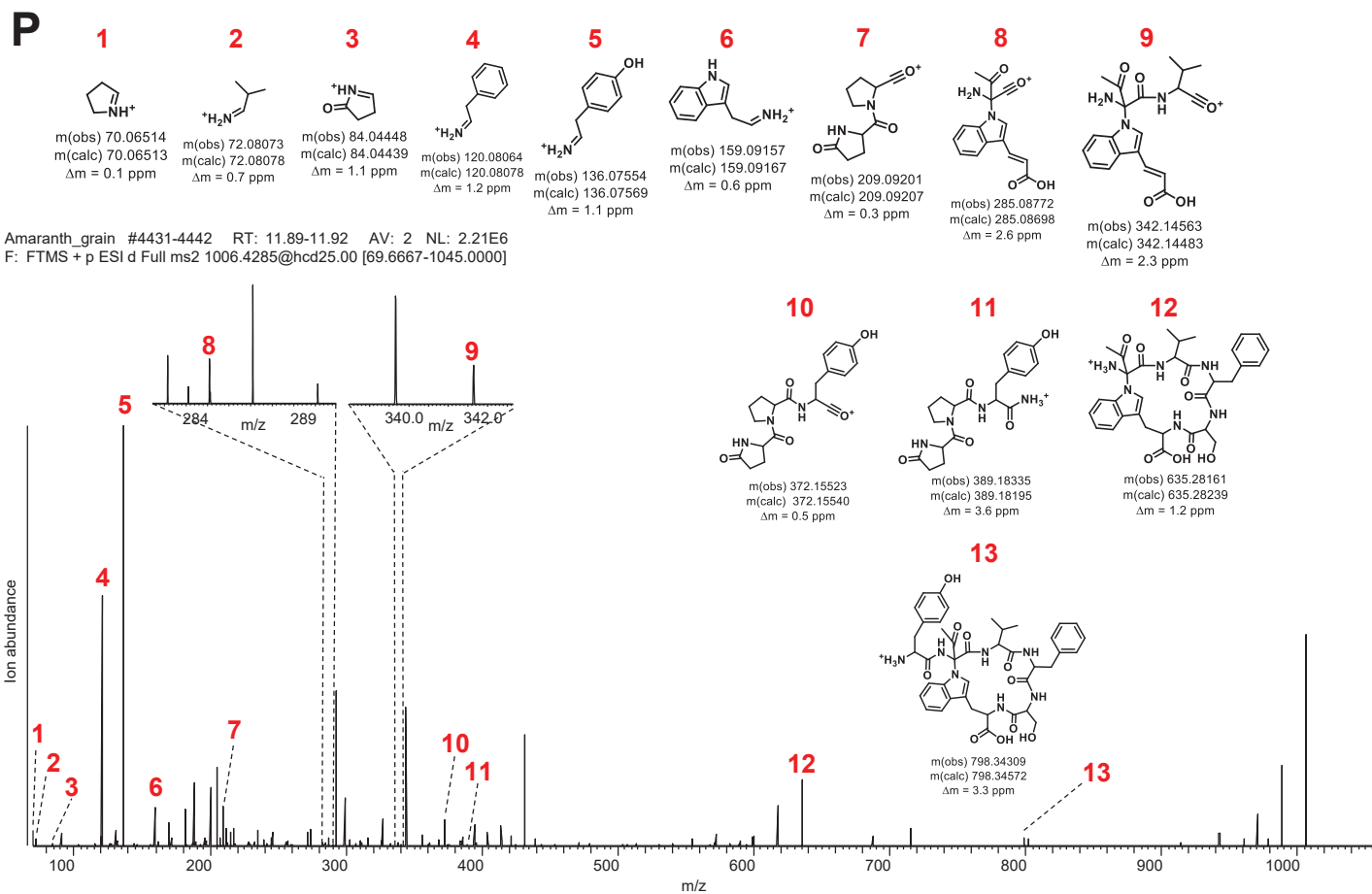


Figure S27 | Detection of candidate dehydrothreonine-lyciumin derivatives in Amaranthaceae. (P) MS/MS analysis of predicted lyciumin A and C dehydrothreonine derivative chemotypes of *Amaranthus hypochondriacus*.

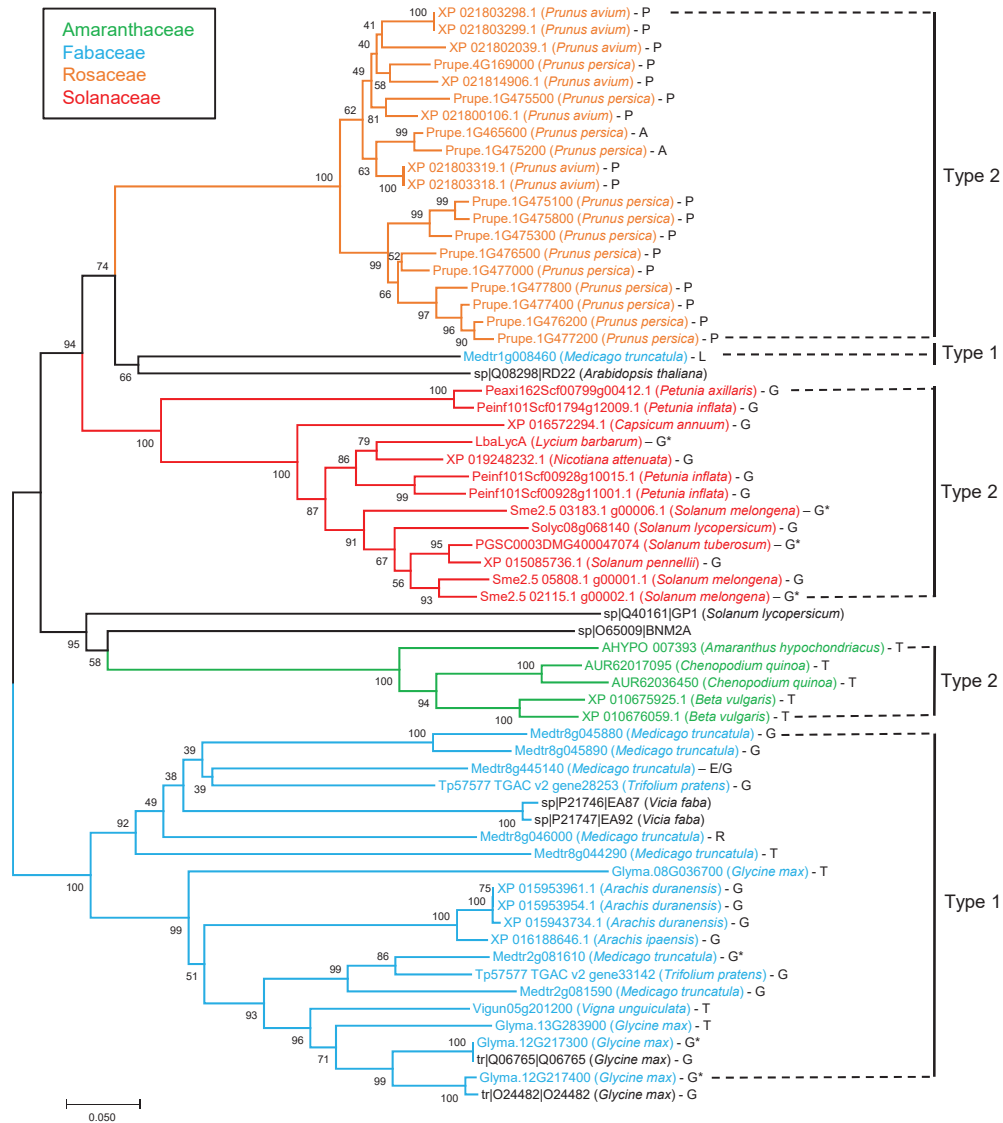


Figure S28 | Phylogenetic analysis of predicted and characterized lyciumin precursors from analyzed plant genomes. A neighbor-joining phylogenetic tree of the BURP-domain sequences of lyciumin precursors predicted from plant genomes and founding members of BURP domain protein family generated with 2000 bootstrap generations using the p-distance method. The scale measures evolutionary distances in substitutions per amino acid. Precursors with characterized chemotypes are noted with an asterisk. Predicted cyclization sites at the fourth core peptide position of precursor peptides are noted after species name as capital letter (Abbreviations: A – alanine, G – glycine, L – leucine, P – proline, R – arginine, T – threonine).

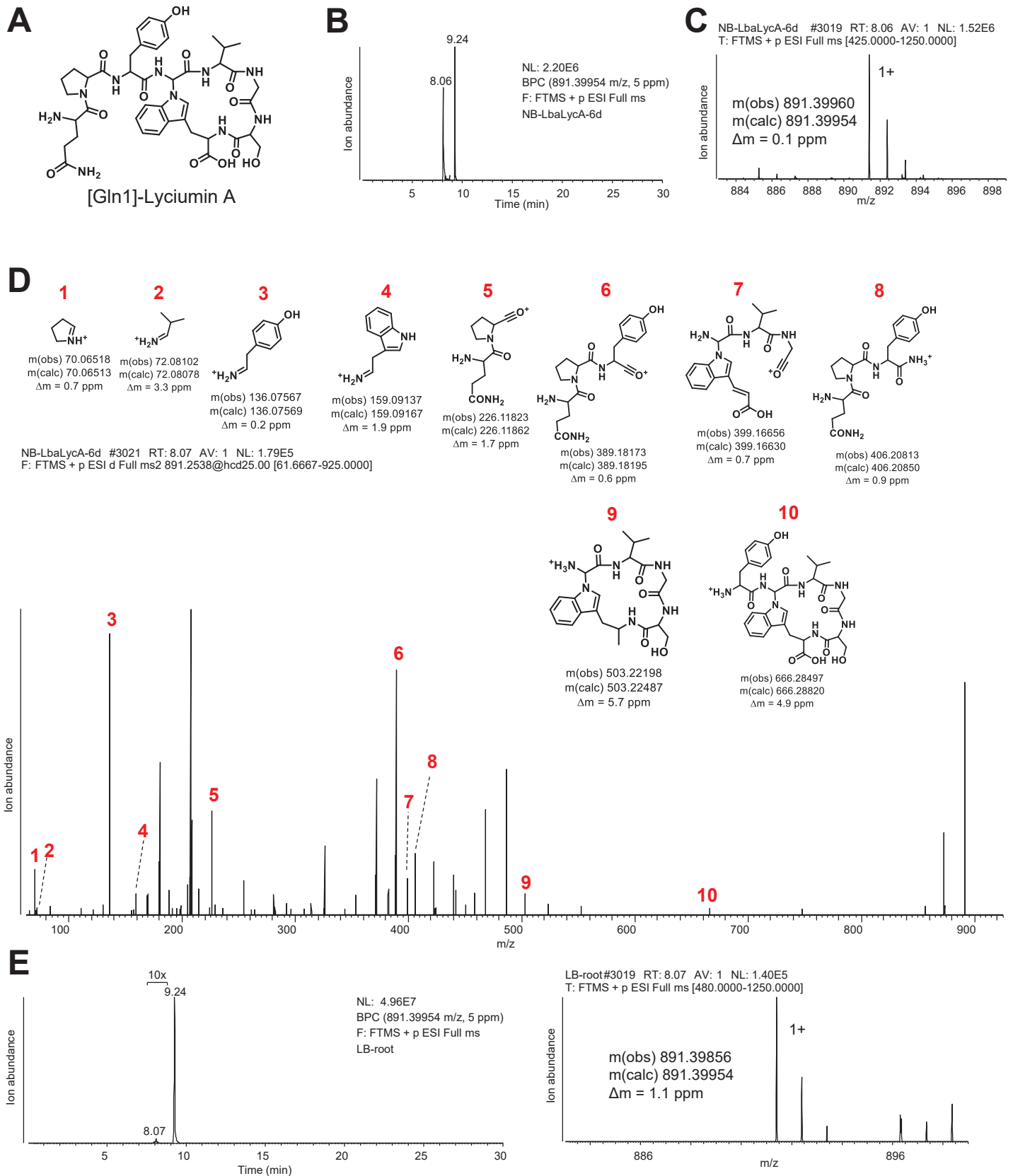


Figure S29 | Detection of [Gln1]-lyciumins after heterologous expression of *LbaLycA* in *Nicotiana benthamiana*. (A) [Gln1]-lyciumin A chemotype. (B) LC-MS chemotyping of [Gln1]-lyciumin A chemotype in peptide extract of *N. benthamiana* six days after infiltration with *A. tumefaciens* LBA4404 pEAQ-HT-*LbaLycA*. (C) MS analysis of [Gln1]-lyciumin A chemotype in peptide extract of *N. benthamiana* six days after infiltration with *A. tumefaciens* LBA4404 pEAQ-HT-*LbaLycA*. (D) MS/MS analysis [Gln1]-lyciumin A chemotype in peptide extract of *N. benthamiana* leaves six days after infiltration with *A. tumefaciens* LBA4404 pEAQ-HT-*LbaLycA*. (E) LC-MS chemotyping of [Gln1]-lyciumin A chemotype in peptide extract of *Lycium barbarum* root.

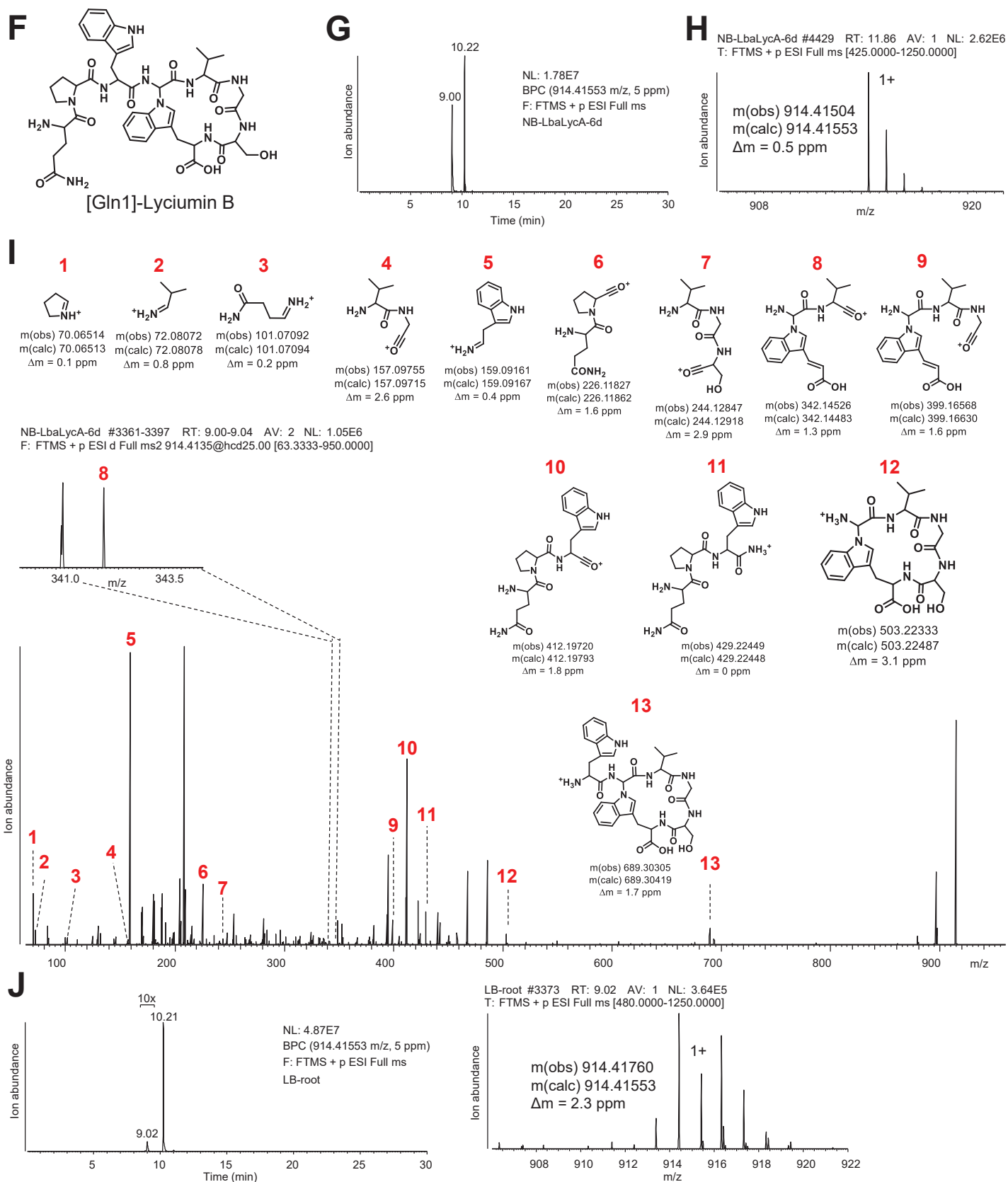


Figure S29 | Detection of [Gln1]-lyciumins after heterologous expression of *LbaLycA* in *Nicotiana benthamiana*. (F) [Gln1]-lyciumin B chemotype. (G) LC-MS chemotyping of [Gln1]-lyciumin B chemotype in peptide extract of *N. benthamiana* six days after infiltration with *A. tumefaciens* LBA4404 pEAQ-HT-*LbaLycA*. (H) MS analysis of [Gln1]-lyciumin B chemotype in peptide extract of *N. benthamiana* six days after infiltration with *A. tumefaciens* LBA4404 pEAQ-HT-*LbaLycA*. (I) MS/MS analysis [Gln1]-lyciumin B chemotype in peptide extract of *N. benthamiana* six days after infiltration with *A. tumefaciens* LBA4404 pEAQ-HT-*LbaLycA*. (J) LC-MS chemotyping of [Gln1]-lyciumin B chemotype in peptide extract of *Lycium barbarum* root.

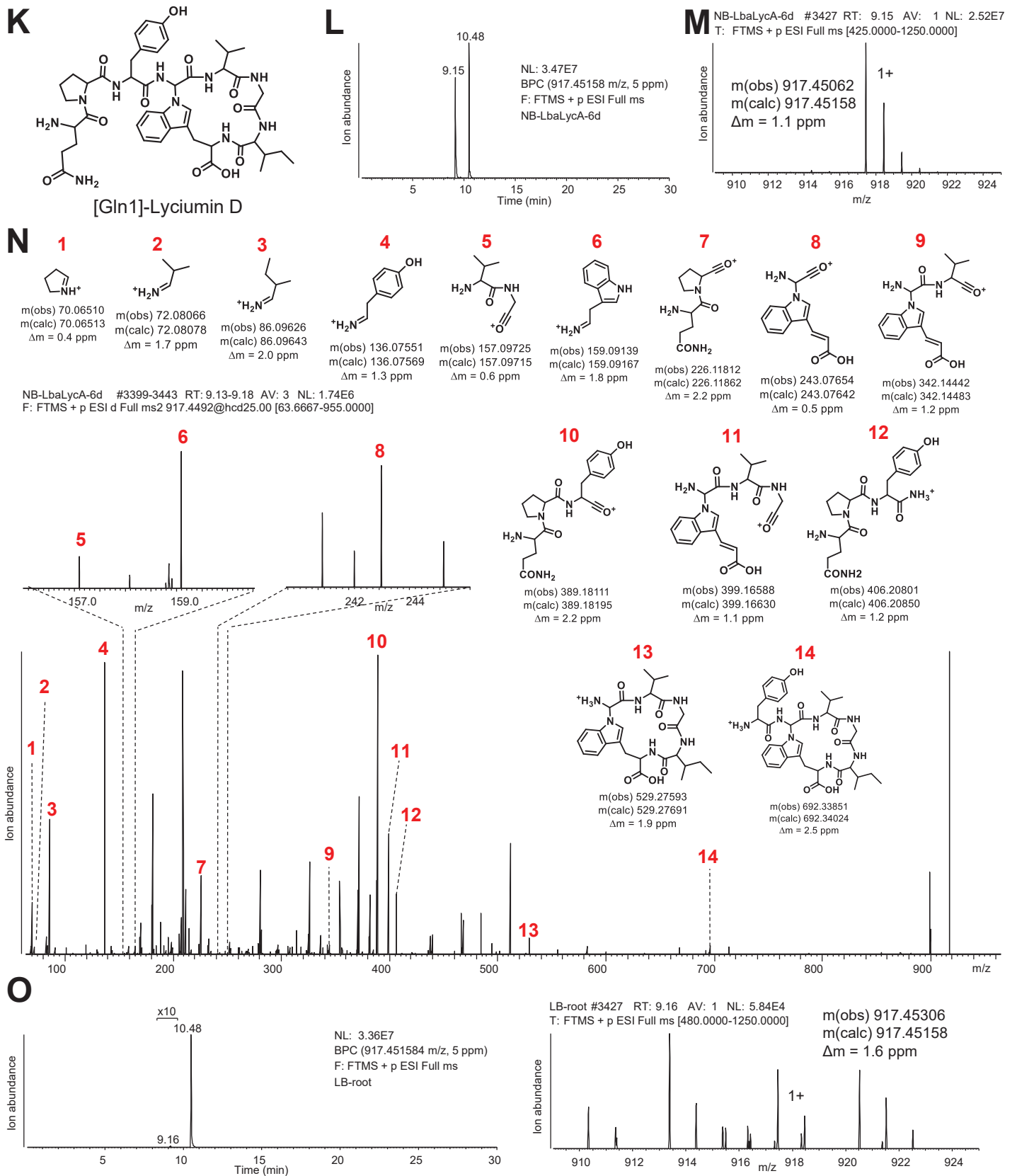


Figure S29 | Detection of [Gln1]-lyciumins after heterologous expression of *LbaLycA* in *Nicotiana benthamiana*. (K) [Gln1]-lyciumin D chemotype. (L) LC-MS chemotyping of [Gln1]-lyciumin D chemotype in peptide extract of *N. benthamiana* six days after infiltration with *A. tumefaciens* LBA4404 pEAQ-HT-*LbaLycA*. (M) MS analysis of [Gln1]-lyciumin D chemotype in peptide extract of *N. benthamiana* six days after infiltration with *A. tumefaciens* LBA4404 pEAQ-HT-*LbaLycA*. (N) MS/MS analysis [Gln1]-lyciumin D chemotype in peptide extract of *N. benthamiana* six days after infiltration with *A. tumefaciens* LBA4404 pEAQ-HT-*LbaLycA*. (O) LC-MS chemotyping of [Gln1]-lyciumin D chemotype in peptide extract of *Lycium barbarum* root.

A

>LbaQC

MPLLNPRFLVISLIVLLSITVFREAEASYRVYKVKVVNEFPHPDQAYTQGLLYAENNTLFESTGLYGRSSVRKVALLDGKVERLHEMESSYFGEGLTLLGE
 RLFQLTWLLDTGFIYDRYNFSKFKKFTTHMQDGWGLATDGKVLFGSDGTSTLYKIDPKTMKVIRKQVVKSQGHEVRYLNELEYVKAEVWANVYVTDCIARI
 SPKDGTVIGWILLQSLREELISRGYKDFEVLNGIAWDRDGRIFVTGKLPKLFKIKLLPLTPNDPLAGEINNLICIPKTSFLEI

B

Gene	Size [aa]	RSEM [TPM]	Transcript rank (Total transcript #)	Similarity/Identity [%/%] to precursor co-localized <i>Chenopodium quinoa</i> QC (AUR62017096-RA)
<i>LbaQC</i>	287	42	3365 (100355)	72/61
<i>LbaLycA</i>	543	13397	13 (100355)	-

Figure S30 | Characterization of *Lycium barbarum* glutamine cyclotransferase (LbaQC). (A) LbaQC sequence with predicted secretory pathway signaling peptide underlined (SignalP v4.1). (B) Bioinformatic analysis of candidate lyciumin-glutamine cyclotransferase LbaQC from root transcriptome of *Lycium barbarum*.

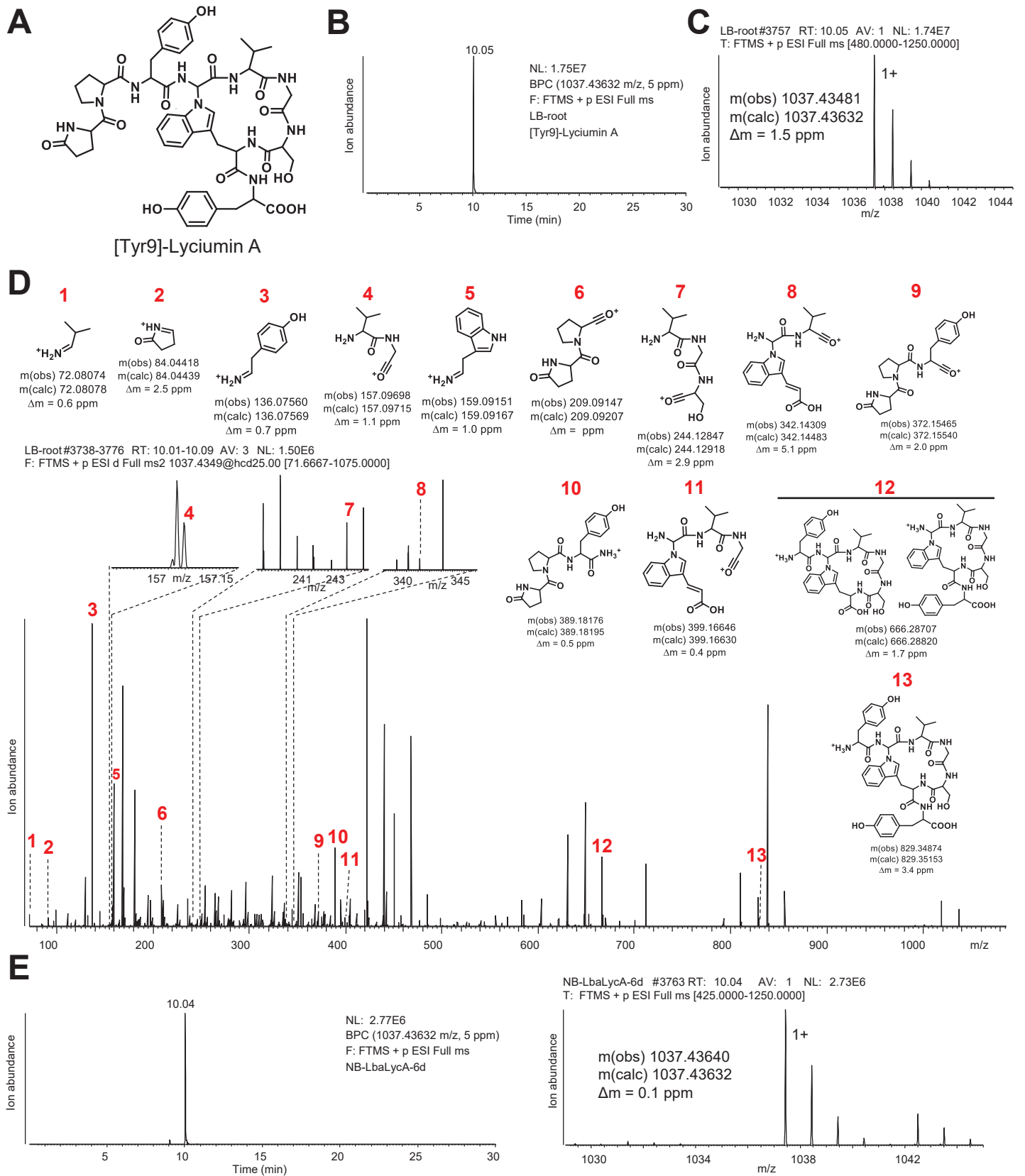


Figure S31 | Detection of C-terminally extended lyciumins after *LbaLycA* heterologous expression in *Nicotiana benthamiana*. (A) [Tyr9]-lyciumin A chemotype. (B) LC-MS chemotyping of [Tyr9]-lyciumin A chemotype in peptide extract of *Lycium barbarum* root. (C) MS analysis of [Tyr9]-lyciumin A chemotype in peptide extract of *Lycium barbarum* root. (D) MS/MS analysis [Tyr9]-lyciumin A chemotype in peptide extract of *Lycium barbarum* root. (E) LC-MS chemotyping of [Tyr9]-lyciumin A chemotype in peptide extract of *N. benthamiana* six days after infiltration with *A. tumefaciens* LBA4404 pEAQ-HT-*LbaLycA*.

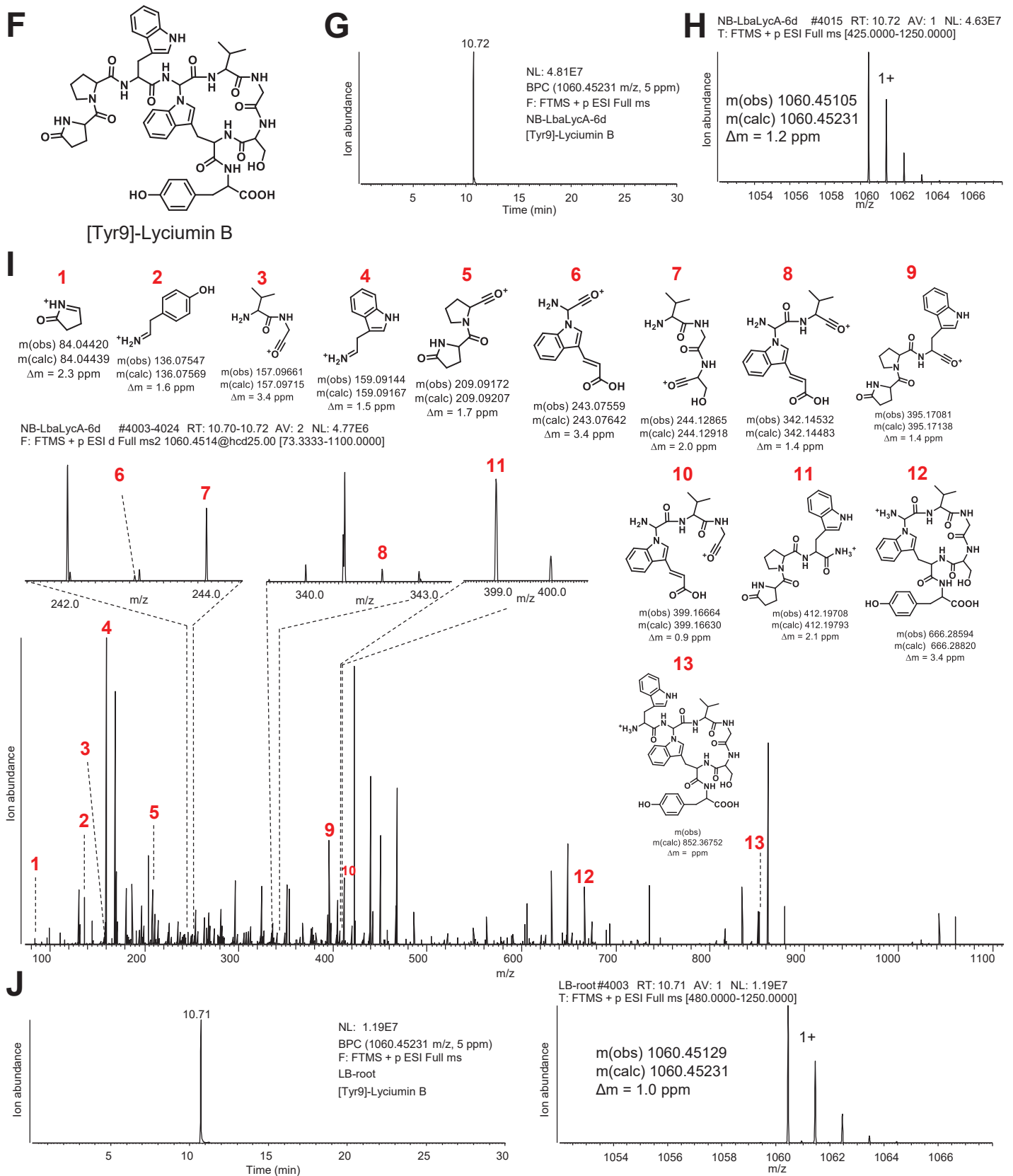


Figure S31 | Detection of C-terminally extended lyciumins after *LbaLycA* heterologous expression in *Nicotiana benthamiana*. (F) [Tyr9]-lyciumin B chemotype. (G) LC-MS chemotyping of [Tyr9]-lyciumin B chemotype in peptide extract of *N. benthamiana* six days after infiltration with *A. tumefaciens* LBA4404 pEAQ-HT-*LbaLycA*. (H) MS analysis of [Tyr9]-lyciumin B chemotype in peptide extract of *N. benthamiana* six days after infiltration with *A. tumefaciens* LBA4404 pEAQ-HT-*LbaLycA*. (I) MS/MS analysis [Tyr9]-lyciumin B chemotype in peptide extract of *N. benthamiana* six days after infiltration with *A. tumefaciens* LBA4404 pEAQ-HT-*LbaLycA*. (J) LC-MS chemotyping of [Tyr9]-lyciumin B chemotype in peptide extract of *Lycium barbarum* root.

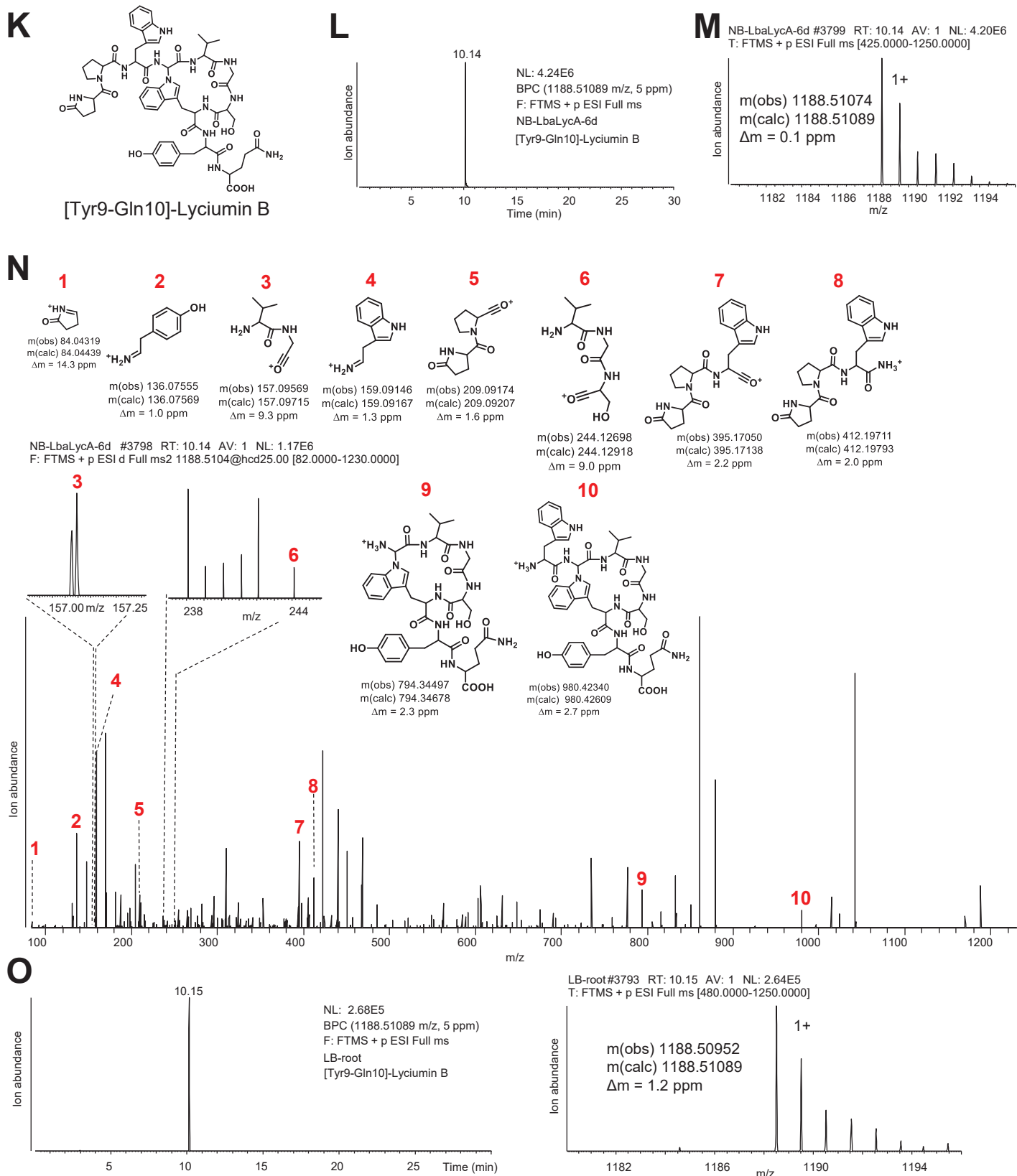


Figure S31 | Detection of C-terminally extended lyciumins after *LbaLycA* heterologous expression in *Nicotiana benthamiana*. (K) [Tyr9-Gln10]-lyciumin B chemotype. (L) LC-MS chemotyping of [Tyr9-Gln10]-lyciumin B chemotype in peptide extract of *N. benthamiana* six days after infiltration with *A. tumefaciens* LBA4404 pEAQ-HT-*LbaLycA*. (M) MS analysis of [Tyr9-Gln10]-lyciumin B chemotype in peptide extract of *N. benthamiana* six days after infiltration with *A. tumefaciens* LBA4404 pEAQ-HT-*LbaLycA*. (N) MS/MS analysis [Tyr9-Gln10]-lyciumin B chemotype in peptide extract of *N. benthamiana* six days after infiltration with *A. tumefaciens* LBA4404 pEAQ-HT-*LbaLycA*. (O) LC-MS chemotyping of [Tyr9-Gln10]-lyciumin B chemotype in peptide extract of *Lycium barbarum* root.

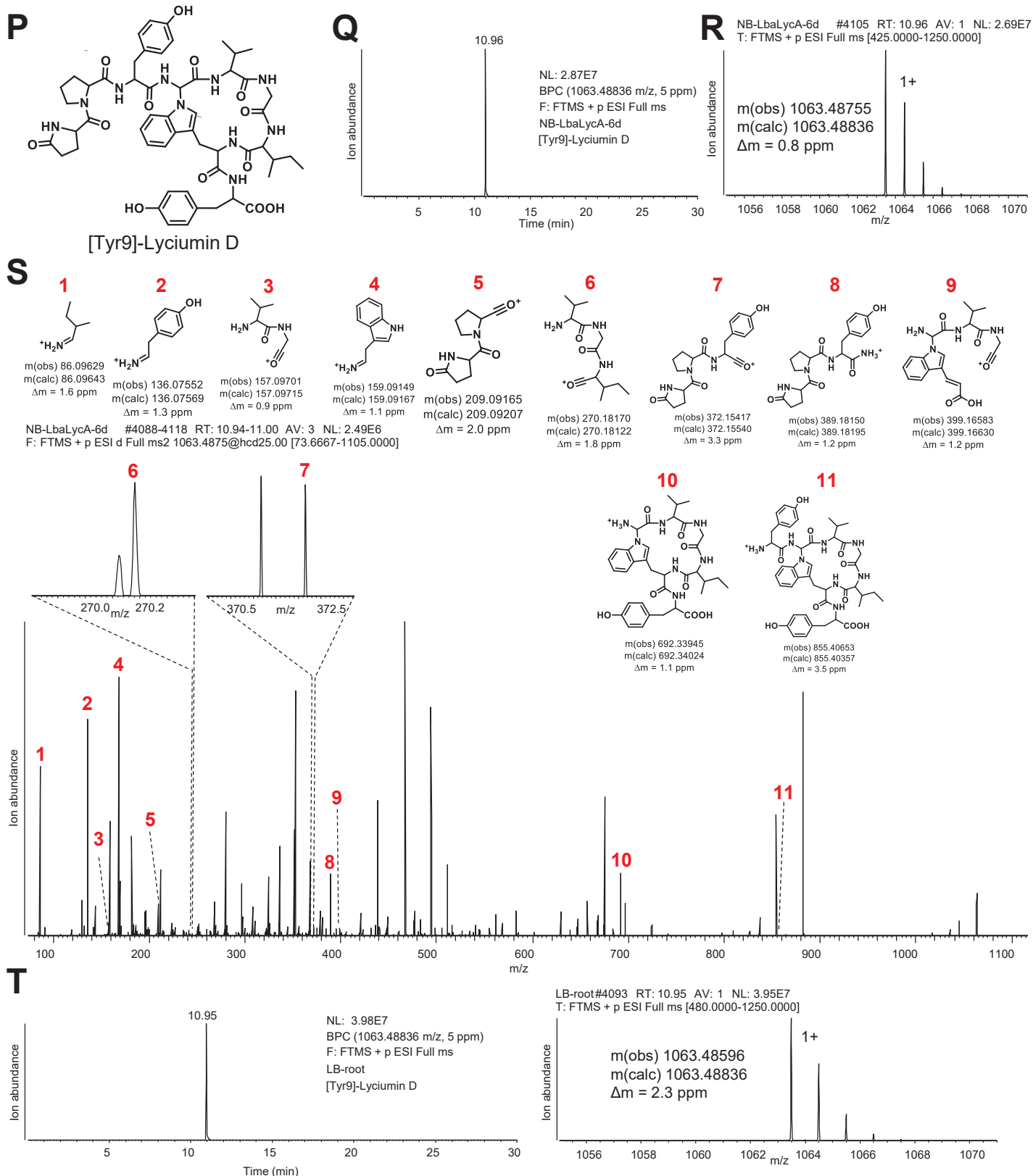


Figure S31 | Detection of C-terminally extended lyciumins after *LbaLycA* heterologous expression in *Nicotiana benthamiana*. (P) [Tyr9]-lyciumin D chemotype. (Q) LC-MS chemotyping of [Tyr9]-lyciumin D chemotype in peptide extract of *N. benthamiana* six days after infiltration with *A. tumefaciens* LBA4404 pEAQ-HT-*LbaLycA*. (R) MS analysis of [Tyr9]-lyciumin D chemotype in peptide extract of *N. benthamiana* six days after infiltration with *A. tumefaciens* LBA4404 pEAQ-HT-*LbaLycA*. (S) MS/MS analysis [Tyr9]-lyciumin D chemotype in peptide extract of *N. benthamiana* six days after infiltration with *A. tumefaciens* LBA4404 pEAQ-HT-*LbaLycA*. (T) LC-MS chemotyping of [Tyr9]-lyciumin D chemotype in peptide extract of *Lycium barbarum* root.

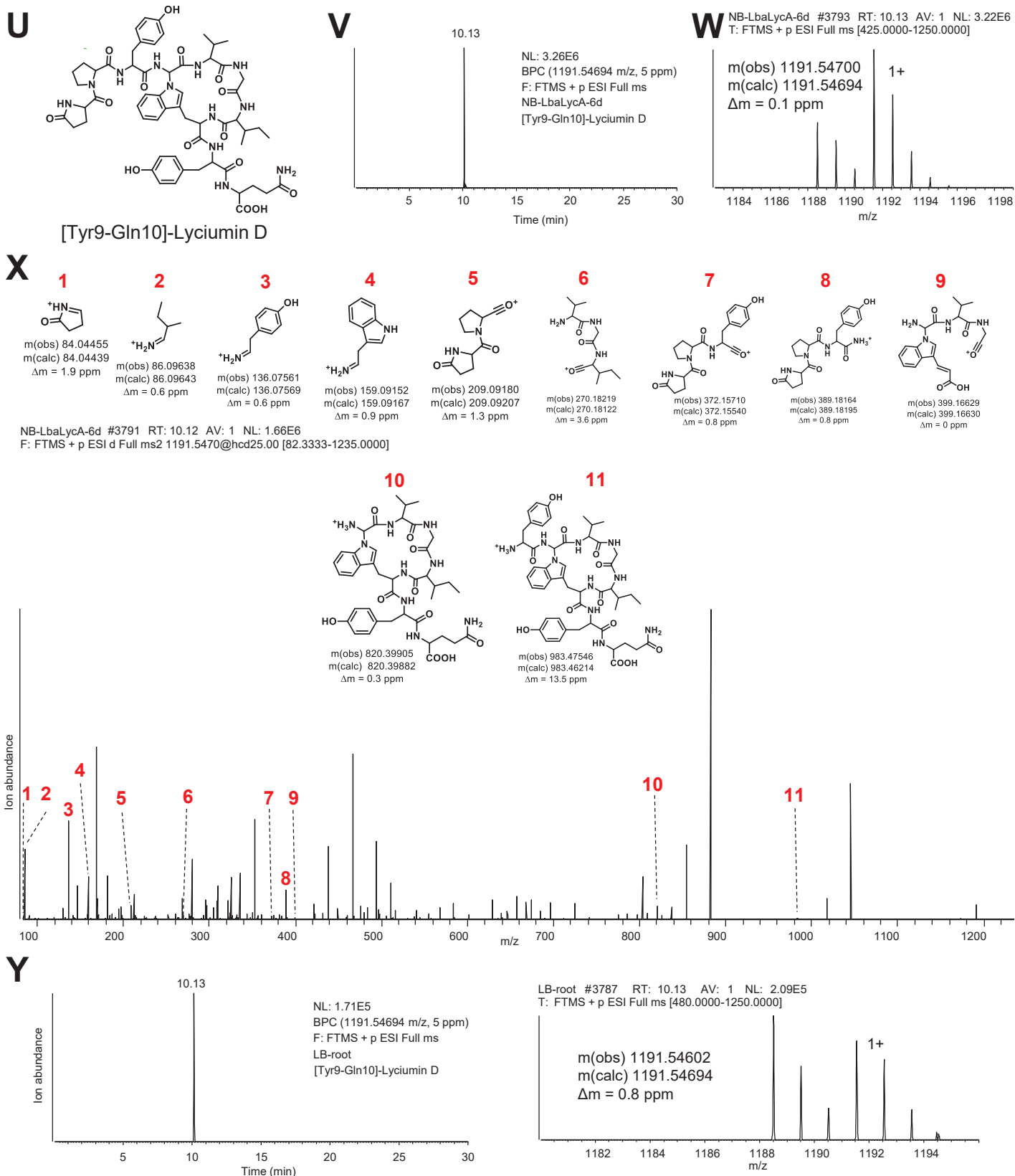


Figure S31 | Detection of C-terminally extended lyciumins after *LbaLycA* heterologous expression in *Nicotiana benthamiana*. (U) [Tyr9-Gln10]-lyciumin D chemotype. (V) LC-MS chemotyping of [Tyr9-Gln10]-lyciumin D chemotype in peptide extract of *N. benthamiana* six days after infiltration with *A. tumefaciens* LBA4404 pEAQ-HT-*LbaLycA*. (W) MS analysis of [Tyr9-Gln10]-lyciumin D chemotype in peptide extract of *N. benthamiana* six days after infiltration with *A. tumefaciens* LBA4404 pEAQ-HT-*LbaLycA*. (X) MS/MS analysis [Tyr9-Gln10]-lyciumin D chemotype in peptide extract of *N. benthamiana* six days after infiltration with *A. tumefaciens* LBA4404 pEAQ-HT-*LbaLycA*. (Y) LC-MS chemotyping of [Tyr9-Gln10]-lyciumin D chemotype in peptide extract of *Lycium barbarum* root.

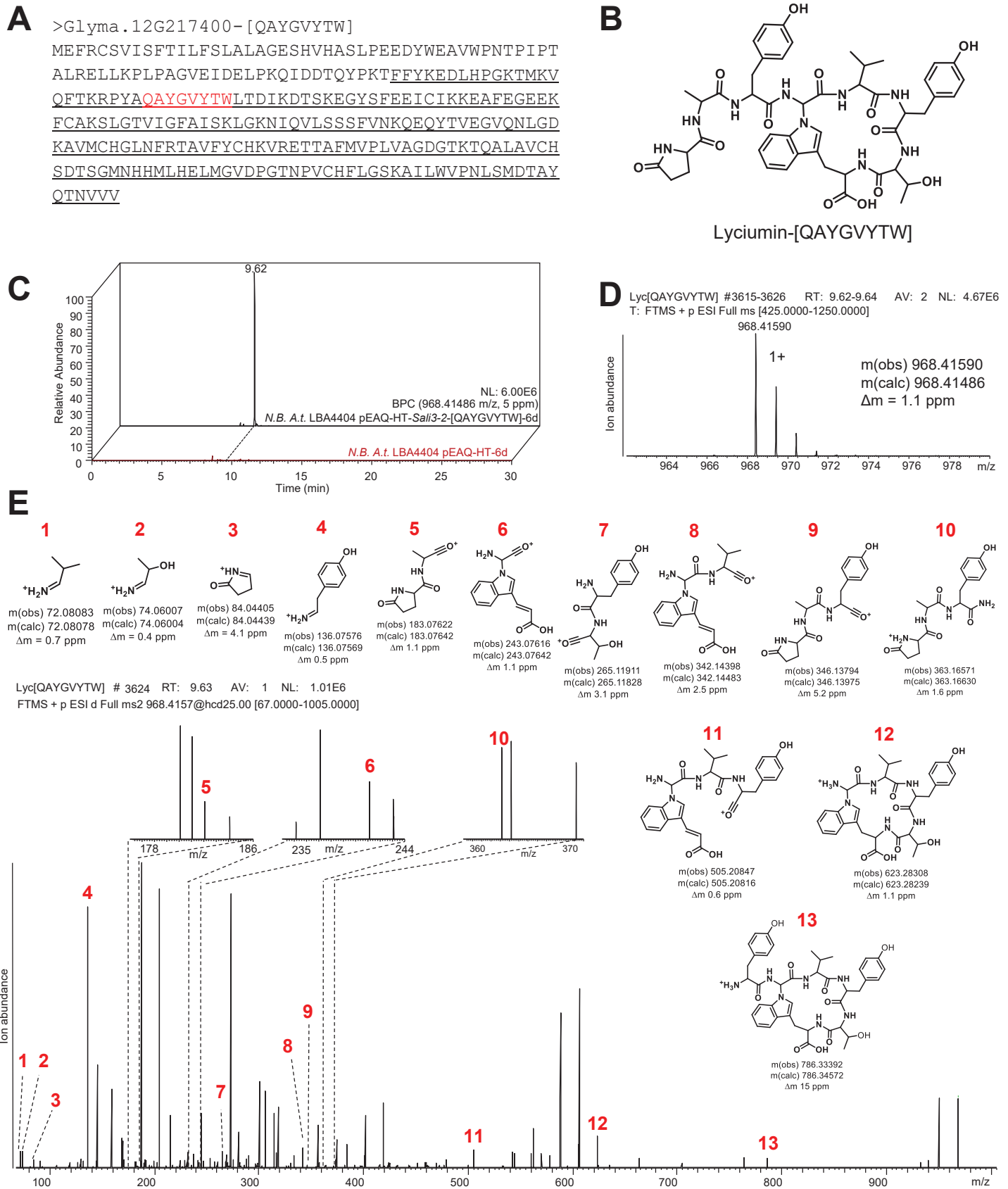


Figure S32 | Heterologous expression of *Sali3-2*-[QAYGVYTW] in *Nicotiana benthamiana*. (A) *Sali3-2*-[QAYGVYTW] lyciumin precursor peptide (BURP domain underlined, core peptide highlighted in red). (B) Predicted [QAYGVYTW]-lyciumin chemotype. (C) LC-MS chemotyping of predicted [QAYGVYTW]-lyciumin in peptide extract of *N. benthamiana* leaves infiltrated with *A. tumefaciens* LBA4404 pEAQ-HT-*Sali3-2*-[QAYGVYTW] for six days. (D) MS analysis of predicted [QAYGVYTW]-lyciumin chemotype. (E) MS/MS analysis of predicted [QAYGVYTW]-lyciumin chemotype.

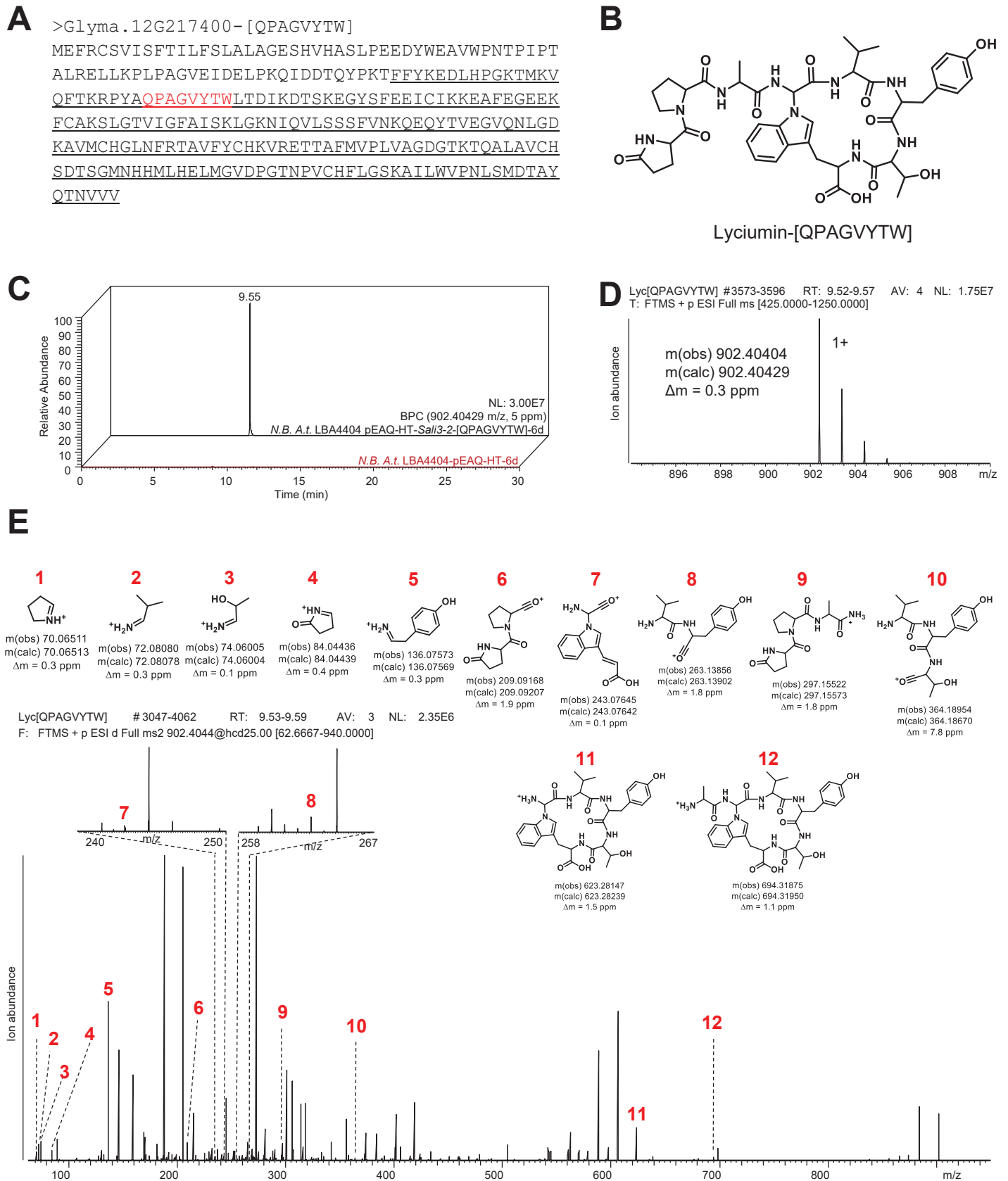


Figure S33 | Heterologous expression of *Sali3-2*-[QPAGVYTW] in *Nicotiana benthamiana*. (A) *Sali3-2*-[QPAGVYTW] lyciumin precursor peptide (BURP domain underlined, core peptide highlighted in red). (B) Predicted [QPAGVYTW]-lyciumin chemotype. (C) LC-MS chemotyping of predicted [QPAGVYTW]-lyciumin in peptide extract of *N. benthamiana* leaves infiltrated with *A. tumefaciens* LBA4404 pEAQ-HT-*Sali3-2*-[QPAGVYTW] for six days. (D) MS analysis of predicted [QPAGVYTW]-lyciumin chemotype. (E) MS/MS analysis of predicted [QPAGVYTW]-lyciumin chemotype.

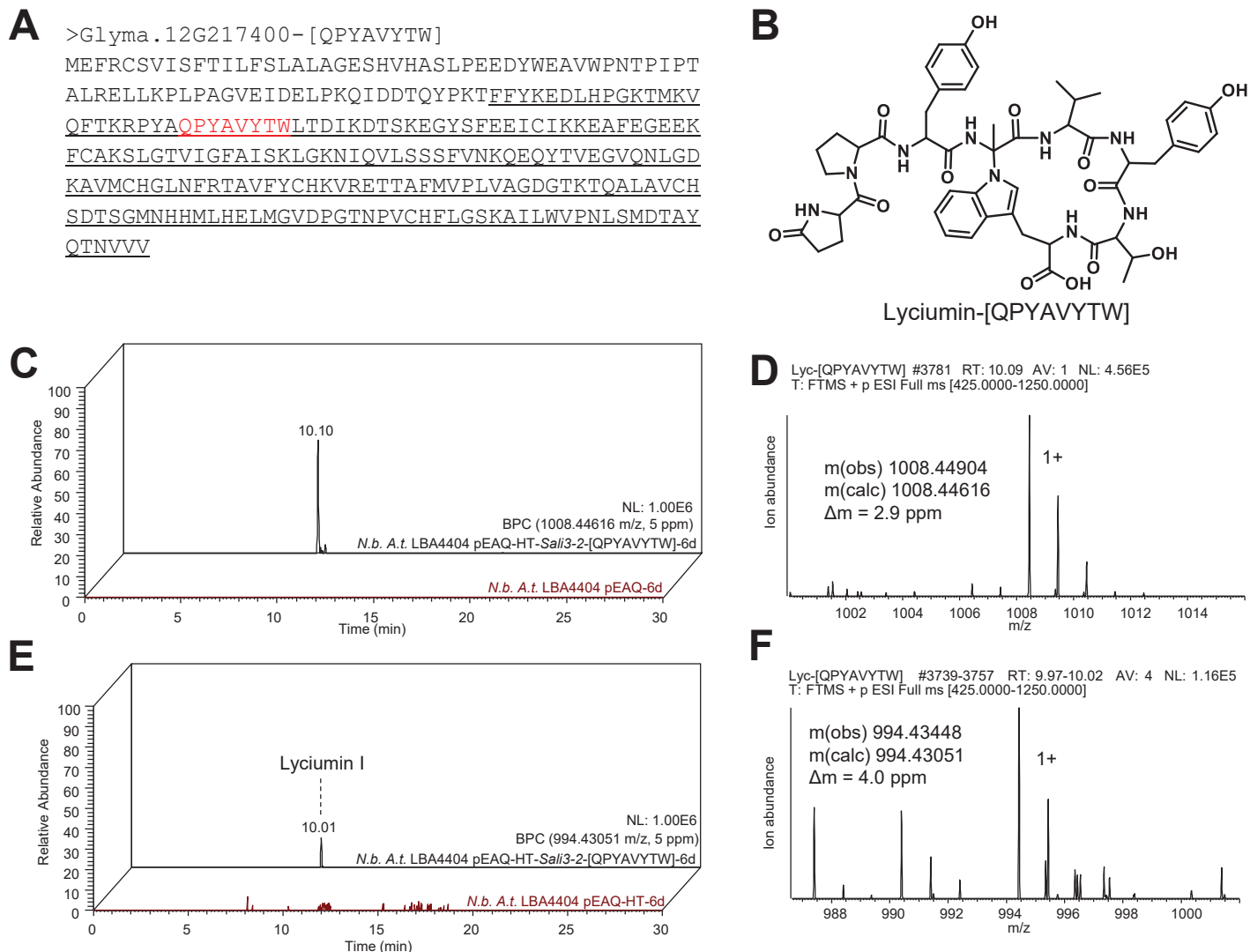


Figure S34 | Heterologous expression of *Sali3-2*-[QPYAVYTW] in *Nicotiana benthamiana*. (A) *Sali3-2*-[QPYAVYTW] lyciumin precursor peptide (BURP domain underlined, core peptide highlighted in red). (B) Predicted [QPYAVYTW]-lyciumin chemotype. (C) LC-MS chemotyping of predicted [QPYAVYTW]-lyciumin in peptide extract of *N. benthamiana* leaves infiltrated with *A. tumefaciens* LBA4404 pEAQ-HT-*Sali3-2*-[QPYAVYTW] for six days. (D) MS analysis of predicted [QPYAVYTW]-lyciumin chemotype. (E) LC-MS chemotyping of lyciumin I in peptide extract of *N. benthamiana* leaves infiltrated with *A. tumefaciens* LBA4404 pEAQ-HT-*Sali3-2*-[QPYAVYTW] for six days. (F) MS analysis of predicted lyciumin I chemotype.

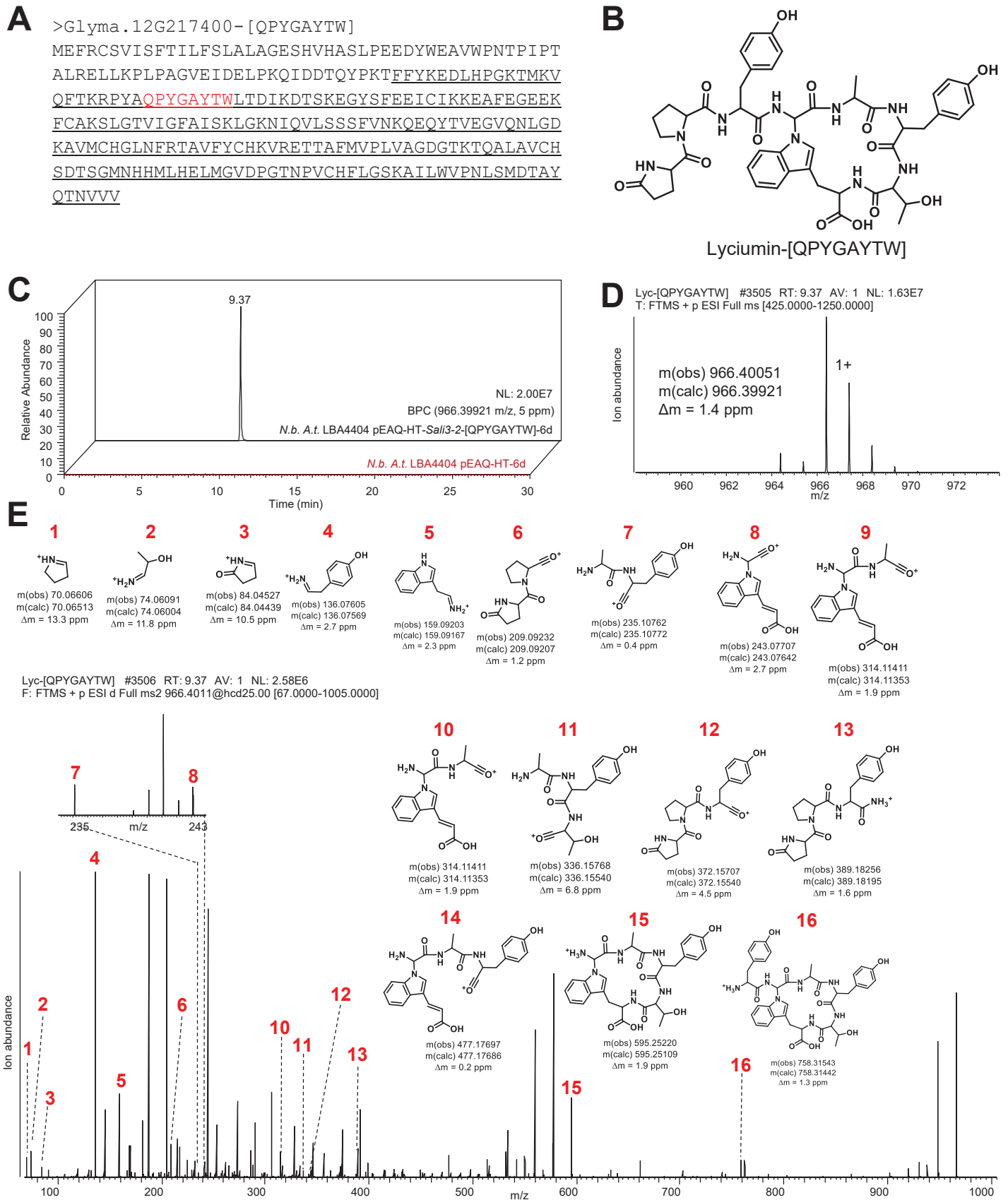


Figure S35 | Heterologous expression of *Sali3-2*-[QPYGAYTW] in *Nicotiana benthamiana*. (A) *Sali3-2*-[QPYGAYTW] lyciumin precursor peptide (BURP domain underlined, core peptide highlighted in red). (B) Predicted [QPYGAYTW]-lyciumin chemotype. (C) LC-MS chemotyping of predicted [QPYGAYTW]-lyciumin in peptide extract of *N. benthamiana* leaves infiltrated with *A. tumefaciens* LBA4404 pEAQ-HT-*Sali3-2*-[QPYGAYTW] for six days. (D) MS analysis of predicted [QPYGAYTW]-lyciumin chemotype. (E) MS/MS analysis of predicted [QPYGAYTW]-lyciumin chemotype.

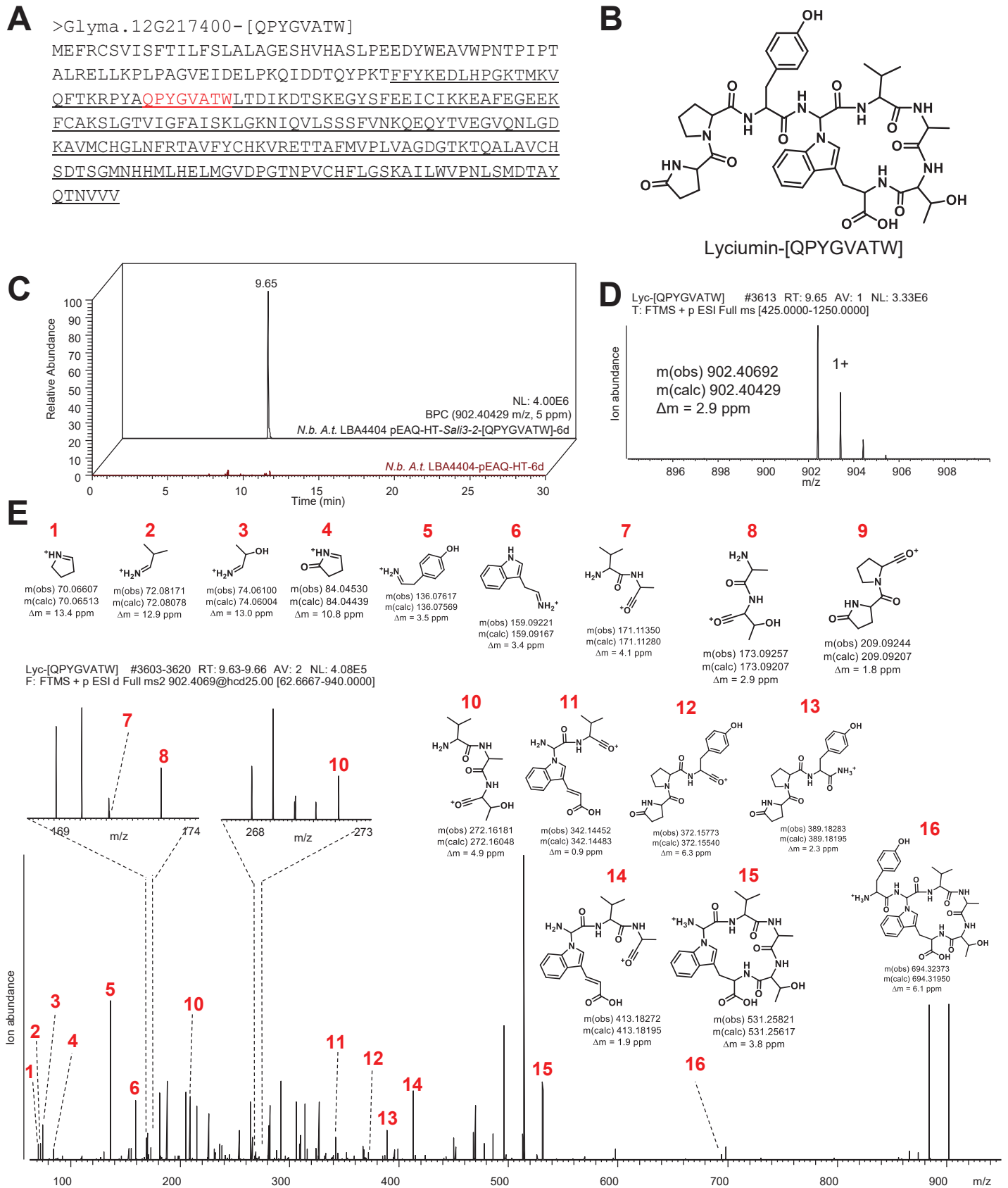


Figure S36 | Heterologous expression of *Sali3-2*-[QPYGVATW] in *Nicotiana benthamiana*. (A) *Sali3-2*-[QPYGVATW] lyciumin precursor peptide (BURP domain underlined, core peptide highlighted in red). (B) Predicted [QPYGVATW]-lyciumin chemotype. (C) LC-MS chemotyping of predicted [QPYGVATW]-lyciumin in peptide extract of *N. benthamiana* leaves infiltrated with *A. tumefaciens* LBA4404 pEAQ-HT-*Sali3-2*-[QPYGVATW] for six days. (D) MS analysis of predicted [QPYGVATW]-lyciumin chemotype. (E) MS/MS analysis of predicted [QPYGVATW]-lyciumin chemotype.

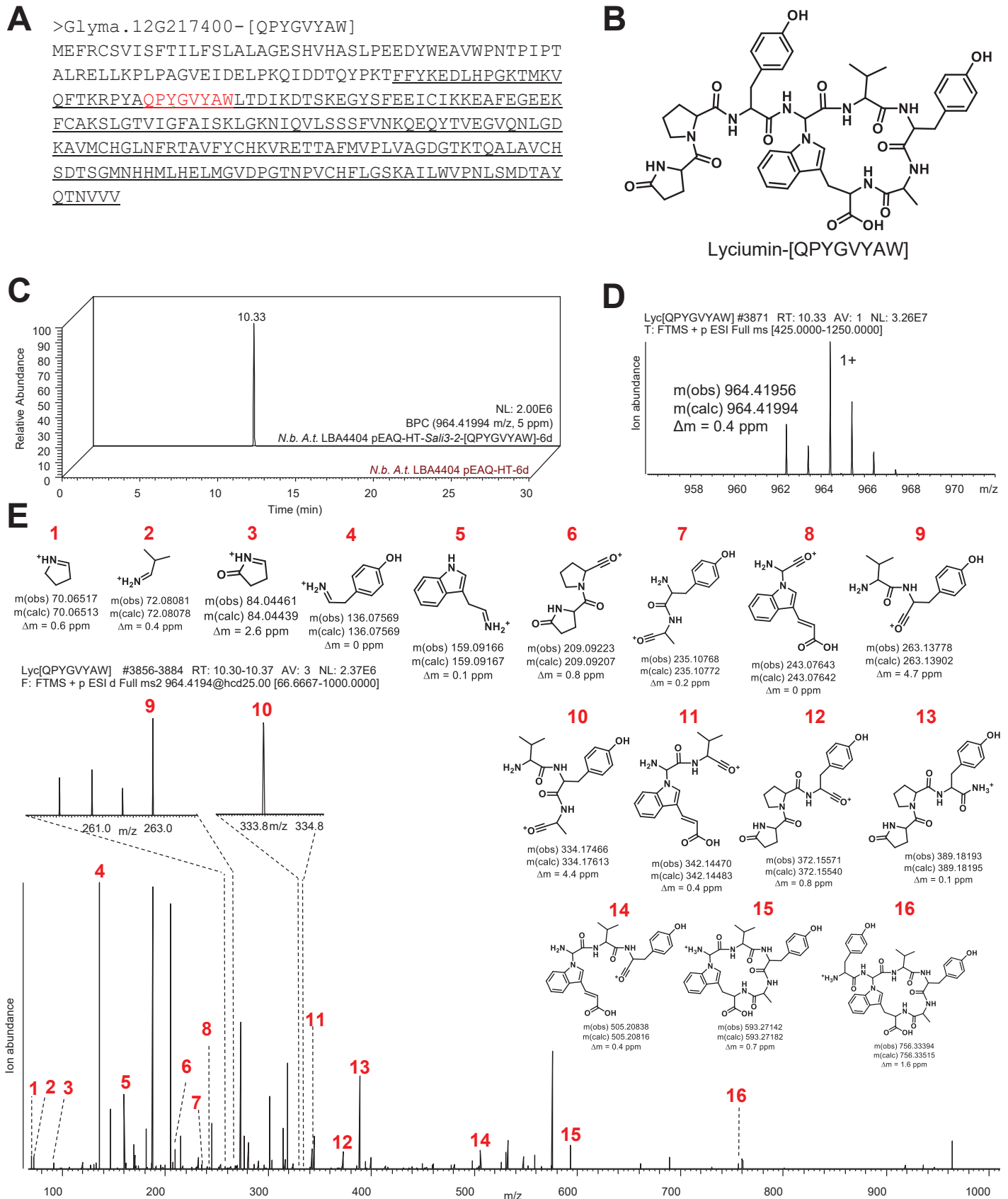


Figure S37 | Heterologous expression of *Sali3-2*-[QPYG^VVYAW] in *Nicotiana benthamiana*. (A) *Sali3-2*-[QPYG^VVYAW] lyciumin precursor peptide (BURP domain underlined, core peptide highlighted in red). (B) Predicted [QPYG^VVYAW]-lyciumin chemotype. (C) LC-MS chemotyping of predicted [QPYG^VVYAW]-lyciumin in peptide extract of *N. benthamiana* leaves infiltrated with *A. tumefaciens* LBA4404 pEAQ-HT-*Sali3-2*-[QPYG^VVYAW] for six days. (D) MS analysis of predicted [QPYG^VVYAW]-lyciumin chemotype. (E) MS/MS analysis of predicted [QPYG^VVYAW]-lyciumin chemotype.

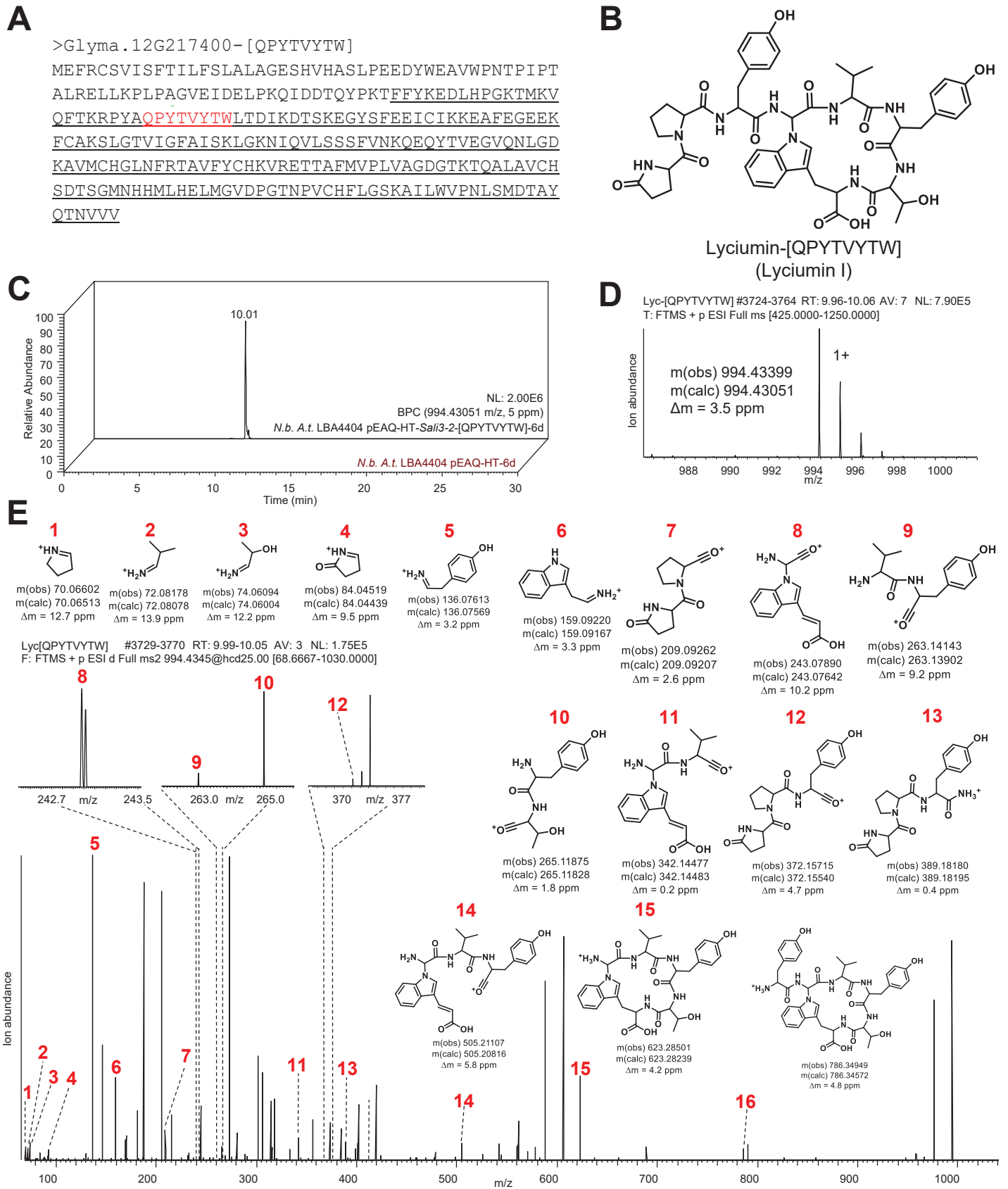


Figure S38 | Heterologous expression of *Sali3-2*-[QPYTVYTW] in *Nicotiana benthamiana*. (A) *Sali3-2*-[QPYTVYTW] lyciumin precursor peptide (BURP domain underlined, core peptide highlighted in red). (B) Predicted [QPYTVYTW]-lyciumin chemotype. (C) LC-MS chemotyping of predicted [QPYTVYTW]-lyciumin in peptide extract of *N. benthamiana* leaves infiltrated with *A. tumefaciens* LBA4404 pEAQ-HT-*Sali3-2*-[QPYTVYTW] for six days. (D) MS analysis of predicted [QPYTVYTW]-lyciumin chemotype. (E) MS/MS analysis of predicted [QPYTVYTW]-lyciumin chemotype.

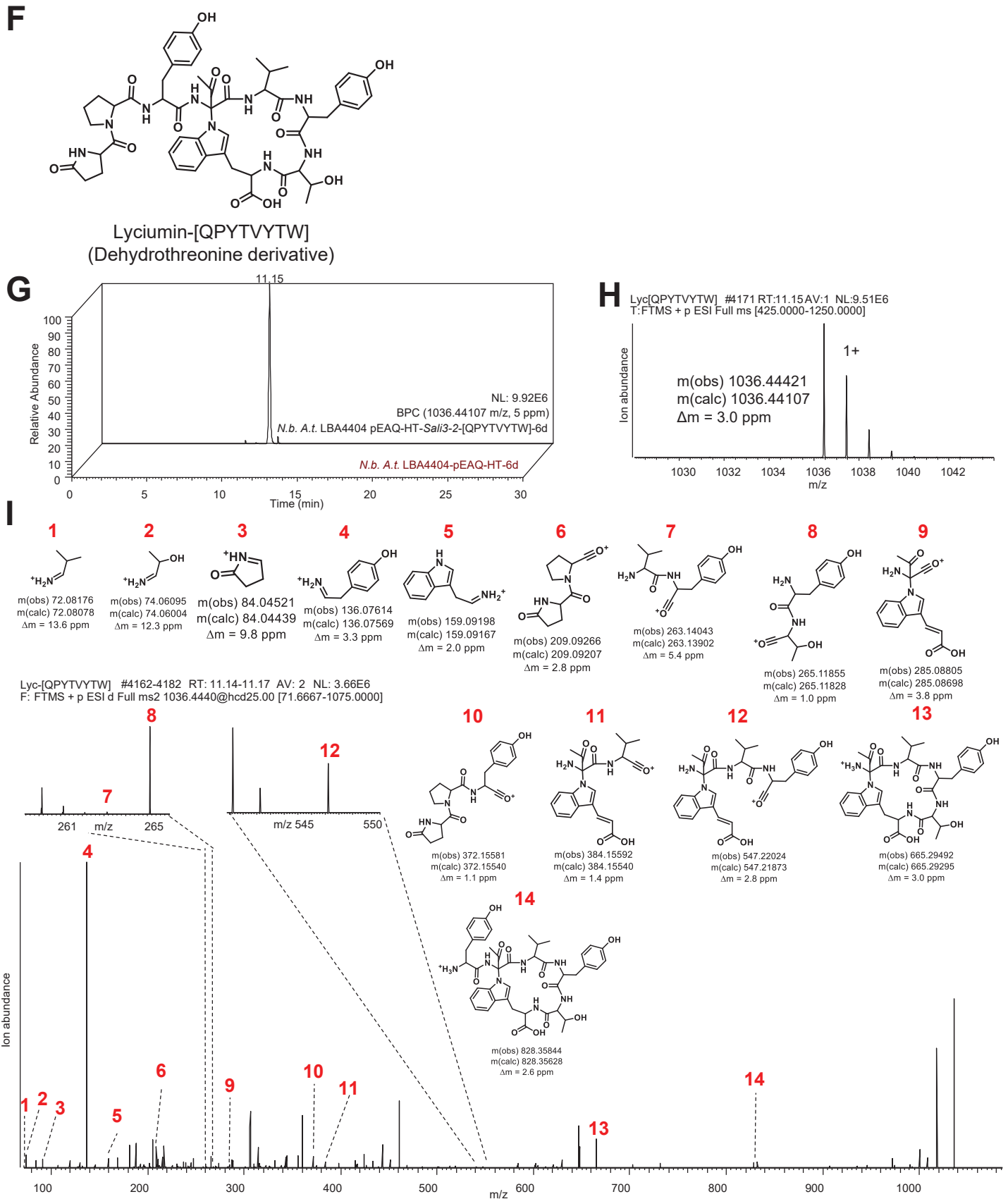


Figure S38 | Heterologous expression of *Sali*3-2-[QPYTVYTW] in *Nicotiana benthamiana*. (F) Predicted [QPYTVYTW]-dehydrothreonine lyciumin chemotype. (G) LC-MS chemotyping of predicted [QPYTVYTW]-dehydrothreonine lyciumin in peptide extract of *N. benthamiana* leaves infiltrated with *A. tumefaciens* LBA4404 pEAQ-HT-*Sali*3-2-[QPYTVYTW] for six days. (H) MS analysis of predicted [QPYTVYTW]-dehydrothreonine lyciumin chemotype. (I) MS/MS analysis of predicted [QPYTVYTW]-dehydrothreonine lyciumin chemotype.

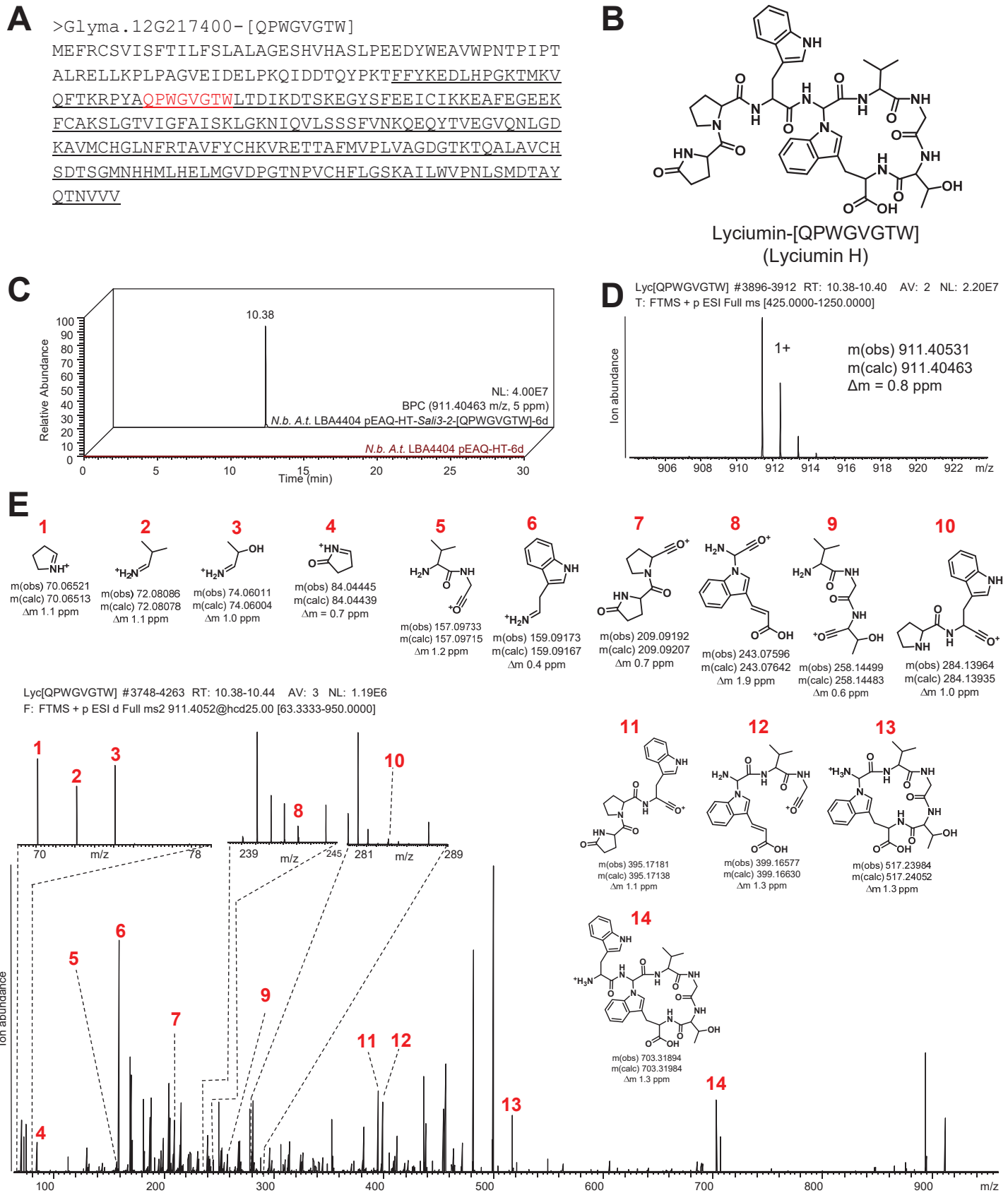


Figure S39 | Heterologous expression of *Sali3-2*-[QPWGVGTW] in *Nicotiana benthamiana*. (A) *Sali3-2*-[QPWGVGTW] lyciumin precursor peptide (BURP domain underlined, core peptide highlighted in red). (B) Predicted [QPWGVGTW]-lyciumin chemotype. (C) LC-MS chemotyping of predicted [QPWGVGTW]-lyciumin in peptide extract of *N. benthamiana* leaves infiltrated with *A. tumefaciens* LBA4404 pEAQ-HT-*Sali3-2*-[QPWGVGTW] for six days. (D) MS analysis of predicted [QPWGVGTW]-lyciumin chemotype. (E) MS/MS analysis of predicted [QPWGVGTW]-lyciumin chemotype.

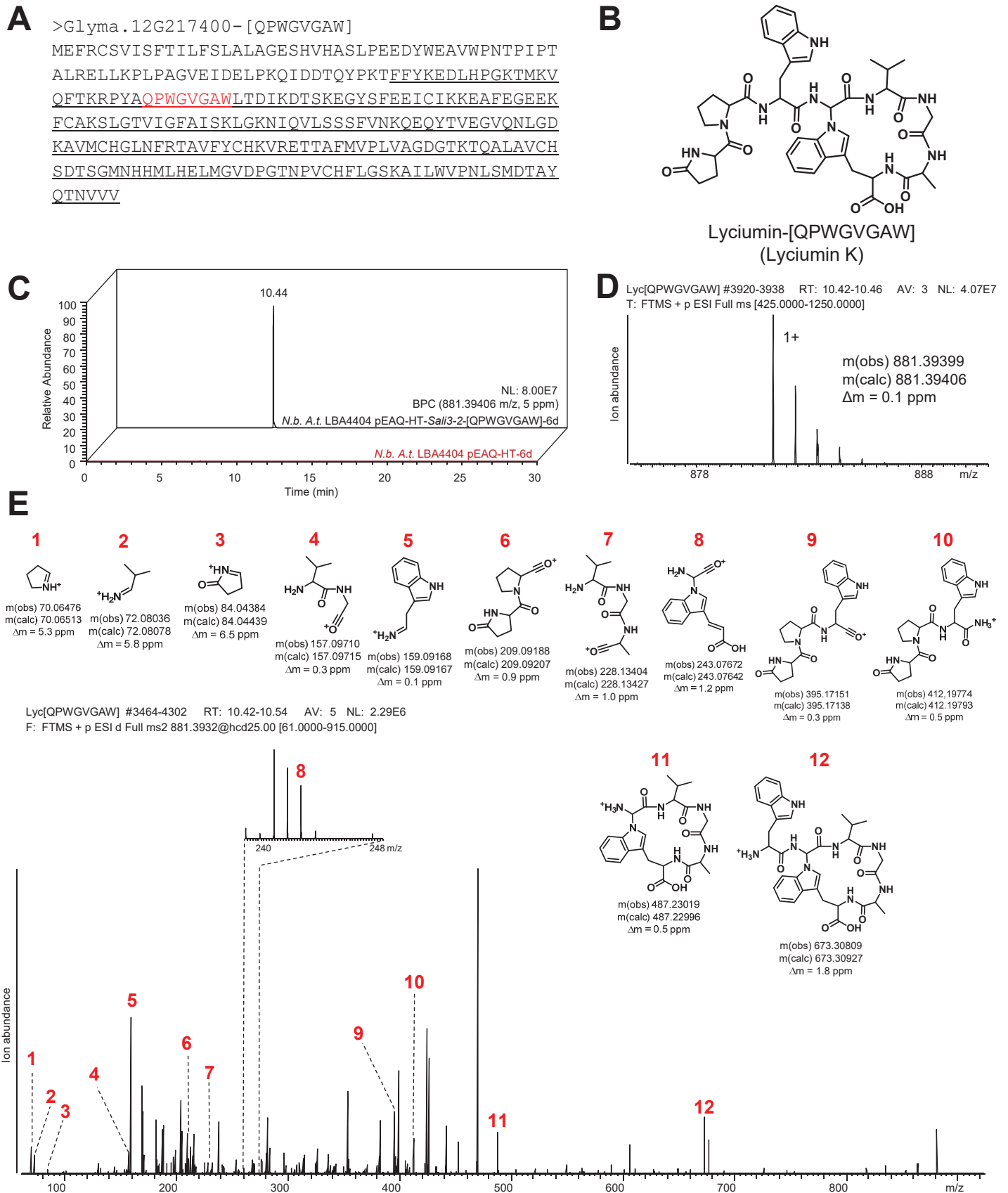


Figure S40 | Heterologous expression of *Sali3-2*-[QPWVGAW] in *Nicotiana benthamiana*. (A) *Sali3-2*-[QPWVGAW] lyciumin precursor peptide (BURP domain underlined, core peptide highlighted in red). (B) Predicted [QPWVGAW]-lyciumin chemotype. (C) LC-MS chemotyping of predicted [QPWVGAW]-lyciumin in peptide extract of *N. benthamiana* leaves infiltrated with *A. tumefaciens* LBA4404 pEAQ-HT-*Sali3-2*-[QPWVGAW] for six days. (D) MS analysis of predicted [QPWVGAW]-lyciumin chemotype. (E) MS/MS analysis of predicted [QPWVGAW]-lyciumin chemotype.

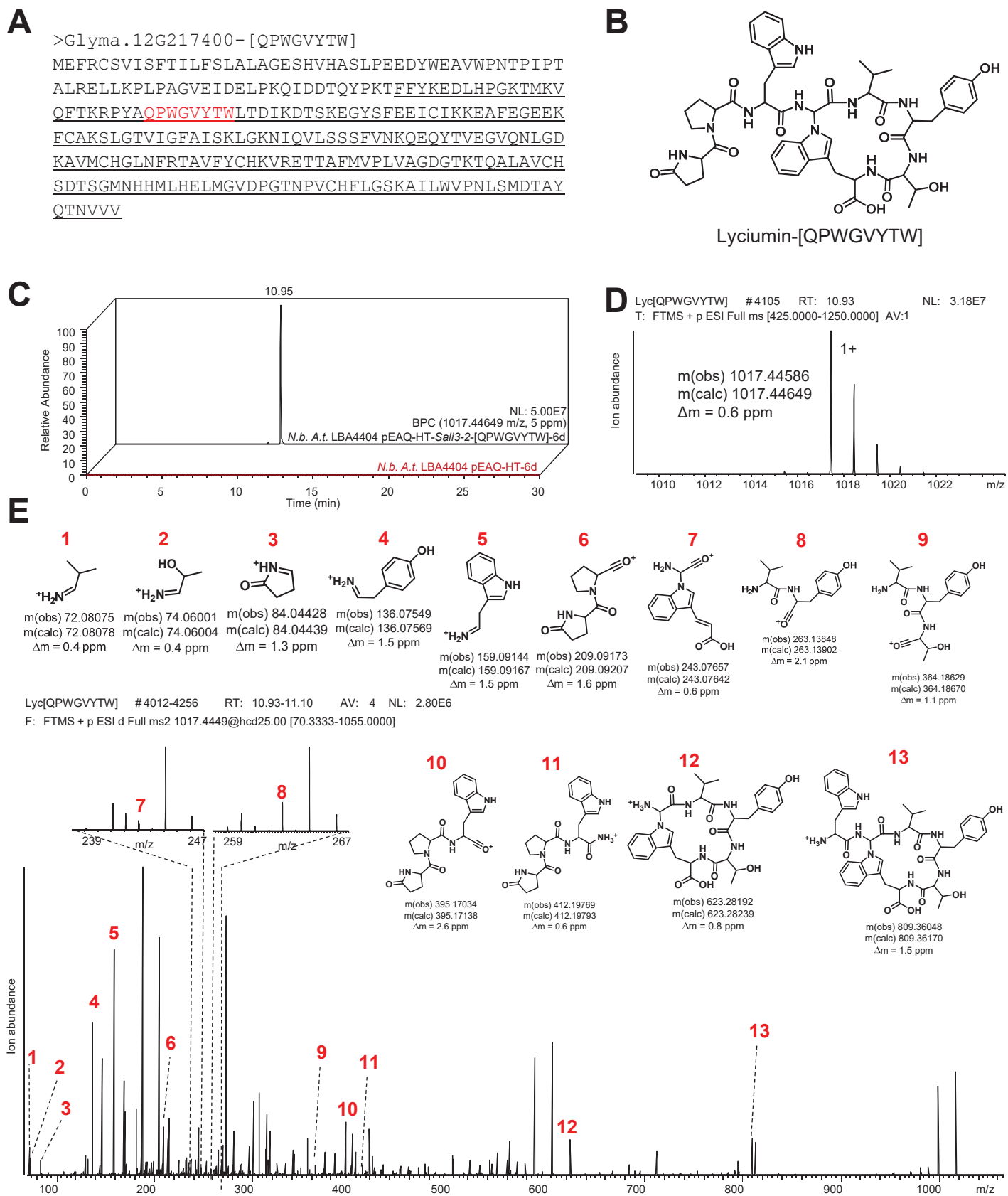


Figure S41 | Heterologous expression of *Sali3-2*-[QPWGVYTW] in *Nicotiana benthamiana*. (A) *Sali3-2*-[QPWGVYTW] lyciumin precursor peptide (BURP domain underlined, core peptide highlighted in red). (B) Predicted [QPWGVYTW]-lyciumin chemotype. (C) LC-MS chemotyping of predicted [QPWGVYTW]-lyciumin in peptide extract of *N. benthamiana* leaves infiltrated with *A. tumefaciens* LBA4404 pEAQ-HT-*Sali3-2*-[QPWGVYTW] for six days. (D) MS analysis of predicted [QPWGVYTW]-lyciumin chemotype. (E) MS/MS analysis of predicted [QPWGVYTW]-lyciumin chemotype.

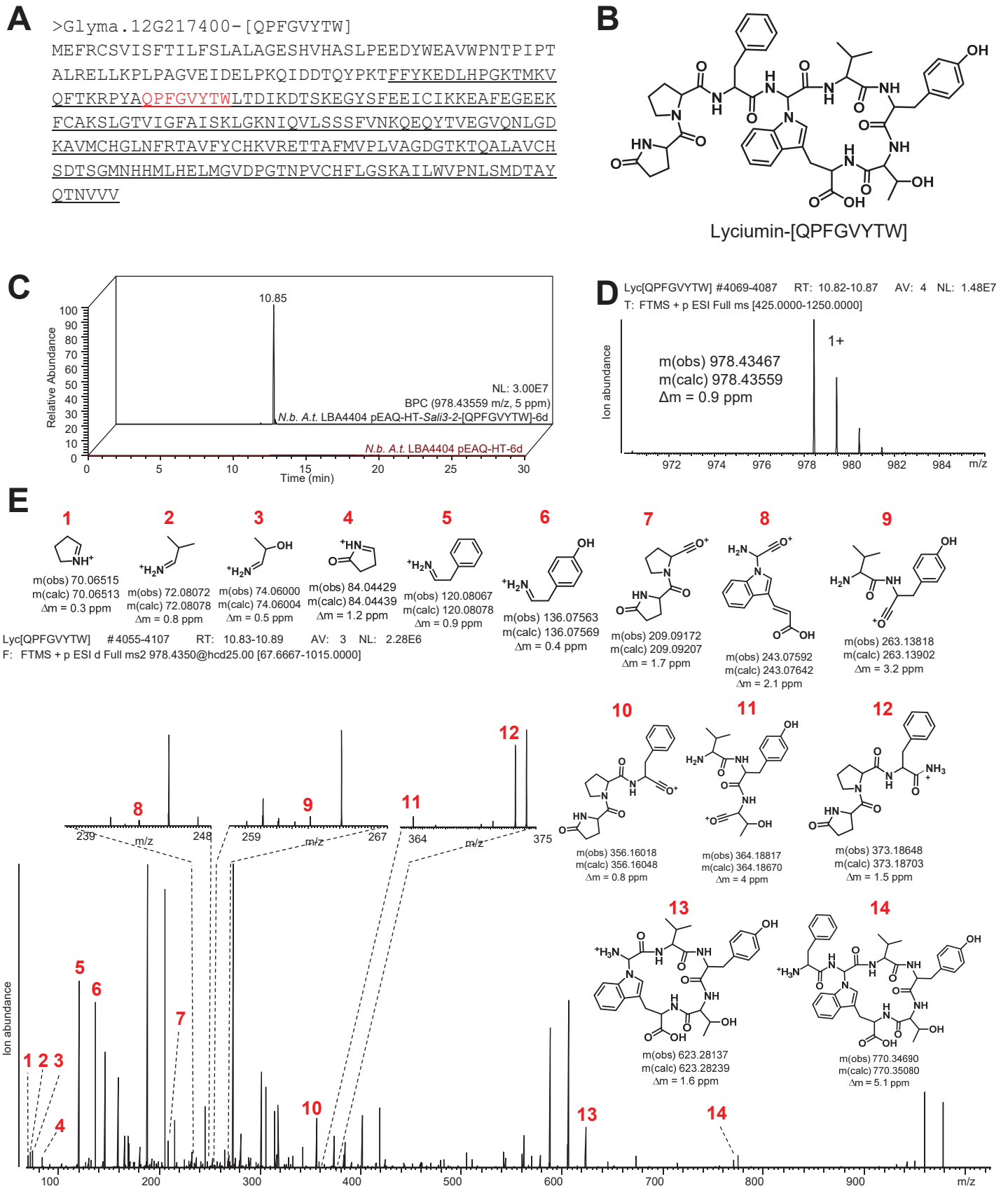


Figure S42 | Heterologous expression of *Sali3-2*-[QPF \overline{G} VYTW] in *Nicotiana benthamiana*. (A) *Sali3-2*-[QPF \overline{G} VYTW] lyciumin precursor peptide (BURP domain underlined, core peptide highlighted in red). (B) Predicted [QPF \overline{G} VYTW]-lyciumin chemotype. (C) LC-MS chemotyping of predicted [QPF \overline{G} VYTW]-lyciumin in peptide extract of *N. benthamiana* leaves infiltrated with *A. tumefaciens* LBA4404 pEAQ-HT-*Sali3-2*-[QPF \overline{G} VYTW] for six days. (D) MS analysis of predicted [QPF \overline{G} VYTW]-lyciumin chemotype. (E) MS/MS analysis of predicted [QPF \overline{G} VYTW]-lyciumin chemotype.

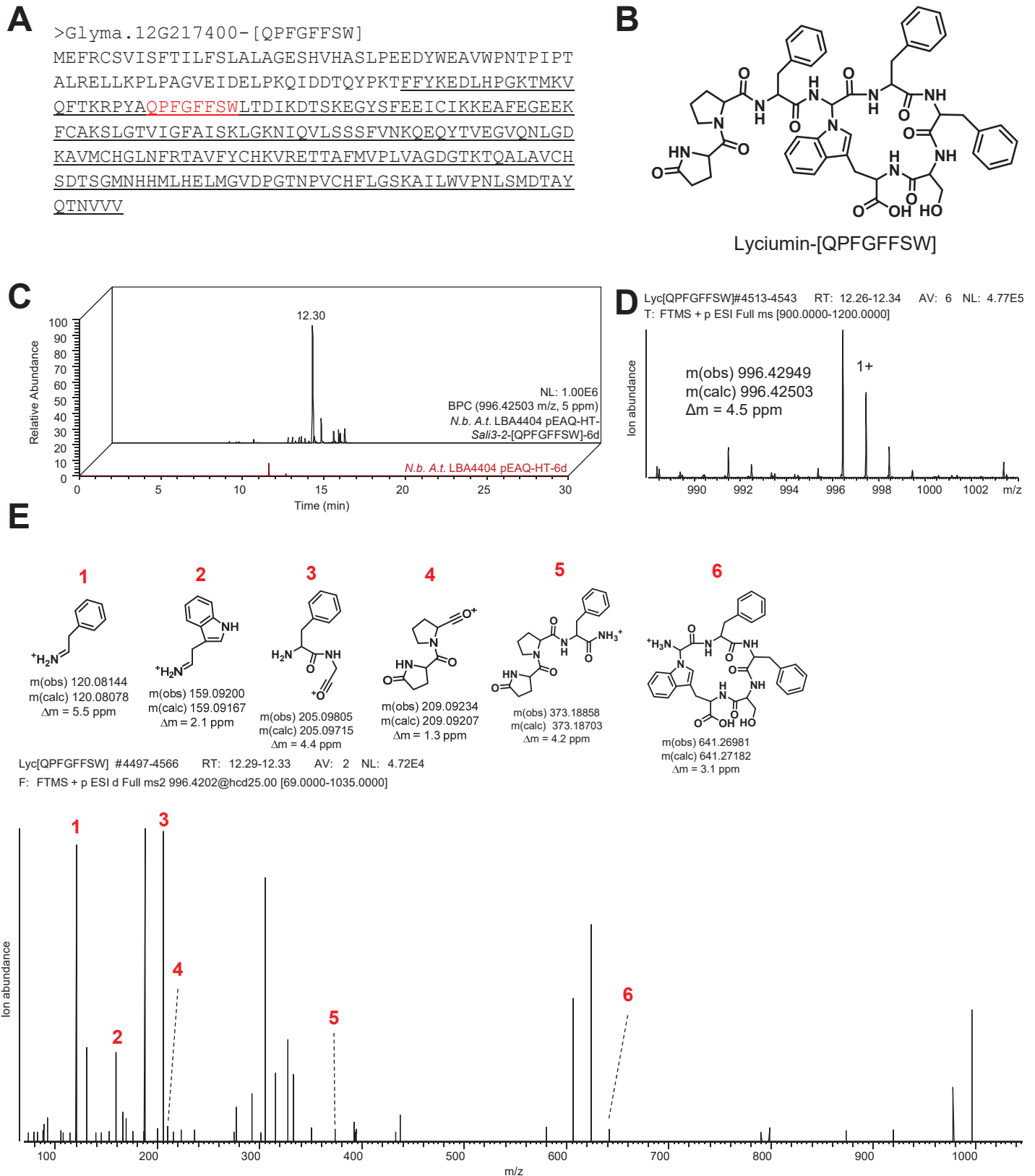


Figure S43 | Heterologous expression of *Sali3-2*-[QPF_GFFSW] in *Nicotiana benthamiana*. (A) *Sali3-2*-[QPF_GFFSW] lyciumin precursor peptide (BURP domain underlined, core peptide highlighted in red). (B) Predicted [QPF_GFFSW]-lyciumin chemotype. (C) LC-MS chemotyping of predicted [QPF_GFFSW]-lyciumin in peptide extract of *N. benthamiana* leaves infiltrated with *A. tumefaciens* LBA4404 pEAQ-HT-*Sali3-2*-[QPF_GFFSW] for six days. (D) MS analysis of predicted [QPF_GFFSW]-lyciumin chemotype. (E) MS/MS analysis of predicted [QPF_GFFSW]-lyciumin chemotype.

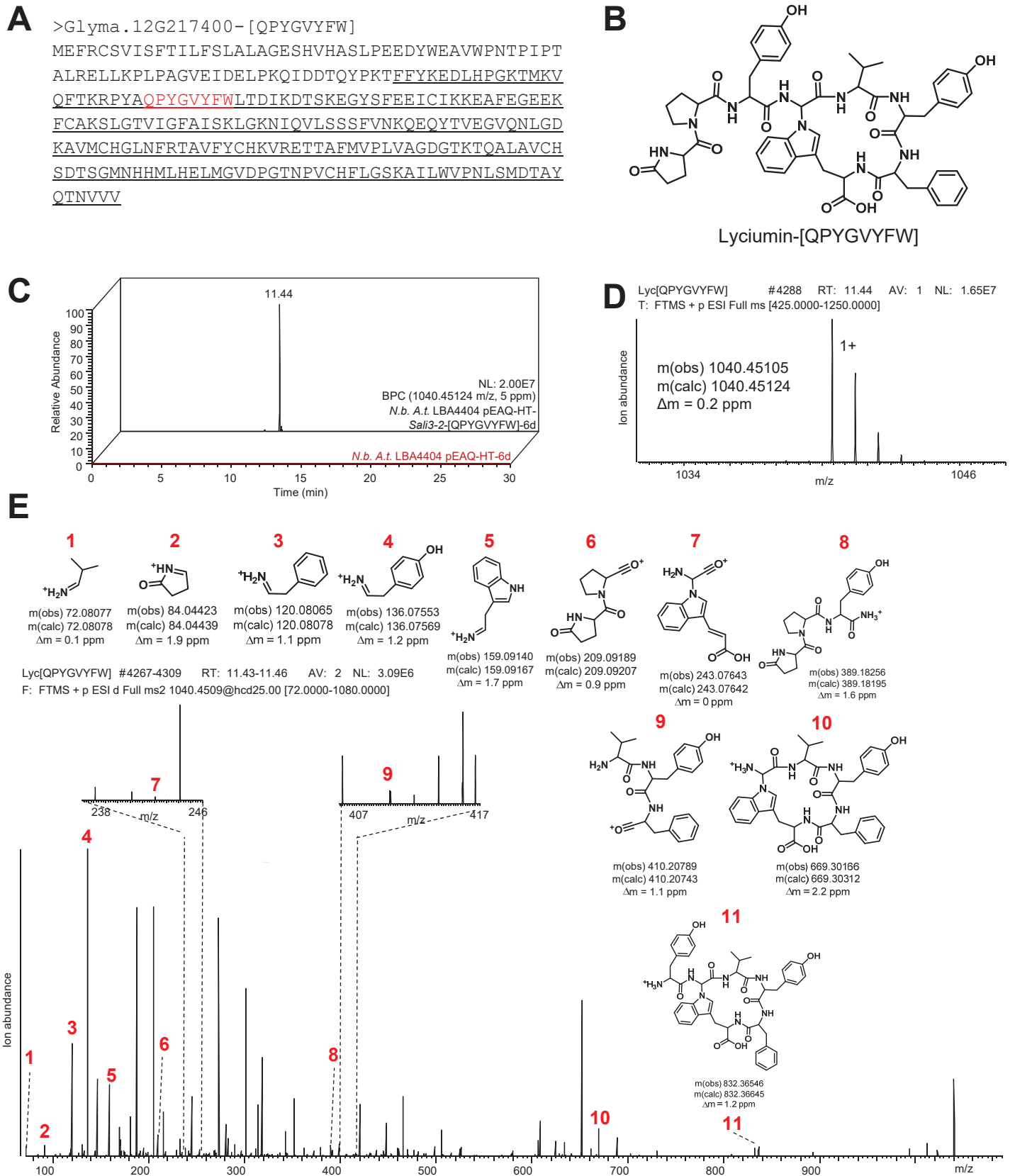


Figure S44 | Heterologous expression of *Sali3-2*-[QPYGVYFW] in *Nicotiana benthamiana*. (A) *Sali3-2*-[QPYGVYFW] lyciumin precursor peptide (BURP domain underlined, core peptide highlighted in red). (B) Predicted [QPYGVYFW]-lyciumin chemotype. (C) LC-MS chemotyping of predicted [QPYGVYFW]-lyciumin in peptide extract of *N. benthamiana* leaves infiltrated with *A. tumefaciens* LBA4404 pEAQ-HT-*Sali3-2*-[QPYGVYFW] for six days. (D) MS analysis of predicted [QPYGVYFW]-lyciumin chemotype. (E) MS/MS analysis of predicted [QPYGVYFW]-lyciumin chemotype.

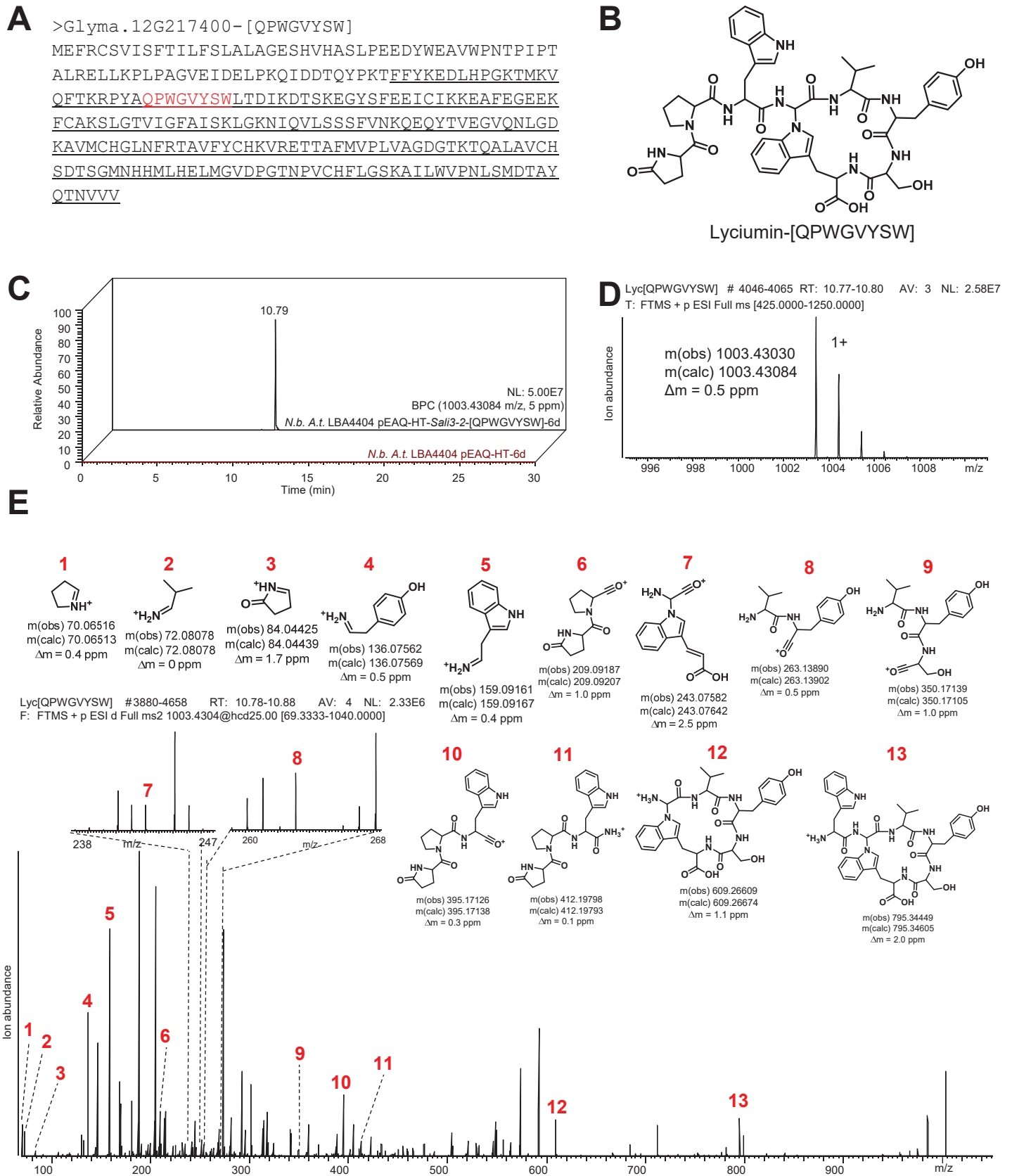


Figure S45 | Heterologous expression of *Sali3-2*-[QPWGVYSW] in *Nicotiana benthamiana*. (A) *Sali3-2*-[QPWGVYSW] lyciumin precursor peptide (BURP domain underlined, core peptide highlighted in red). (B) Predicted [QPWGVYSW]-lyciumin chemotype. (C) LC-MS chemotyping of predicted [QPWGVYSW]-lyciumin in peptide extract of *N. benthamiana* leaves infiltrated with *A. tumefaciens* LBA4404 pEAQ-HT-*Sali3-2*-[QPWGVYSW] for six days. (D) MS analysis of predicted [QPWGVYSW]-lyciumin chemotype. (E) MS/MS analysis of predicted [QPWGVYSW]-lyciumin chemotype.

References

1. Bassüner R *et al.* (1988) Abundant embryonic mRNA in field bean (*Vicia faba* L.) codes for a new class of seed proteins: cDNA cloning and characterization of the primary translation product. *Plant Mol Biol* 11(3): pp 321–334.
2. Yamaguchi-Shinozaki K, Shinozaki K (1993) The plant hormone abscisic acid mediates the drought-induced expression but not the seed-specific expression of rd22, a gene responsive to dehydration stress in *Arabidopsis thaliana*. *Mol Gen Genet* 238(1-2): pp 17–25.
3. Zheng L, Heupel RC, DellaPenna D (1992) The b Subunit of Tomato Fruit Polygalacturonase Isoenzyme 1: Isolation, Characterization, and Identification of Unique Structural Features. *Plant Cell* 4(9): pp 1147–1156.
4. Boutilier KA *et al.* (1994) Expression of the BnmNAP subfamily of napin genes coincides with the induction of Brassica microspore embryogenesis. *Plant Mol Biol* 26(6): pp 1711–1723.
5. Edgar RC (2004) MUSCLE: multiple sequence alignment with high accuracy and high throughput *Nucleic Acids Res* 32(5): pp 1792–1797.
6. Kumar S, Stecher G, Tamura K (2016) MEGA7: Molecular Evolutionary Genetics Analysis version 7.0 for bigger datasets MEGA7: Molecular Evolutionary Genetics Analysis Version 7.0 for Bigger Datasets *Mol Biol Evol* 33, pp 1870–1874.
7. Nei M, Kumar S (2000) Molecular Evolution and Phylogenetics. Oxford University Press, New York.
8. Morita H, Yoshida N, Takeya K, Itokawa H, Shiota O (1996) Configurational and conformational analyses of a cyclic octapeptide, lyciumin A, from *Lycium chinense* Mill. *Tetrahedron* 52(8): pp 2795–2802.
9. Yahara S *et al.* (1993) Cyclic peptides, acyclic diterpene glycosides and other compounds from *Lycium chinense* Mill. *Chem Pharm Bull* 41(4): pp 703–709.
10. Morita H, Suzuki H, Kobayashi J (2004) Celogenamide A, a New Cyclic Peptide from the Seeds of *Celosia argentea*. *J Nat Prod* 67(9): pp 1628–1630.
11. Li B, Dewey CN (2011) RSEM: accurate transcript quantification from RNA-Seq data with or without a reference genome. *BMC Bioinform* 12(1): pp 323.
12. Potato Genome Sequencing Consortium (2011) Genome sequence and analysis of the tuber crop potato. *Nature* 475(7355): pp 189–195.
13. Grabherr MG *et al.* Full-length transcriptome assembly from RNA-Seq data without a reference genome. *Nat Biotechnol* 29(7): pp 644–652.
14. Waese J *et al.* (2017) ePlant: Visualizing and Exploring Multiple Levels of Data for Hypothesis Generation in Plant Biology. *Plant Cell* 29: pp 1806–1821.
15. Benedito VA *et al.* (2008) A gene expression atlas of the model legume *Medicago truncatula*. *Plant J* 55(3): pp 504–513.
16. Libault M *et al.* (2010) An integrated transcriptome atlas of the crop model *Glycine max*, and its use in comparative analyses in plants. *Plant J* 63(1): pp 86–99.
17. Severin AJ *et al.* (2010) RNA-Seq Atlas of *Glycine max*: a guide to the soybean transcriptome. *BMC Plant Biol* 10(1): pp 160.
18. Priyam A *et al.* (2015) Sequenceserver: a modern graphical user interface for custom BLAST databases. *Biorxiv* 033142.
19. Gibson DG *et al.* (2009) Enzymatic assembly of DNA molecules up to several hundred kilobases. *Nat Methods* 6(5): pp 343–345.
20. Sainsbury F, Thuenemann EC, Lomonosoff GP (2009) pEAQ: versatile expression vectors for easy and quick transient expression of heterologous proteins in plants. *Plant Biotechnol J* 7(7): pp 682–693.
21. Wang MX *et al.* (2016) Sharing and community curation of mass spectrometry data with Global Natural Products Social Molecular Networking. *Nat Biotechnol* 34(8): pp 828–837.